



universität
wien

DIPLOMARBEIT

Titel der Diplomarbeit

Identification of small RNAs in Staufen2 complexes
from rat brain

angestrebter akademischer Grad

Magister/Magistra der Naturwissenschaften (Mag. rer.nat.)

Verfasserin:	Sabine Spath
Matrikel-Nummer:	0202491
Studienrichtung (lt. Studienblatt):	Molekulare Biologie (A490)
Betreuerin:	Dr. Anetta Konecna

Wien, am 15. Juni 2008

TABLE OF CONTENTS

Abstract	1
Zusammenfassung	2
1 Introduction	3
1.1 Small RNAs.....	3
1.1.1 Generation of miRNAs and siRNAs.....	3
1.1.2 RISC and miRNP associated proteins	5
1.1.3 Function of miRNAs.....	6
1.1.4 miRNAs in the nervous system.....	8
1.2 RNA granules	11
1.2.1 Processing bodies.....	11
1.2.2 Neuronal granules.....	12
1.3 RNA localization in neurons	13
1.4 Aim of the project.....	14
2 Materials and methods	16
2.1 Materials	16
2.1.1 Reagents and consumables.....	16
2.1.2 Enzymes.....	19
2.1.3 Antibodies	20
2.1.4 Plasmids and primers	20
2.1.5 Animals	21
2.1.6 Cells.....	21
2.1.7 Buffers and solutions.....	21
2.1.8 Equipment.....	27
2.2 Methods.....	28
2.2.1 Molecular Biology	28
2.2.2 Cloning of GST-Stau2 _{CT} into pGEX-6P-2	29
2.2.3 Expression and purification of proteins	32
2.2.4 Analysis of proteins	34
2.2.5 Gel filtration of rat brain lysates	35
2.2.6 Preparation of antibody-coupled beads for IP.....	37
2.2.7 Immunoprecipitation of Stau2-containing RNPs.....	38
2.2.8 RNA methods.....	40

2.2.9	Immunoprecipitation of Stau2-containing RNPs for RNA experiments.....	40
2.2.10	RNA gel electrophoresis	41
2.2.11	3'-end RNA labeling with [³² P] pCp.....	42
2.2.12	End point RT-PCR for selected miRNAs	43
3	Results.....	45
3.1	Purification of GST-Stau2 _{CT} for antibody production.....	45
3.1.1	Cloning of Stau2 _{CT} into pGEX-6P-2	45
3.1.2	Expression and purification of the PreScission protease.....	45
3.1.3	Expression and purification of Stau2 proteins	47
3.2	Protein composition of Stau2 complexes.....	52
3.2.1	Affinity purification of anti-Stau2 antibodies and preparation of antibody-coupled beads	52
3.2.2	Protein candidates in Stau2 complexes	53
3.3	RNA composition of Stau2 complexes.....	56
3.3.1	RNA isolation from Stau2 RNPs.....	56
3.3.2	RNA labeling experiments – a search for miRNAs.....	58
3.3.3	Gel filtration experiments to separate different Stau2 complexes.....	62
3.3.4	The S100 fraction as an input for labeling experiments.....	63
3.3.5	RT-PCR.....	67
4	Discussion	70
4.1	Protein candidates in Stau2 complexes	70
4.1.1	Stau2 is associated with ribosomes.....	71
4.1.2	RISC proteins in Stau2 complexes	72
4.2	RNA composition of Stau2 complexes.....	72
4.2.1	miRNAs are associated with Stau2 complexes	72
4.2.2	miRNAs in different Stau2 complexes.....	74
4.2.3	Stau2 and export of pre-miRNAs	75
4.3	Future perspectives.....	75
5	References	77
6	Appendix.....	82
6.1	Abbreviations.....	82
6.2	Acknowledgements	85
6.3	Curriculum Vitae	86

ABSTRACT

microRNAs (miRNAs) are ~22 nt long non-coding RNAs which are involved in post-transcriptional gene regulation via mRNA silencing or degradation. miRNAs are abundant in the nervous system, where they have key roles in development and possibly in synaptic plasticity.

Both RNA localization as well as stimulus-dependent local protein synthesis critically contribute to synaptic plasticity. During transport, the silencing of mRNAs within neuronal ribonucleoprotein particles (RNPs) can be achieved either by translational regulator-proteins or by miRNAs. Stau2 (Stau2), an RNA-binding protein (RBP) investigated in the Kiebler lab, belongs to the family of dsRBPs and is mainly expressed in the nervous system. Stau2 was shown to be involved in memory formation in *Drosophila melanogaster*. In hippocampal neurons, Stau2 proteins are core components of distinct RNA-containing particles that reach out to distal dendrites.

Recent evidence suggested a link between Stau2 and miRNAs. The export of Stau2 from the nucleus depends on Exportin-5, the main export factor for precursor-miRNAs. Therefore, this project aimed at investigating whether small non-coding RNAs, especially miRNAs, are part of Stau2-containing complexes in the rat brain.

Immunoprecipitation, using affinity-purified anti-Stau2 antibodies, was performed to isolate Stau2 RNPs including all associated proteins and RNAs. On the protein level, the presence of different RISC-associated components like Ago, PACT, FMRP and eIF6 in Stau2 complexes suggested a participation of the miRNA pathway.

On the RNA level, the specific association of small RNAs at the size of 20-22 nt with Stau2 RNPs in E17 rat brain provided further evidence for a connection between miRNAs and Stau2 complexes, as shown by radioactive labeling of RNA isolated after Stau2 immunoprecipitation. In addition, RT-PCR proved the presence of 5 candidate miRNAs, miR-18, 26a, 128a, 134 and let-7c, in Stau2 complexes. In the future, RNA isolated from Stau2 immunoprecipitations will be cloned and sequenced to obtain a complete list of miRNAs associated with Stau2 complexes.

A hypothesis to explain this association between miRNAs and Stau2 would be that the miRNA translationally silences its target mRNAs during transport in Stau2 complexes. Upon a specific stimulus, the suppression would be relieved allowing translation to occur at the synapse.

ZUSAMMENFASSUNG

MikroRNAs (miRNAs) sind ~22 nt lange, nicht kodierende RNAs, welche Gene post-transkriptionell regulieren können, indem sie die Translation hemmen oder den Abbau der mRNA auslösen. Im Nervensystem spielen miRNAs eine zentrale Rolle in der Entwicklung und wahrscheinlich auch bei der synaptischen Plastizität.

Hierfür sind RNA-bindende Proteine (RBPs), welche mRNAs an die Synapsen lokalisieren, ebenso wichtig wie eine Stimulus-abhängige lokale Proteinsynthese. Während des Transports ist die Translation der mRNAs in neuronalen Ribonukleoprotein-Partikeln (RNPs) unterbunden, was entweder durch Regulator-Proteine oder durch miRNAs bewerkstelligt werden kann. Das im Kiebler Labor untersuchte Protein Stau2 (Stau2) gehört zur Familie der dsRBPs und wird hauptsächlich im Nervensystem exprimiert. In der Taufliege *Drosophila melanogaster* spielt es eine Rolle bei der Gedächtnisbildung. In hippocampalen Neuronen stellen Stau2-Proteine wichtige Komponenten in RNA-enthaltenden Partikeln dar, welche sich bis in die distalen Dendriten erstrecken.

Kürzlich wurde ein Zusammenhang zwischen Stau2 und miRNAs vorgeschlagen, da der Export von Stau2 aus dem Kern von Exportin-5 abhängig ist, dem primären Exportfaktor für Vorläufer-miRNAs. Deshalb war die Hauptaufgabe dieses Projekts zu untersuchen, ob kleine nicht-kodierende RNAs, im Besonderen miRNAs, in Stau2 Partikeln enthalten sind.

Über Immunoprecipitationen mit affinitätsgereinigten Antikörpern gegen Stau2 gelang es, Stau2 RNPs mit allen enthaltenen Proteinen und RNAs zu isolieren. Auf Proteinebene wurden verschiedene RISC-assoziierte Komponenten wie Ago, PACT, FMRP und eIF6 in Stau2 Komplexen gefunden, was auf eine Beteiligung von miRNAs hindeutet.

Auf RNA-Ebene gelang mittels radioaktiver Markierung von RNA der Nachweis kleiner RNAs mit einer Größe von 20-22 nt in den Stau2 Komplexen. Dies ist ein weiterer Hinweis auf einen Zusammenhang zwischen miRNAs und Stau2 Partikeln. Zusätzlich wurde das Vorhandensein von miR-18, 26a, 128a, 134 und let-7c in Stau2 Komplexen mittels RT-PCR nachgewiesen. In Folge soll die in den Stau2 Immunoprecipitationen vorkommende RNA kloniert und sequenziert werden, um eine vollständige Liste aller Stau2-assoziierten miRNAs zu erhalten.

Eine Hypothese um den Zusammenhang zwischen miRNAs und Stau2 zu erklären, wäre dass miRNAs eventuell eine Funktion in der Inhibierung der Translation von mRNAs in den Stau2 Komplexen erfüllen. Während des Transports sind mRNAs in RNPs durch miRNAs gebunden, was die Translation verhindert. Dies wird später durch einen spezifischen Stimulus aufgehoben, welcher eine lokale Translation an der Synapse ermöglicht.

1 INTRODUCTION

1.1 SMALL RNAs

In the 1990s, the first microRNAs (miRNAs), *lin-4* and *let-7*, were discovered by genetic experiments in *Caenorhabditis elegans* (*C. elegans*). Since this time, extensive research took place in this field leading to the identification of the so-called short interfering RNAs (siRNAs), the effector molecules of RNA interference (RNAi) in plants, animals and fungi (reviewed in He and Hannon 2004; Grosshans and Filipowicz 2008). Up to now, different classes of small, non-coding regulatory RNAs were identified (reviewed in Grosshans and Filipowicz 2008; Filipowicz et al. 2005; Rana 2007). First, miRNAs, which are 20-25 nucleotides (nt) in length, are encoded by specific genes and processed from single-stranded RNAs which are folded into hairpins. They can function via repression of translation or degradation of mRNAs. Second, siRNAs, which are 20-25 nt in length and formed by cleavage of long double-stranded RNAs (originally coming from viral infections). siRNAs are incorporated into the RNA-induced silencing complex (RISC) and capable of cleaving target mRNAs. Besides these two most prominent classes, there were also other groups identified, e.g. Piwi-associated RNAs (piRNAs) or repeat-associated small interfering RNA (rasiRNA). Still, the field of small RNAs is growing and new classes are likely to be identified.

1.1.1 GENERATION OF MIRNAS AND SIRNAS

The generation of miRNAs takes place in several steps, as shown in Figure 1.1 (reviewed in Filipowicz et al. 2008; Filipowicz et al. 2005). miRNAs are transcribed by Polymerase II from either independent miRNA genes or from introns of protein-coding genes. These primary transcripts (pri-miRNAs) are first processed by the Drosha/Pasha complex in the nucleus. Drosha belongs to the RNase III family, which are nuclear proteins of 130-160 kD in size, containing two RNase III catalytic domains and one double-stranded RNA-binding domain (dsRBD). Pasha, named DiGeorge syndrome critical region gene-8 (DGCR8) in mammals, is a dsRNA-binding protein (dsRBP) and like Drosha essential for the processing of pri-miRNAs to ~70 nt long hairpins called precursor (pre)-miRNAs. These pre-miRNAs are transported from the nucleus to the cytoplasm via the Exportin-5 nuclear transport receptor complex in a Ran GTP-dependent manner.

In a second cleavage step Dicer, another RNase III enzyme, is involved in the processing of the hairpins to yield a ~22 nt miRNA duplex. Dicer recognizes the 2 nt 3' overhang from

pre-miRNAs generated by Drosha via the Piwi Argonaute Zwiille (PAZ) domain. Cleavage by Dicer itself also leads to the generation of a 2 nt 3' overhang. This cleavage step requires two other dsRBPs, Loquacious in *Drosophila melanogaster* (*D. melanogaster*) and human immunodeficiency virus (HIV-1) *trans*-activating response (TAR) RNA-binding protein (TRPB) in mammals.

From the mature miRNA duplex, the strand with the 5' terminus located at the thermodynamically less-stable end is selected to function as the mature miRNA, called the guide strand. This miRNA is assembled into miRNA-containing ribonucleoprotein particles (miRNPs) together with the Argonaute (Ago) proteins. The remaining strand of the duplex, the passenger strand, is degraded.

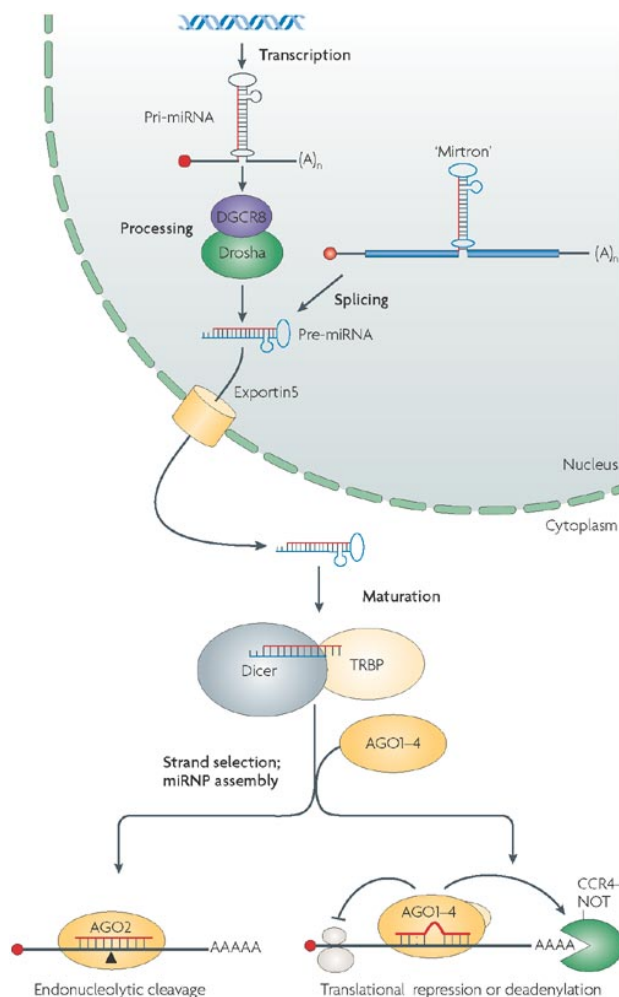


Figure 1.1 - Biogenesis of miRNAs

After transcription by PolII the pri-miRNAs are processed by the Drosha/DGCR8 complex to yield pre-miRNAs. These ~70 nt long hairpins are transported to the cytoplasm via the Exportin-5 export factor. Cleavage by Dicer, yielding a ~22 nt mature miRNA, involves the dsRBP TRPB in mammals. The guide strand from the mature miRNA duplex is assembled into miRNPs together with Argonaute proteins. Binding of miRNPs to target RNAs leads to either cleavage or translational repression, dependent on the mode of base-pairing. (from Filipowicz et al. 2008)

The biogenesis of siRNAs is slightly different. In this case, the origin is a double-stranded RNA coming from a viral infection, anti-sense transcription or transfection. This dsRNA is cleaved by Dicer to yield a 22 nt siRNA duplex. Similarly, the guide strand gets incorporated into the RISC complex which is composed amongst others of Ago2 and Dicer (Filipowicz et al. 2005).

1.1.1.1 DIFFERENCES BETWEEN miRNAs AND siRNAs

One main difference between siRNAs and miRNAs is their molecular origin. Another distinct feature is their mode of target recognition. In general, small RNAs recognize their target RNAs by sequence-specific base-pairing. The effect of the small RNA-mRNA interaction depends on the degree of complementarity between these two sequences. If the base-pairing is nearly perfect, the target mRNA is cleaved in the middle of the siRNA/miRNA-mRNA duplex. This is the case for siRNAs and most plant miRNAs (Jones-Rhoades et al. 2006). In contrast, the base-pairing of animal miRNAs with mRNAs is imperfect, but still follows some rules. First, perfect base-pairing at the 5' end in the seed region (miRNA nucleotides 2-8); second, the presence of a bulge or mismatches in the central region to exclude endonucleolytic cleavage and third, a reasonable complementarity at the miRNA 3' end to stabilize the interaction (Doench and Sharp 2004; Brennecke et al. 2005; Grimson et al. 2007). This imperfect base-pairing leads to either translational inhibition or degradation of the mRNA.

1.1.2 RISC AND miRNP ASSOCIATED PROTEINS

After their generation, mature small RNAs are incorporated into the RISC (in case of siRNAs) or into miRNPs (in case of miRNAs). However, these two complexes share protein components and sometimes the term RISC is used for both, siRNAs and miRNAs. It is possible that a common core exists, which can associate with a variety of accessory proteins. The main components of the complexes containing siRNAs or miRNAs are Argonaute proteins, which are able to bind the 2 nt 3' overhang of small RNAs via their PAZ domain. The Argonaute family consists of highly basic proteins of ~100 kD in size, containing PAZ and PIWI domains. They can be subdivided in PIWI and EIF2C/AGO proteins. In mammals, four Ago proteins exist (Ago1-4), which are expressed in various adult tissues including the nervous system. Ago2 is the only member having slicer activity and is therefore capable of cleaving siRNA/miRNA-mRNA duplexes (Meister et al. 2004). All four Ago proteins associate with miRNAs and are involved in translational repression.

In addition to Ago family members, other proteins have been identified to associate with the RISC/miRNPs: Fragile-X mental retardation protein (FMRP), known as a translational inhibitor (Jin et al. 2004) and its *Drosophila* homologue Fragile-X-related protein (dFXR), vasa intronic gene (Caudy et al. 2002), tudor staphylococcal nuclease (Caudy et al. 2003), R2D2 (Liu et al. 2003) as well as members of the Gemin family (Mourelatos et al. 2002). Further identified as RISC-associated proteins contributing to translational repression were armitage/MOV10, a

putative RNA helicase (Tomari et al. 2004) and RCK/p54, a DEAD-box helicase (Chu and Rana 2006). Depletion of either of them from mammalian cells impairs gene silencing by miRNAs. From two other RISC components, Dicer and TRBP, involved in production of miRNAs and siRNAs from precursor molecules, only TRBP contributes to RISC function (Haase et al. 2005). Finally, the eukaryotic initiation factor (eIF) 6 also accounts for translational repression and is discussed in detail later.

1.1.3 FUNCTION OF MIRNAS

1.1.3.1 TRANSLATIONAL REPRESSION AND MRNA DEGRADATION

The exact mechanism by which miRNAs can down-regulate translation is currently under extensive investigation and the results obtained so far are controversial (reviewed in Filipowicz et al. 2008; Wu and Belasco 2008, pointed out in Figure 1.2). First studies involving sucrose density-gradient centrifugation revealed a shift of targeted mRNAs to translationally active polysomes of lower mass, meaning fewer ribosomes per message. This would suggest an inhibition at the initiation of translation (Pillai et al. 2005). Further studies showed that Ago has cap-binding ability and can therefore compete with eIF4E for binding the cap structure of the mRNA, resulting in inhibition of translation initiation (Kiriakidou et al. 2007). Another mechanism proposed is the prevention of 60S ribosomal subunit joining (Chendrimada et al. 2007). It was reported, that eIF6 and 60S ribosomal subunits co-purify with the Ago-Dicer-TRBP complex. eIF6 was initially identified to interact with the 60S subunit and thereby preventing its interaction with the 40S subunit (Russell and Spremulli 1978). The partial depletion of eIF6 in human cells and *C. elegans* rescued mRNA targets from miRNA inhibition.

Other groups, however, have found no change in the polysome profile of targeted messages combined with the evidence that miRNAs can also repress cap-independent translation via an internal ribosomal entry site (IRES). These results rather suggest inhibition after initiation, at the elongation step (Maroney et al. 2006; Nottrott et al. 2006; Petersen et al. 2006). The inhibition could take place either through slowed elongation or ribosome 'drop-off'. A third possibility displays the degradation of the nascent peptide (Nottrott et al. 2006).

Independent of translational inhibition, deadenylation and subsequent degradation of miRNA targets was shown. Binding of the miRNPs can lead to the deadenylation of the mRNA by the deadenylase CCR4-NOT. This initiates the 5' decapping by loss of poly(A)-binding proteins, exposing the message to exonucleolytic digestion from the 5' end (Giraldez et al. 2006; Wu et al. 2006).

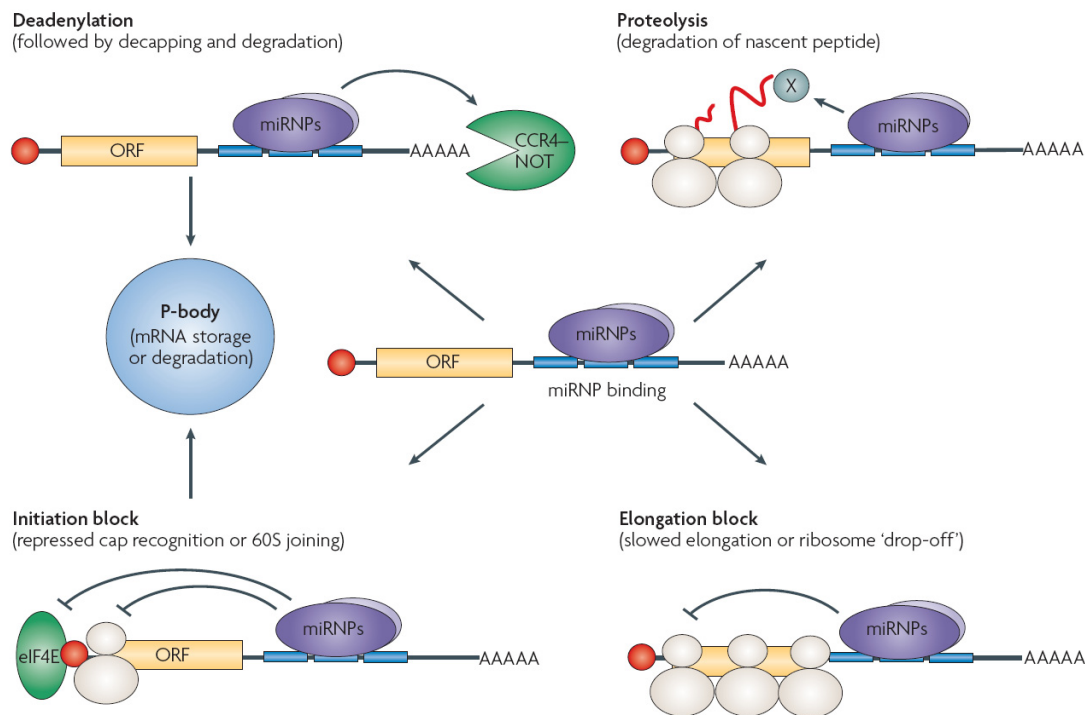


Figure 1.2 – Putative functions of miRNAs in the cell

miRNAs can repress translation either by inhibition at the initiation or elongation step, but can also cause proteolysis of the nascent peptide. Another effect of miRNPs is the degradation of the mRNA, triggered by deadenylation and decapping. (from Filipowicz et al. 2008)

1.1.3.2 TRANSLATIONAL ACTIVATION

Although miRNAs have long been thought to only down-regulate protein synthesis, new data indicate that they can also stimulate translation under certain conditions (Vasudevan and Steitz 2007; Vasudevan et al. 2007). Thus, a miRNA that inhibits translation in proliferating mammalian cells can have the opposite effect after cell-cycle arrest caused by serum starvation or treatment with the replication inhibitor aphidicolin. This effect depends on binding of the miR-369-3 to the 3'-untranslated region (UTR) of the target mRNA, in this case the tumor necrosis factor- α (TNF α) mRNA. The same serum starvation dependent up-regulation was shown for targets of miRNA let-7 and the artificial miRNA cxc4. The main protein involved is FXR1. Together with Ago2, it mediates the positive effect on translation of the targeted mRNA by miRNA-dependent binding to AU-rich elements (ARE) in the TNF α 3'-UTR. Moreover, compared to Ago2, which can associate with target mRNAs under both conditions (repression and activation), FXR1 does so only in non-dividing cells. These findings lead to a very intriguing model that miRNPs and RBPs might act synergistically to either repress or activate mRNA translation.

1.1.3.3 RELIEF OF MIRNA-MEDIATED REPRESSION

Another possibility for fine-tuning or regulating miRNA function is the relieve of miRNA-mediated repression. Work by Bhattacharyya and others showed that in human hepatoma cells, *cationic amino acid transporter 1 (CAT1)* mRNA is translationally repressed by the liver-specific miR-122 (Bhattacharyya et al. 2006). Upon stress, this repression is relieved by binding of the RBP HuR, to the 3'-UTR of *CAT1* and subsequent re-entry of the mRNA into translating polysomes. HuR belongs to the family of embryonic lethal abnormal vision (ELAV) proteins, recognizes AU-rich elements and was implicated in modulation of mRNA translation and stability (Brennan and Steitz 2001).

Recently, Kedde and colleagues provided evidence that the RBP Dead end (Dnd1) is able to block the interaction with miRNAs by binding target mRNAs and therefore relieves the repression (Kedde et al. 2007). Experiments in human teratoma cells showed that down-regulation of endogenous Dnd1 reduces the expression of a reporter gene, depended on the presence of functional miRNA-binding sites. In zebrafish, Dnd1 counteracts the inhibition of *nanos* mRNA by miR-430. The group proposed a model, where Dnd1 binds to U-rich regions in the 3'-UTR and either physically blocks access of a miRNA to its binding site or changes the subcellular localization of the mRNA.

Other examples for the relief of miRNA-mediated translational repression have been reported in neurons and are discussed later.

1.1.4 MIRNAS IN THE NERVOUS SYSTEM

The nervous system is a rich source of miRNAs with a diversity of functions that affect a large number of neuronal genes. To date, many miRNAs have been found to play a role in developmental processes (reviewed in Kosik 2006). For example, miRNAs are encoded within the Homeobox (Hox) gene cluster, which determines a distinct protein patterning along the anterior-posterior axis during *Drosophila* development (Pearson et al. 2005).

Another process is the establishment and maintenance of cell identity: miRNA-124a and miR-9 are implicated in the decision of mouse neuronal precursor cells to adopt either neuronal or glial fate and can shift the proportion of differentiating cells into the direction of neurons (Krichevsky et al. 2006). Also in the axonal path-finding, miRNAs were shown to have a function: In zebrafish, axon guidance abnormalities were associated with defects in Dicer function (Giraldez et al. 2005). Furthermore, functional RISC (composed of Ago3, Ago4, Dicer and FMRP) is present in developing axons of cultured rat neurons (Hengst et al. 2006).

1.1.4.1 DENDRITIC MIRNAS AND SYNAPTIC PLASTICITY

Long-lasting memory formation requires new protein synthesis (Montarolo et al. 1986; Davis and Squire 1984). Furthermore, to date, an activity-dependent translation of several mRNAs has been shown in neurons (Aakalu et al. 2001). Therefore, based on the current knowledge about miRNA functions, it is very tempting to hypothesize a role of miRNAs in regulating local protein translation at the synapse.

First support for this hypothesis came from the finding that miR-134 regulates the expression of *LIM-domain kinase 1* (*Limk1*) mRNA at the synapse (Schratt et al. 2006). miR-134 is expressed in the hippocampus and *in situ* hybridization shows a punctate pattern in dendrites of cultured hippocampal neurons. Previously, *Limk1* was reported to affect the spine structure by regulating actin filament dynamics through inhibition of the actin depolymerizing factor cofilin (Bamburg 1999). When *Limk1* mRNA is translationally repressed by binding of miR-134 (at a single binding site), the dendritic spine size is negatively regulated. Upon synaptic stimulation by brain-derived neurotrophic factor (BDNF), the activated TrkB/mTOR signaling pathway relieves the miR-134-mediated repression and leads to enhanced *Limk1* protein synthesis and spine growth. At the same time, miR-134 shifts to the polysome-associated pool of mRNAs (unpublished observation), suggesting that miR-134 itself may not dissociate from the *Limk1* mRNA to allow for its translation. BDNF could therefore alter the activity of some other translational regulators in this complex (Schratt et al. 2006).

In an interesting related study, the expression of miR-132 was found to be regulated by BDNF, which functions through the activation of the transcription factor cAMP-response element binding protein (CREB) (Vo et al. 2005). A computational search predicted the GTPase-activating protein P250GAP, which regulates the Rho family, as a target of miR-132. Both miR-132 overexpression and knock-down of P250GAP expression induced neurite outgrowth in transfected rat primary cortical neurons, a phenocopy of the effects of ectopic CREB activity. Taken together, these observations indicate that CREB functions through the miR132-mediated silencing of P250GAP to promote neurite growth.

Latest data show that RISC indeed acts at the synapse at least in *D. melanogaster* (Ashraf et al. 2006). Synaptic protein synthesis was measured using a fluorescent reporter of calcium/calmodulin-dependent protein kinase II α (CaMKII α). Thereby protein synthesis of CaMKII α but also of Staufen (*Stau*) and Kinesin Heavy Chain (KHC) was found to be dependent on Armitage (named MOV10 in mammals), a protein required for RISC function. Proteasome-mediated degradation of Armitage upon external stimulation of olfactory

neurons in *D. melanogaster* led to the relief of suppression followed by *CaMKII α* mRNA translation. The group concluded that degradative control of the RISC pathway underlies the pattern of synaptic protein synthesis associated with a stable memory.

Taken together with the fact that many miRNAs are specifically expressed in the brain and three of the four mammalian ELAV proteins, HuB, HuC and HuD are restricted to neurons, it is likely that reversible miRNA-mediated regulation has an important role in brain development and function (Filipowicz et al. 2008). An overview how miRNAs regulate protein expression in neurons is shown in Figure 1.3.

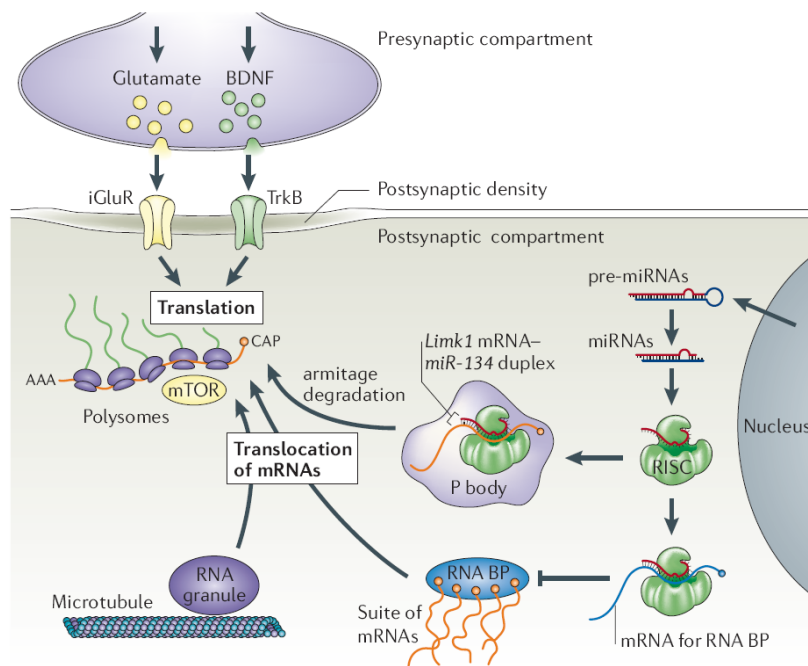


Figure 1.3 – miRNA-mediated effects at the synapse

Synaptic stimulation by glutamate or BDNF affects the translation of mRNAs in dendritic spines. Translational repression can take place in P-bodies, RNA granules or RBP platforms. Reactivation of translation might be controlled by the degradation of Armitage as well as release of mRNA cargo following synaptic stimulation. (from Kosik 2006)

Linking the miRNA-mediated translation to synaptic stimulation leads to the following model: A miRNA-mRNA duplex (e.g. miR-134/*Limk1* mRNA) can translocate from the so-called processing bodies (P-bodies), where translation is repressed, to polysomes. Other means of release of silenced mRNAs in dendrites include RNA granules, which can release their mRNA cargo following synaptic stimulation, or RBP-platforms, which are capable of carrying a suite of mRNAs (Kosik 2006). Reactivation of translation might be controlled by the degradation of Armitage. The stimulation of the ionotropic glutamate receptors (iGluR) by glutamate or of TrkB receptors by BDNF affects the translation of specific mRNAs in dendritic spines.

An important question left is how miRNAs are transported to the dendrite. One possibility is that they hitch-hike on a target mRNA that contains dendritic localization signals. Alternatively, dendritic miRNAs might be processed from pre-miRNAs in the dendrite. This

mechanism would require the independent transport of pre-miRNAs to the dendritic spines as well as the presence of RISC and Dicer at the synapse (reviewed in Kosik 2006).

By combining laser-capture and multiplex real-time reverse transcription (RT) PCR, Kye and colleagues were able to quantify miRNAs in the neuritic and somatic compartment separately. Most neuronal miRNAs were detected in dendrites (Kye et al. 2007); for some miRNAs *in situ* hybridization was performed, showing a granular staining for miR-26a, 92, 124a, let-7d. In the same study, the mRNA for the microtubule-associated protein 2 (MAP2) was validated as target mRNA for miR-26a.

1.2 RNA GRANULES

Different classes of RNA granules have been identified. They differ in their protein composition and function (Anderson and Kedersha 2006). Two of them, P-bodies and neuronal granules (e.g. transport RNPs) are discussed in more detail here.

1.2.1 PROCESSING BODIES

P-bodies contain components of the 5'-3' mRNA decay machinery, of the nonsense-mediated decay (NMD) pathway and factors involved in miRNA-guided translational silencing (Anderson and Kedersha 2006). The core components are conserved from yeast to mammals, including the decapping enzyme complex DCP1–DCP2, the decapping activators RCK/p54, Pat1, RAP55 and EDC3 and the heptameric Lsm1–7 protein complex. P-bodies also contain other mRNA decay enzymes: the deadenylase complex CAF1–CCR4–NOT and the 5'-3' exonuclease XRN1. They lack ribosomes and all translation initiation factors with the exception of eIF4E (Filipowicz et al. 2008; Anderson and Kedersha 2006).

P-bodies are considered as storage sites of translationally repressed mRNAs, including those repressed by miRNAs, as well as a place of mRNA degradation (Anderson and Kedersha 2006). In general, these mRNAs are not associated with ribosomes. Indeed, ribosomes and P-bodies compete for mRNAs and repression of translation initiation may be sufficient to target mRNAs to P-bodies. Upon specific signals, such repressed mRNAs can even be released into the cytoplasm for further translation (Sossin and DesGroseillers 2006).

Different hypotheses linking miRNA-mediated repression and P-bodies in mammals have been formulated (Wu and Belasco 2008). Either it is the ability of miRNAs to direct target messages to P-bodies what contributes to their effect on translational repression or, more likely, P-bodies represent a transient depot for silenced mRNAs until further use.

1.2.2 NEURONAL GRANULES

Neuronal transport RNPs harbor translationally silenced mRNAs that are transported to dendritic synapses, where they are released and translated in response to specific exogenous stimuli. They consist of mRNAs, small and large ribosomal subunits, translation initiation factors and RBPs that regulate mRNA function. Despite the presence of intact ribosomes, it is important to note that translation is repressed in these structures until they arrive at the synapse, where translation may require an activating stimulus (Anderson and Kedersha 2006).

Different components have been identified in neuronal granules (reviewed in Kiebler and Bassell 2006; Sossin and DesGroseillers 2006). KIF5 motor protein, which is involved in their transport to the dendrites, several RNA-binding proteins such as Stau1 and 2, FMRP, ZIP-code binding protein 1 (ZBP1) and other *trans*-acting factors. The mechanism how mRNAs are silenced in RNA granules is still under intense investigation. One option is repression through RBPs: β -actin mRNA is silenced during transport via ZBP1, but also FMRP was shown to be involved in mRNA translational repression *in vitro* and *in vivo* (Hüttelmaier et al. 2005; Zalfa et al. 2006). Another possibility is silencing through miRNAs, e.g. *Limk1* by miR-134 in mammals (see above) and *CaMKII α* mRNA in *D. melanogaster* (Schratt et al. 2006; Ashraf et al. 2006).

1.2.2.1 THE STAUFEN FAMILY

Staufen belongs to the family of dsRBPs, which contain three to five copies of the dsRBDs. In the *Drosophila* oocyte, Staufen plays an important role in localization of *bicoid* and *oskar* mRNAs to the anterior and posterior pole, respectively (reviewed in St Johnston 2005).

In mammals, there are two Staufen genes that encode two distinct Staufen proteins, Stau1 and Stau2 (Wickham et al. 1999; Duchaine et al. 2002). Stau1 is ubiquitously expressed whereas Stau2 is mainly present in the nervous system. Moreover, two isoforms for Stau1 and four isoforms for Stau2 are generated through alternative splicing (Monshausen et al. 2001; Duchaine et al. 2002). Both Staufen proteins are predominantly found in the cytoplasm around the perinuclear region and are associated with the endoplasmic reticulum. In hippocampal neurons, Staufen proteins additionally appear within distinct RNA-containing particles reaching up to the distal dendrites (Kiebler et al. 1999; Duchaine et al. 2002).

Subsequent work showed, that Staufen-containing RNPs move along microtubules from the cell body into dendrites, suggesting a functional role of Staufen proteins in the dendritic localization of mRNAs (Köhrmann et al. 1999).

1.3 RNA LOCALIZATION IN NEURONS

RNA localization is necessary in many different cell types and organisms during various biological processes. Neurons are highly polarized cells, containing long protrusions and forming a large number of synapses. Therefore, in the nervous system, the localization of RNAs plays an important role both during development (outgrowth and guidance of growth cones) and in the adult organism (for modification of synapses undergoing plasticity during learning).

An important question is why localization of RNAs rather than of proteins to specific compartments is more advantageous to the cell. First, localization of RNAs and their local translation is believed to contribute to synapse-specific modifications. Other reasons are based on efficiency: local translation abolishes the need of regulating the activity of the proteins before they reach their target region. Furthermore, it makes it possible to regulate expression independently in different regions of the cell. Overall RNA transport provides additional spatial control and leads to a faster and more economical protein production (Dahm et al. 2007).

Several steps are important in RNA localization, which are summarized in Figure 1.4. First, the RNA is processed in the nucleus. During this process, *cis*-acting sequence elements are recognized by RBPs, "labeling" the RNA for subsequent localization. Second, after the nuclear export other factors bind to obtain a fully competent cytoplasmic RNP. Third, the RNP associates with motors mediating its transport along microtubules. One example is ZBP2 which associates with β -actin mRNA in the nucleus and facilitates its cytoplasmic localization. In the cytoplasm, β -actin mRNA RNPs are remodeled recruiting ZBP1 and then transported to neurites or growth cones (Gu et al. 2002; Zhang et al. 2001). During transport, mRNAs are translationally silenced. Fourth, following activation at the synapse, the protein is made by local translation and contributes to synaptic plasticity (Dahm et al. 2007).

Localized RNAs contain *cis*-acting localization elements (LEs), recognized by RBPs. These LEs are generally present in the 3'-UTR. In the nervous system, LEs are found in e.g. the mRNAs for the immediate-early gene arg 3.1 (Arc) as well as β -actin, CaMKII α , MAP2 and myelin basic protein (MBP). Also non-coding RNAs were found to be localized, e.g. brain cytoplasmic 1 (BC1) RNA and miRNAs (reviewed in Dahm et al. 2007).

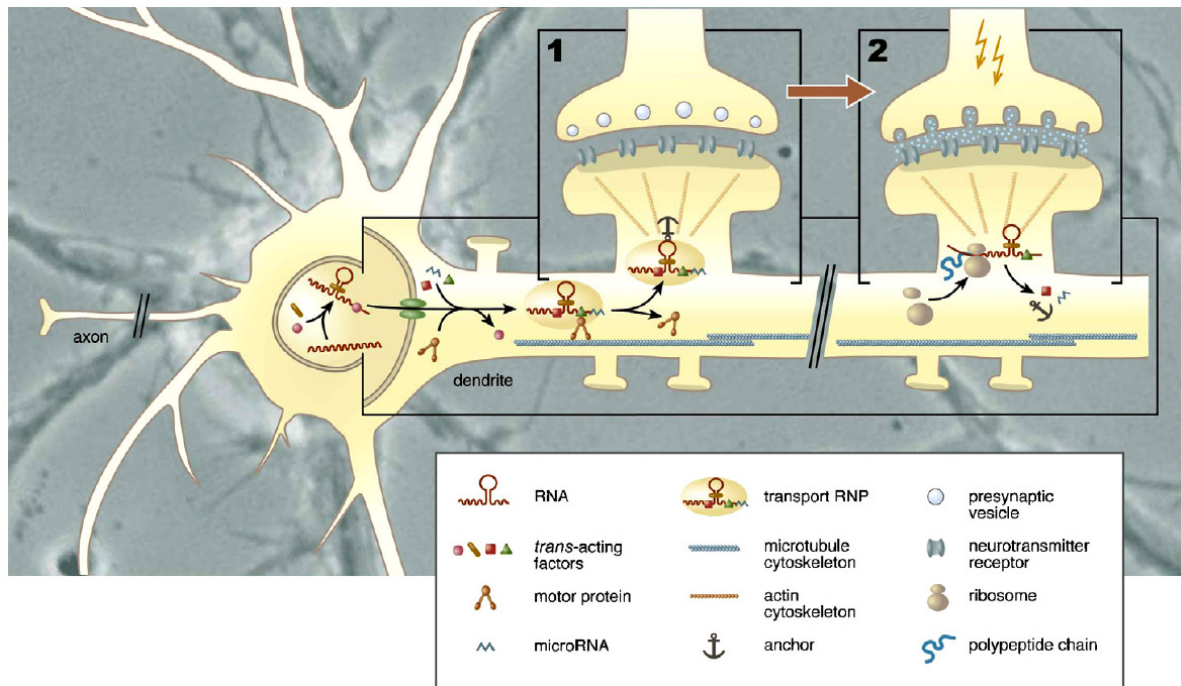


Figure 1.4 - RNA localization in mammalian neurons

After processing of the RNA in the nucleus it is recognized by RBPs and exported to the cytoplasm. A fully competent RNP is obtained upon binding of additional factors. This RNPs associate with motor proteins mediating their transport via microtubules. Important to note is that mRNAs are translationally silenced during transport. Synaptic activation leads to local translation, thereby contributing to synaptic plasticity. (from Dahm et al. 2007)

1.4 AIM OF THE PROJECT

Different studies indicate an involvement of Stau2 in the formation of long-term memory (Dubnau et al. 2003; Ashraf et al. 2006). Dubnau et al. reported an involvement of the pumilio/staufen pathway in *Drosophila* long-term memory (Dubnau et al. 2003). Based on a genetic screen, *in vivo* disruption of Staufen yielded defective memory. In the study by Ashraf and colleagues described in section 1.1.4.1, *Drosophila* Staufen protein was found to be subjected to miRNA-dependent regulation. Upon degradation of Armitage, a RISC-associated factor, protein synthesis of Staufen increases, which may facilitate the synaptic transport of mRNAs (Ashraf et al. 2006). However, a detailed understanding of the function of Stau2 in mammals is still missing.

The composition of Stau-containing particles in rat brain is currently investigated in the Kiebler lab (Mallardo et al. 2003; D. Karra and M. Kiebler, in preparation). Previously, it was shown that Stau2, if mutated in the RBD3, accumulated in the nucleolus in contrast to the

prominent cytoplasmic localization of the wild-type protein (Macchi et al. 2004). Furthermore, Macchi and colleagues found that the export of Stau2 out of the nucleus is dependent on Exportin-5, which is the main export factor for pre-miRNAs. Exportin-5 was shown to interact *in vitro* with RBD3 of wild-type Stau2 in an RNA-dependent manner but not with mutated Stau2. Upon down-regulation of Exportin-5, the largest isoform (62 kD) of Stau2 accumulates in the nucleolus (Macchi et al. 2004). Stau2 was shown to bind dsRNA in a sequence independent manner but rather interacts with stem-loops containing 12 uninterrupted base pairs *in vitro* (Ramos et al. 2000). Since pre-miRNAs are folded into hairpin structures, this work suggested for the first time a possible link between Stau2 and the generation of miRNAs.

In the *Drosophila* oocyte, Stau2 plays an important role in localization of *bicoid* and *oskar* mRNAs (St Johnston 2005). In addition, an involvement of Stau in translational activation of *oskar* mRNA in *D. melanogaster* was also shown (Micklem et al. 2000). However, the exact function of Stau2 in mammals remains to be investigated.

As described in section 1.3, localized mRNAs are thought to be silenced during transport. This could be achieved either by proteins and/or by miRNAs. The only evidence for functional dendritic miRNAs to date, is the regulation of *Limk1* by miR-134 at the synapse, which was shown to have an effect on spine growth. Based on these findings, it was of great interest for my project to investigate whether small non-coding RNAs (especially miRNAs) are part of Stau2-containing complexes in rat brains.

Furthermore, by combining data from the mRNA composition of Stau2 particles (A. Konecna and M. Kiebler, unpublished) with data on small RNAs, new pairs of mRNA-miRNA are expected to be identified. This could then lead to a detailed understanding of miRNA-mediated silencing of mRNAs during transport with regards to how many and which mRNAs are regulated by miRNAs.

2 MATERIALS AND METHODS

2.1 MATERIALS

2.1.1 REAGENTS AND CONSUMABLES

Reagents

Acrylamide mix, 30%	Roth
Acetic acid	Roth
Acetone	Roth
Adenosine triphosphate (ATP)	Fluka
Agar	Sigma
Agarose	Roth
Ammonium peroxodisulfate (APS)	Roth
Ampicillin	Roth
β -Mercaptoethanol	Sigma
Bovine serum albumin (BSA)	Serva
Bromphenol blue	Serva
Coomassie Brilliant blue	Merck
Deoxycholate (DOC)	Sigma
Detector TM Block	KPL
Dialysis membrane MWCO 6-8000	SpectraPor
Diethyl pyrocarbonate (DEPC)	Sigma
Dimethylpimelimidate dihydrochloride (DMP)	Sigma
DL-Dithiothreitol (DTT)	Sigma
Ethanol, absolute	Roth
Ethanol, technical	Roth
Ethanolamine	Sigma
Ethidium bromide	Fluka
Ethylenediaminetetraacetic acid (EDTA), disodium salt	Sigma
Filter, 0.45 μ m	Schleicher & Schuell
Filter, Steritop 0.2 μ m	Millipore
Formaldehyde, 37%	Roth

GeneRuler™ 1 kb DNA Ladder (0.5 µg/µl)	Fermentas
GeneRuler™ 100 bp DNA Ladder (0.5 µg/µl)	Fermentas
Glutardialdehyde	Roth
Glutathione Sepharose™ 4 Fast Flow (GSFF)	GE
L-Glutathione, reduced	Sigma
Glycerol	Sigma
Glycine	Merck
2-[4-(2-Hydroxyethyl)-1-piperazinyl]-ethanesulfonic acid (HEPES)	Sigma
Hydrochloric acid, 37%	Roth
Isopropanol (2-Propanol)	Roth
Isopropylthiogalactoside (IPTG)	Roth
Leupeptin	Serva
Loading Dye Solution, 6x	Fermentas
MagneGST Glutathione particles	Promega
Magnesium chloride	Fluka
Methanol, technical	Roth
Methanol	Roth
N,N,N',N'-Tetramethylethylenediamine (TEMED)	Roth
Nitrocellulose membrane, 0.22 µm	Schleicher & Schuell
Nonidet™ P 40 Substitute (NP-40)	Sigma
O'GeneRuler™ DNA Ladder, low range (0.1 µg/µl)	Fermentas
Orange Loading Dye Solution, 6x	Fermentas
PageRuler™ Prestained Protein Ladder	Fermentas
PBS Dulbecco, w/o Ca ²⁺ Mg ²⁺	Biochrom
Pefabloc (AEBSF)	Roche
Pepstatin	Roche
Ponceau S	Merck
Potassium acetate	Merck
Potassium chloride	Sigma
Precision Plus Protein™ All Blue Standard	Bio-Rad
Protease inhibitor cocktail tablets, EDTA free	Roche
Protein A Sepharose (from Staph. aureus)	Sigma
Protein Assay Dye Reagent Concentrate	Bio-Rad
RiboLock Ribonuclease Inhibitor 40 u/µl	Fermentas
Ribonuclease A	Sigma

RNase A + T mix	Fermentas
Sephacryl S300-High Resolution	Amersham Pharmacia
Silver nitrate	Merck
Sodium acetate	Merck
Sodium azide	Roth
Sodium chloride	Merck
Sodium dodecylsulfate (SDS)	Serva
Sodium hydroxide	Merck
Sucrose	Sigma
SYBR [®] GOLD nucleic acid stain	Invitrogen
Trichloric acid (TCA)	Merck
Tris(hydroxymethyl)aminomethane (Tris)	Roth
Triton X-100	Roth
Trizma hydrochloride	Sigma
Tryptone	Roth
Tween 20	Roth
Vivaspin Concentrator (10 kD MWCO)	Vivascience
Vivaspin Concentrator (50 kD MWCO)	Vivascience
Whatman chromatography paper	Multimed
Yeast extract	Roth
Yeast tRNAs	Roche

RNA grade reagents

Acid Phenol:Chloroform, MB grade	Ambion
Acrylamide/Bis (19:1), 40%	Ambion
Ammonium peroxodisulfate (APS)	Roth
Cytidine 3',5'-bis [α - ³² P] phosphate (pCp) (10 mCi/ml; 3000 Ci/mmol)	GE
Dimethyl sulfoxide (DMSO)	Sigma
Formaldehyde, 37%	Merck
Formamide (deionized)	Ambion
Gel loading buffer II	Ambion
Glycogen, RNA grade (20 mg/ml)	Fermentas
Magnesium chloride for molecular biology, 1 M	Sigma

MicroSpin G-25 columns	GE
Morpholinopropane sulfonic acid (MOPS)	Serva
N,N,N',N'-Tetramethylethylenediamine (TEMED)	Roth
Non-stick RNase free tubes	Ambion
Imaging Screen K, 20x25 cm	Biorad
2-Propananol, for molecular biology, min 99%	Sigma
RNase ZAP	Sigma
Sodium acetate pH 5.5, 3 M	Ambion
Sodium chloride for molecular biology, 5 M	Sigma
Sodium dodecyl sulfate (SDS) 10%	Sigma
10x TBE electrophoresis buffer	Fermentas
Top Vision LE GQ Agarose	Fermentas
Trizma hydrochloride solution	Sigma
Urea	Ambion
Water, DNase + RNase free	Sigma

Kits

Molecular Weight marker kit, for GF chromatography,	Sigma
GenElute™ Plasmid MiniPrep Kit,	Sigma
QIAquick Gel Extraction Kit,	Qiagen
2x Rapid Ligation Kit,	Promega
QIAquick PCR purification Kit,	Qiagen
<i>miVana</i> ™ miRNA Isolation Kit,	Ambion
<i>miVana</i> ™ qRT-PCR miRNA Detection Kit,	Ambion

2.1.2 ENZYMES

DNase I	Boehringer Mannheim
Lysozyme	Sigma
BamHI (10 u/μl) + buffer	Fermentas
EcoRV (20 u/μl) + buffer/BSA	NEB
NotI (10 u/μl) + buffer	Fermentas
SalI (10 u/μl) + buffer	Fermentas
T4 RNA Ligase (10 u/μl)	Fermentas
T4 DNA Ligase (3 u/μl)	Promega
Taq DNA polymerase (5 u/μl)	Fermentas

2.1.3 ANTIBODIES

Rabbit anti-Stau2_{FL} (rabbit H7) 1:1000 (WB)

Antigen: His-Stau2_{FL}

Generated by Dipl.-Biol. Daniela Karra (Kiebler Lab), see D. Karra, 2008, PhD thesis

Rabbit anti-Stau2_{CT} (rabbit R) 1:1000 (WB)

Antigen: GST-Stau2_{CT}

Generated by Dr. Anke Deitinghoff (Kiebler Lab)

Primary antibodies for Western blotting

Ag	size (kD)	species	dilution	company
Upf1	130	goat	1:500	Abcam
Ago2	95	Mab	1:250	Abnova
PACT	36	rabbit	1:1000	Dr. G. Meister
eIF6	26	Mab	1:1000	BD Transduction Labs
FMRP	70 – triple band	mouse	1:500	Chemicon
eEF1a	53	Mab	1:1000	Biomedica
eIF4E	25	Mab	1:1000	BD Transduction Labs
S6	32	Mab	1:500	Cell signaling
L7a	34	rabbit	1:5000	Prof. Dr. A. Ziemiecki

2.1.4 PLASMIDS AND PRIMERS

pGEX vectors (GST Gene Fusion System): pGEX-4T-2 and pGEX-6P-1, GE Healthcare

resistance: ampicillin

pGEX-4T-2 containing Stau2_{CT} (Thr 379 until stop 512), inserted at NotI/SalI sites

resistance: ampicillin

from Dr. L. DesGroseiller, University of Montreal, Canada

GST-3C (PreScission protease):

containing N-terminally GST-tagged 3C (PreScission) protease

resistance: ampicillin

from Andi Geerlof at the EMBL outstation in Hamburg

Primers for RT-PCR (Ambion)

hsa-miR-18 (AM 30065)

hsa-miR-26a (AM 30123)

hsa-miR-128a (AM 30026)

hsa-miR-134 (AM 30034)

hsa-let-7c (AM 30002)

2.1.5 ANIMALS

Animals were obtained from the Medical University Vienna, Core Unit of Biomedical Research, Division of Laboratory Animal Science and Genetics, Himberg

Rats (*Rattus norvegicus domesticus*) Strain: Him:OFA Sprague-Dawley (SD)

Adult: 9-11 weeks old, pregnant female rats

E17: embryos (E17) from adult rats (brains used for biochemistry were missing the hippocampi)

Brains were removed by Sabine Thomas, John Vessey, Julia Riefler and Krzysztof Wieczorek

Rabbits, mast hybrids, New Zealand White Basis
used for antibody production

2.1.6 CELLS

BL21 (DE3) pLysS: F⁻, *ompT hsdS_B (r_B⁻ r_B⁻) gal dcm* (DE3); pLysS (cam^r), Invitrogen

TOP 10, F⁻ *mcrA Δ(mrr-hsdRMS-mcrBC) φ80/lacZΔM15 ΔlacX74 recA1 araD139 Δ(araIeu)*

7697 *galU galK rpsL* (Str^r) *endA1 nupG*, Invitrogen

2.1.7 BUFFERS AND SOLUTIONSMolecularbiology and cloning

50x TAE (2 l)

484 g Tris base

114.2 ml acetic acid

200 ml EDTA (0.5 M, pH 8.0)

Adjust pH to 7.5 - 7.8

1x TAE

dilute from 50x TAE

Expression and purification of proteins

2x YT (for 200 ml)	3.2 g tryptone 2 g yeast extract 1 g NaCl Autoclave
LB (for 1 l)	10 g tryptone 5 g yeast extract 10 g NaCl Autoclave
PBS Dulbecco, w/o Ca ²⁺ Mg ²⁺	140 mM NaCl 2.7 mM KCl 16 mM disodium hydrogen phosphate 1.8 mM potassium dihydrogen phosphate Adjust pH to 7.1 with HCl

PreScission protease

Lysis Buffer	50 mM TrisHCl, pH 8.0 200 mM NaCl 1 mM DTT 1 ST Lysozyme and DNase I
Wash Buffer	50 mM TrisHCl, pH 8.0 300 mM NaCl 1 mM DTT
Elution Buffer	50 mM TrisHCl, pH 8.0 200 mM NaCl 1 mM DTT 10 mM L-glutathione reduced
Dialysis Buffer	50 mM TrisHCl 200 mM NaCl 1 mM DTT

10 mM EDTA
20% glycerol
adjust pH to 8.0

Stau2 proteins

Lysis Buffer 50 mM Tris pH 7.5
 500 mM NaCl
 0,1% TritonX-100 – add after resuspension of the cells
 2 mM DTT
 8% glycerol
 Lysozyme 1 mg/ml final
 Protease inhibitors: Pefablock, Leustatin, Pepstatin; 1x

ATP/MgCl₂ buffer 10 mM ATP
 10 mM MgCl₂ in water

Dialysis Buffer (GST-Stau2_{CT}) PBS

Dialysis Buffer (Stau2_{CT}) PBS + 8% glycerol

Buffer A 50 mM Tris pH 7.5
 8% glycerol

Buffer B Buffer A + 20 mM glutathione, set pH to 8

Cleavage Buffer 50 mM TrisHCl, pH 7.0
 150 mM NaCl
 1 mM DTT
 1 mM EDTA

Analysis of proteins

Minigels, 0.75 mm:

	Separation gel (5 ml/gel)		Stacking gel (2 ml/ gel)	
	10% [ml]	12% [ml]		4% [ml]
H ₂ O	1.9	1.6	H ₂ O	1.4
30% acrylamide	1.7	2.0	30% acrylamide	0.33
1.5 M Tris pH 8.8	1.3	1.3	1 M Tris pH 6.8	0.25
10% SDS	0.05	0.05	10% SDS	0.02
	Mix well			Mix well
10% APS	0.05	0.05	10% APS	0.02
TEMED	0.002	0.002	TEMED	0.002

6× Laemmli-buffer (SDS-PAGE): 10% SDS
350 mM TrisHCl pH 6.8
30% glycerol
0.1% Bromphenol blue
600 mM DTT

10x SDS running buffer 0.25 M Tris
1.92 M glycine
1% SDS

Coomassie staining solution 0.1% Coomassie Brilliant Blue
40% methanol
10% acetic acid

Coomassie destaining solution 40% methanol
10% acetic acid

Fixation solution (silver) 15 ml ethanol
5 ml acetic acid
Up to 50 ml water

Reducing and crosslinking (silver) 15 ml ethanol
3.4 g sodium acetate

	0.1 g sodium thiosulfate (5x H ₂ O) 0.25 ml glutaraldehyde (25%) Up to 50 ml water
Silver incubation	0.1 g silver nitrate 10 µl formaldehyde Up to 50 ml water
Developing solution (silver)	2.5 g sodium carbonate 10 µl formaldehyde Up to 100 ml water
10× Blotting buffer (Towbin)	250 mM Tris 1.92 M glycine
1× Blotting buffer	10% 10× blotting buffer 20% methanol 70% H ₂ O
Ponceau-S solution	0.2% Ponceau S 3% TCA in water
10× TBS	150 mM Tris 1.5 M NaCl Set pH to 7.5
TBS-T	1x TBS with 0.1% (v/v) Tween 20
Blocking solution (1x Detector TM Block)	0.2 g Detector Block powder 20 ml 5x Detector Block solution 80 ml water
 <i><u>Gel filtration</u></i>	
GF buffer	50 mM HEPES 150 mM KCl

pH 7.3, 0.22 µm filtered

Homogenization solution (HS) 10 mM HEPES pH 7.5
320 mM sucrose
1 tablet of protease inhibitor cocktail, Roche
2 µl RiboLock/ml

Immunoprecipitation

Tris buffer (for affinity purification) 250 mM NaCl
25 mM TrisHCl pH 8.5

4x BEB (brain extraction buffer) 100 mM HEPES pH 7.3
600 mM KCl
32% glycerol
0.4% NP-40

RNA methods

DEPC water ddH₂O including 0.1% of DEPC was constantly stirred for
6 h and subsequently autoclaved

10x TBE electrophoresis buffer

Diluted to 1x TBE 89 mM Tris
89 mM boric acid
2 mM EDTA

10x MOPS: 0.4 M MOPS
0.1 M NaAc (3x H₂O)
10 mM EDTA
adjust to pH 7.2 with NaOH

RNA loading dye mix 50% glycerol
10 mM EDTA
0.25% Bromphenol blue

2.1.8 EQUIPMENT

Thermomixer compact, Eppendorf

Vortex VF2 Janke & Kunkel IKA

pH Meter MP 225, Mettler Toledo

Shaker, GFL 3015

Waterbath, GFL

Incubator, shaking, INFORS, Unitron

Incubator, kelvitron t, Heraeus

Balance, KERN ABS

Balance, KERN 440-49N

GeneQuant Pro spectrophotometer, Amersham Pharmacia

Cuvette Suprasil, 10 mm, Hellma

Potter homogenizer, 557, 5ml, B.Braun, Melsungen

Ultrasound processor, UP 400s, dr. hielsche GmbH

BioLogic LP system and BioLogic BioFrac fraction collector

FPLC LCC-500, Pharmacia and Fraction collector Frac-200, Pharmacia LKB

Power Pac 300 power supply for electrophoresis, BIO-RAD

Power Pac HC power supply for electrophoresis, BIO-RAD

Mini-Protean[®] 3 Cell SDS-PAGE-System, BIO-RAD

Trans-Blot Cell blotting chamber, BIO-RAD

Infrared Imager Odyssey Li-Cor Biosciences

PCR-machine, PTC-200 Peltier Thermal Cycler, MJ Research

Peqlab imaging system with UV/IR interference filter type F590 or SYBR[®] photographic filter

Centrifuge 5417 C Eppendorf

Centrifuge 5417 R Eppendorf

Virifuge 3.OR Heraeus

Rotor Heraeus #8074

Centrifuge Avanti[™] J-25, Beckman Coulter

Rotor JLA 10.500, Beckman

Rotor JA 25.50, Beckman

Ultracentrifuge Optima[™] TXL, 120000 rpm, Beckman

Rotor TLA 100.3, Beckman with polycarbonate centrifuge tubes, 13x51 cm, Beckman

Molecular Imager[®] FX (+ Screen Eraser – K), BioRad

2.2 METHODS

2.2.1 MOLECULAR BIOLOGY

2.2.1.1 PREPARATION OF PLASMID DNA

Plasmid DNA (pDNA) was prepared using the GenElute™ Plasmid MiniPrep Kit from Sigma. Four ml of the o/n culture were used to pellet bacteria at 14,000 rpm for 5 min, 4°C. Lysis of the cells and pDNA purification was carried out as stated in the manufacturer's protocol. The elution of pDNA was performed in 50 - 70 µl ddH₂O, whereby the yield was increased by performing an incubation step in ddH₂O for 1 min before the final centrifugation. As a last step, DNA concentration was measured in a 1:20 dilution at 260 nm.

2.2.1.2 PREPARATION OF COMPETENT BL21 CELLS AND TRANSFORMATION

For o/n cultures, 5 ml of LB were inoculated with BL21 cells and grown at 37°C. The next day, 200 µl of the o/n culture were used to inoculate 10 ml of LB which was subsequently grown at 37°C until an OD₆₀₀ ~0.5. The cell suspension was chilled on ice for 10 min and centrifuged at 1,700 g for 8 min at 4°C. The pellet was resuspended in 10 ml of cold 0.1 M CaCl₂, which was prepared freshly and filter sterilized. After incubation on ice for 30 min, cells were pelleted again at 1,700 g for 8 min at 4°C, resuspended in 2 ml cold 0.1 M CaCl₂ and incubated for another 2 h on ice. The competent cells were distributed into 200 µl aliquots, frozen on dry ice and stored at -80°C.

Transformation

Competent cells were thawed on ice and mixed with 10 µl of ligation mix or 10 ng (1 µl) of pDNA. After incubation on ice for 30 min, a heat shock was performed at 42°C for 1 min. Afterwards, cells were chilled on ice for 2 min before incubation with 1 ml of LB at 37°C for 1 h shaking. In case of transforming a ligation mix, cells were pelleted at 950 g for 3 min, resuspended in 100 µl LB medium and plated on LB plates containing the appropriate antibiotics. For pDNA transformation, only 50 – 100 µl of the cell suspension were plated in the same way. Incubation was performed o/n at 37°C.

2.2.1.3 AGAROSE GEL ELECTROPHORESIS

Gels were prepared by dissolving the appropriate amount of agarose in 1x TAE. After cooling down the mixture by constant stirring, 20 µl of ethidium bromide (0.2 mg/ml) were added

per 100 ml of agarose solution. After pouring the gel, it was allowed to polymerize at RT. Samples were prepared by combining them with 6x LD and loaded onto the gel in combination with a suitable marker. Separation of DNA was performed in 1x TAE at 100 V constant.

2.2.2 CLONING OF *GST-STAU2_{CT}* INTO *PGEX-6P-2*

2.2.2.1 CLONING OF *PGEX-6P-2*

The pGEX-6P-2 vector was constructed from pGEX-6P-1 and pGEX-4T-2. The purpose was to combine the MCS of pGEX-4T-2 with the PreScission cleavage site from pGEX-6P-1, which yields pGEX-6P-2. The coding region for GST including the thrombin cleavage site was excised from pGEX-4T-2 with BamHI and EcoRV and replaced by the coding region for GST containing the PreScission cleavage site from pGEX-6P-1. Two successive restriction digestions were performed as follows.

1 st restriction	50 μ l	1 st restriction	50 μ l
PGEX-4T-2 pDNA	40 μ l = 6.2 μ g	PGEX-6P-1 pDNA	44 μ l = 7.0 μ g
ddH ₂ O	4 μ l	10x buffer BamHI	5 μ l
10x buffer BamHI	5 μ l	BamHI	10 u (1 μ l)
BamHI	10 u (1 μ l)		

In general, restriction digestions were incubated at 37°C for 1.5 h, then 0.5 μ l fresh enzyme was added and incubated for another 45 min at 37°C. The restriction digestion was purified from the previous buffer using the QiaQuick PCR purification kit. The pDNA was finally eluted in 46 μ l ddH₂O, 3 μ l were saved for test purposes and the resulting 43 μ l were subjected to a second round of restriction digestion.

2 nd restriction	50 μ l	2 nd restriction	50 μ l
PGEX-4T-2 pDNA (BamHI cleaved)	43 μ l	PGEX-6P-1 pDNA (BamHI cleaved)	43 μ l
10x buffer NEB3	5 μ l	10x buffer NEB3	5 μ l
100x BSA	0.5 μ l	100x BSA	0.5 μ l
EcoRV	20 u (1 μ l)	EcoRV	20 u (1 μ l)

Restriction digestions were performed as before. The restriction digestion (50 μ l) was separated by 1% agarose gel electrophoresis. The fragments for pGEX-4T-2 (3187 bp) as well as for pGEX-6P-1 (1798 bp) were excised from the gel and eluted using the QIAquick Gel Extraction Kit according to the manual. The final elution volume was 30 μ l of ddH₂O. For constructing the new pGEX-6P-2 the two fragments were ligated in the following way:

ligation	10 μ l
pGEX-4T-2 (BamHI, EcoRV cleaved)	2 μ l
pGEX-6P-1 (BamHI, EcoRV cleaved)	2 μ l
2x ligation buffer	5 μ l
T4 DNA Ligase	3 u (1 μ l)

The ligation was performed for 1 h at RT and the whole ligation mixture was transformed into 100 μ l TOP 10 competent cells. Seven colonies were randomly picked, grown o/n in 4 ml of LB amp and used for pDNA preparation. In order to find positive clones, a restriction digestion was performed as follows:

test restriction	15 μ l
PGEX-6P-2 pDNA	8 μ l
10x buffer O	1.5 μ l
ddH ₂ O	5 μ l
Sal I	5 u (0.5 μ l)

Restriction digestion was performed at 37°C for 2 h and analyzed by 1% agarose gel electrophoresis. The size of the linearized plasmids was compared to SalI digested pGEX-6P-1 vector to check for positive clones. For further cloning one of the positive clones was used.

2.2.2.2 CLONING OF *STAU2*_{CT} INTO PGEX-6P-2

The sequence corresponding to the C-terminal part of the mouse Staufen 2 protein (Thr 379 – stop 512) from pGEX-4T-2 (Duchaine et al. 2002) was cloned into pGEX-6P-2 using NotI/SalI restriction sites. Restriction digestions were performed as follows:

restriction	50 μ l
Stau2 _{CT} in pGEX-4T-2	43 μ l = 8.4 μ g
10x buffer O	5 μ l
NotI	10 u (1 μ l)
SalI	10 u (1 μ l)

restriction	50 μ l
pGEX-6P-2	40 μ l
ddH ₂ O	3 μ l
10x buffer O	5 μ l
NotI	10 u (1 μ l)
SalI	10 u (1 μ l)

The restriction digestions (50 μ l) were separated by 1% agarose gel electrophoresis. The fragments of pGEX-6P-2 (4985 bp) and Stau2_{CT} (734 bp) were excised from the gel and eluted using the QIAquick Gel Extraction Kit according to the manual. The final elution volume was 30 μ l of ddH₂O. The two fragments were ligated in the following reaction:

ligation	10 μ l
pGEX-6P-2 (NotI, SalI cleaved)	3 μ l
Stau2 _{CT} (NotI, SalI cleaved)	1 μ l
2x ligation buffer	5 μ l
T4 DNA Ligase	3 u (1 μ l)

Ligation was performed for 1 h at RT, afterwards 10 μ l ligation mix were transformed into 100 μ l TOP 10 competent cells. Eight colonies were randomly picked, grown o/n in 4 ml of LB amp and used for pDNA preparation. In order to find positive clones which contain the correct insert, a restriction digestion was performed as follows:

test restriction	15 μ l
Stau2 _{CT} in pGEX-6P-2	8 μ l
10x buffer O	1.5 μ l
ddH ₂ O	4.5 μ l
SalI	5 u (0.5 μ l)
NotI	5 u (0.5 μ l)

Restriction digestion was performed at 37°C for 2 h and analyzed by 1% agarose gel electrophoresis together with pGEX-6P-2 as a size control to check for positive clones. For

protein expression, the obtained mStau2_{CT} construct in pGEX-6P-2 was transformed into 200 µl BL21 competent cells and plated on LB amp plates o/n at 37°C.

2.2.3 EXPRESSION AND PURIFICATION OF PROTEINS

2.2.3.1 PURIFICATION OF GST-PRESCISSION PROTEASE

The protocol was developed by Andi Geerlof at the EMBL outstation in Hamburg.

Expression

For the expression of the GST-tagged PreScission protease, two o/n cultures were prepared by inoculating 4 ml of LB amp (0.1 mg/ml) with one colony of pGEX-3C in BL21 and incubating o/n at 37°C. The next morning, cells of the o/n cultures were collected, resuspended in 1 ml fresh LB medium and used for inoculation of 2 times 500 ml LB including 0.5% glucose and 0.1 mg/ml amp. Cells were grown at 37°C until OD₆₀₀ of ~0.6. Cells were chilled on ice for 3 min, induced subsequently with 0.2 mM IPTG and allowed to express the recombinant protein o/n at 20°C. Cells were harvested at 3000 g (4,000 rpm, rotor JLA 10.500) for 15 min at 4°C and stored at -20°C until further use.

Purification

Cells were thawed and resuspended in 20 ml lysis buffer for each 500 ml expression culture. Both suspensions were pooled and subjected to lysis together. A spatula tip of DNase I and of lysozyme was added to the suspension as well as 2 ml of 4 mg/ml Pefabloc protease inhibitor. To break the cells, they were sonicated 8 times for 10 sec (output 7, 100% cycle) on ice and subsequently subjected to 2 freeze/thaw cycles. Cell debris and unbroken cells were first removed by centrifuging the cell lysate for 10 min at 15 000 g (13,500 rpm, JA 25.50 rotor) at 4°C. Afterwards, the lysate supernatant was prepared by a second centrifugation for 1 h at 50,000 g (25,000 rpm, JA 25.50 rotor) at 4°C. Five ml of GSFF were packed in a column and equilibrated with wash buffer at 0.5 ml/min using the BioLogic purification system. The lysate supernatant (35 ml) was loaded onto the column at a flow rate of 0.25 ml/min. Unspecifically bound proteins were washed off with wash buffer at 0.5 ml/min until the baseline was reached as monitored by the absorbance at 280 nm. The peak fractions were pooled and dialyzed o/n against 2 l of dialysis buffer at 4°C. After measuring the concentration, the purified protease was aliquoted into fractions of 0.5 ml and stored at -80°C.

Protein concentration determination

The amount of the PreScission protease was determined by measuring the absorbance at 280 nm of the protein solution after dialysis. The concentration was calculated using a specific extinction coefficient of 1.005 (i.e. a protease solution of 1 mg/ml gives an A_{280} of 1.005). The predicted molecular weight of GST-3C is 46.4 kDa.

The concentration of the PreScission protease was determined to be 7.36 mg/ml. The activity can be roughly estimated - based on the specific activity of highly purified protease using this protocol - with 1000 U/mg. Therefore, it was assumed that the protease preparation had an activity of 7,360 U/ml.

Preparation of samples for SDS-PAGE

In general, samples for SDS-PAGE to monitor the purification process were prepared from total lysate, supernatant, flow-through (FT) and washing steps by diluting 1:1 (5 μ l sample + 5 μ l PBS) as well as from the eluate (2 μ l and 10 μ l).

2.2.3.2 EXPRESSION OF GST-STAU2_{CT}

For the expression, o/n cultures were inoculated with one colony of BL21 containing GST-Stau2_{CT} in pGEX-6P-2 as described in section 2.2.3.1. The next morning, 400 ml of 2x YT amp (0.1 mg/ml) were inoculated with 4 ml of the o/n culture and grown at 37°C until OD_{600} of \sim 0.6. Cells were chilled on ice for 3 min and subsequently induced with 0.1 mM IPTG. Cultures were incubated 3 h at 25°C and harvested at 3,000 g (4,000 rpm, rotor JLA 10.500) for 15 min at 4°C. The cells were then stored at -20°C until further use or subjected to purification immediately.

2.2.3.3 PURIFICATION STAU2_{CT}

Cells were thawed (if frozen), resuspended in 40 ml of lysis buffer and incubated 20 min at RT in the presence of lysozyme (1 mg/ml) and 0.1% Triton X-100. To lyse the cells, they were subjected to freeze/thaw-cycles for 2-3 times. To break the DNA completely a spatula tip of DNase I was added and an incubation step took place for additional 10 min at RT. Cell debris and unbroken cells were removed by centrifuging the cell lysate for 30 min at 20,000 g (13,500 rpm, JA 25.50 rotor) at 4°C. The resulting supernatant was applied to the GSFF column (5 ml) for 40 min at RT on the shaker. The beads were subsequently washed 3 times with 10 ml of lysis buffer and once with 10 ml of cleavage buffer. Cleavage of the fusion protein was performed on the beads o/n with PreScission protease (80 U/ml of beads)

in cleavage buffer. Finally, the cleaved Stau2_{CT} was eluted 3 times with 5 ml of cleavage buffer and dialyzed o/n at 4°C. Samples for SDS-PAGE were prepared (see section 2.2.3.1).

2.2.3.4 PURIFICATION OF GST-STAU2_{CT}

Lysis, preparation of the lysis supernatant and binding to the beads was performed as described in section 2.2.3.3. Afterwards, the beads were washed 3 times with 10 ml of lysis buffer. To dissociate bacterial chaperones associated with the overexpressed recombinant protein, the beads were incubated with 5 mM ATP/5 mM MgCl₂ solution 2 times 15 min at RT. The beads were then packed into a column, washed once with 10 ml of Buffer A and connected to the BioLogic purification system. After extensive washing with Buffer A, GST-Stau2_{CT} was eluted with reduced glutathione using a linear gradient of 0% - 100% Buffer B over 50 ml at a flow rate of 0.5 ml/min. The fraction size collected was 1 ml. The peak fractions were pooled and dialyzed o/n against 2 l of PBS at 4°C. If necessary, the resulting protein solution was concentrated to 1.3 – 1.4 mg/ml using Vivaspin concentrators (MWCO 10 kD). Samples for SDS-PAGE were prepared (see section 2.2.3.1).

For antibody production, the purified GST-Stau2_{CT} was aliquoted to 1 mg/tube and used as an antigen for injecting rabbits. Before injection, Preimmune sera (PIS) of six different rabbits were tested for background on Western blots of E17 postnuclear supernatant (PNS) samples. The two rabbits with the lowest signal especially at the size of Stau2 (between 52 and 62 kD) were chosen and injected with the purified GST-Stau2_{CT} (injections and bleeding performed by Harald Höger).

2.2.4 ANALYSIS OF PROTEINS

2.2.4.1 SDS-PAGE

Gels (0.75 mm) for SDS-PAGE based on Laemmli were prepared as described in the material section (Laemmli 1970).

After individual sample preparation, all the samples for SDS-PAGE were combined with 6x Laemmli buffer and boiled for 8 min at 95°C. For analysis, samples were loaded onto the gel together with a suitable marker. Proteins were separated for 90 min at a constant voltage of 100 V which resulted in ~20 mA/gel. After SDS-PAGE, the gel was pre-washed in water and either stained with Coomassie or silver or subjected to Western blotting.

Coomassie

Gels were stained with Coomassie staining solution either o/n at RT or with pre-heated staining solution (to 80°C) for 30 min. Destaining was performed with destaining solution until the background was removed. Finally, after equilibration of the gels in water, they were scanned using the Li-Cor scanner.

Silver staining

The gel was fixed in fixation solution for at least 30 min or o/n and subsequently incubated with reducing/cross-linking solution for 10 min. After 3 washing steps with water, the gel was incubated with silver solution for 15 min. Following a short rinse with water, proteins were visualized with developing solution until an optimal intensity of the bands was obtained. The reaction was stopped with 3% acetic acid for 10 min. Finally, after equilibrating the gel in water, it was scanned using the Peqlab imaging system.

2.2.4.2 WESTERN BLOTTING

For Western blotting, the tank blotting system from BioRad was used. The gel, filter papers and the membrane were soaked in cold blotting buffer and assembled into a sandwich in the following order starting from the cathode: sponge, 2 filter papers, gel, membrane, 2 filter papers and sponge.

Proteins were blotted at constant voltage of 100 V for 90 min under constant stirring of the buffer and cooling on ice. Afterwards, the membrane was stained with Ponceau S to check for the quality of blotting. Blocking of the membrane was performed for at least 30 min at RT in Detector™ Block solution. Incubation with the primary antibody, diluted in Detector™ Block was carried out either for 2 h at RT or o/n at 4°C. The membrane was washed at least 2 times for 15 min at RT with 1x TBST, then the secondary antibody was added for 30-40 min at RT. Finally, the blot was washed as before and scanned using the Li-Cor scanner.

2.2.5 GEL FILTRATION OF RAT BRAIN LYSATES

Preparation of the sample

An aliquot of frozen E17 rat brains (30 brains) was thawed and the tissue was homogenized in 5 ml HS with 10 stokes at 900 rpm at 4°C. The homogenate was centrifuged at 12,500 g for 8 min at 4°C, which resulted in the separation of the postnuclear supernatant (PNS). The PNS was then subjected to a differential centrifugation starting with 40,000 g (27,000 rpm,

TLA 100.3 rotor) for 40 min at 4°C. The resulting supernatant S40 was further centrifuged at 120,000 g (47,000 rpm, TLA 100.3 rotor) for 1 h at 4°C. The final supernatant S100 was then recovered (diluted to 2.5 ml) and filtered through 0.45 µm filter prior to loading onto the S-300HR column.

Gel filtration on Sephacryl S-300HR

The S-300HR 26/60 column was equilibrated with at least 3 column volumes of GF buffer. Two ml of the S100 supernatant were loaded and separated at a flow rate of 0.4 ml/min. Fractions of 3 ml were collected. For the calibration, a run of a sample containing 4 mg of each marker protein from the molecular weight marker kit was separated under the same conditions. The elution volumes of marker proteins were then used as reference for the size of Stau2 RNP complexes.

Protein isolation from the fractions

Proteins from 300 µl of each fraction were subjected to TCA precipitation as described (Bensadoun and Weinstein 1976). Briefly, 0.02% DOC was added to the protein solution (4 µl from the 1.5% stock), vortexed and incubated on ice for 5 min. Then 11% TCA was added (41.3 µl from 80% stock) and incubated on ice for 1 h. Precipitated proteins were recovered by centrifugation at maximum speed (20,000 g) using a top-bench Eppendorf centrifuge. The protein pellet was washed with 1 ml cold acetone (-20°C), centrifuged for 5 min at 14,000 rpm at 4°C and allowed to air-dry. Then the proteins were redissolved in 10 µl of 100 mM Tris pH 8.5 and prepared together with an aliquot of 5 µl of the input (S100) for SDS-PAGE. The samples were submitted to Western Blotting. The remainder of the fractions (2.5 ml) was saved for a subsequent IP experiment. The fractions were combined with 500 µl 50% glycerol in GF buffer in order to freeze them in liquid nitrogen for storage at -80°C.

RNA isolation from the fractions

200 µl of the fractions were used to isolate RNA with the *miVana*TM Kit (see section 2.2.9.1).

Immunoprecipitation from GF fractions of the E17 brain lysates

As an input material, fractions 29 to 37 containing Stau2 protein were pooled (20 ml), concentrated up to 2.5 ml using a Vivaspin concentrator (MWCO 10 kD) and used for a subsequent IP as described in section 2.2.7.

2.2.6 PREPARATION OF ANTIBODY-COUPLED BEADS FOR IP

The protocol used was adopted from Daniela Karra in the lab (D. Karra, 2008, PhD thesis).

2.2.6.1 AFFINITY PURIFICATION OF ANTIBODIES

The immunized serum (from rabbit H7) containing the antibody directed against mouse Stau2_{FL} was thawed and diluted 2-fold with Tris buffer. Magnetic beads (0.9 ml) coated with 4.56 mg of GST-Stau2_{FL} protein (prepared by Martina Schwarz) were equilibrated with Tris buffer. The diluted serum was incubated with the magnetic beads for 3 h at 4°C rotating. Afterwards, the supernatant was saved for testing as well as for a subsequent 2nd round of affinity purification. Beads were then washed 3 times with 40 ml Tris buffer and once with 40 ml of 1.5 M NaCl (in water) for 10 min at 4°C. The bound IgGs were eluted with 5 ml glycine pH 2.5 containing 1 tablet of protease inhibitors for 5 min at RT on the shaker. The glycine elution was collected into a Falcon tube containing 1 ml of 1 M Tris pH 8.5. In parallel, the beads were washed with PBS to restore the pH and stored in PBS with 0.02% NaN₃ at 4°C, ready for the next round of affinity purification.

The eluate containing the purified antibodies was concentrated up to 1 ml using a Vivaspin concentrator MWCO 50 kD by centrifugation at 4,000 rpm (rotor Heraeus #8074), at 4°C. To exchange the buffer, 5 ml of PBS supplemented with protease inhibitors was added to dilute the antibodies and subsequently this mixture was concentrated again up to 1 ml. The concentration of the anti-Stau2 antibody was measured using Bradford method and A280 protein measurement. The specificity and purity of the antibody was analyzed by probing on Western blot of E17 PNS samples. Purified anti-Stau2 antibody was stored in PBS containing 0.02% NaN₃ at 4°C until further use. The serum was used for several rounds of affinity purification.

For purification of antibodies directed against mouse Stau2_{CT} (from rabbit R) the same procedure was performed (done by Anetta Konecna). However, first the serum was depleted of antibodies directed against the GST-tag by application to GSFF coated with GST. Afterwards, magnetic beads (1 ml) coated with 4 mg of GST-Stau2_{CT} protein were used for purification.

2.2.6.2 COUPLING OF THE ANTIBODIES TO PROTEIN A SEPHAROSE

In general, approximately 1 mg of affinity-purified anti-Stau2 antibody was coupled to 500 µl of Protein A Sepharose beads. As a negative control, the same amount of PIS (10 mg/ml, from the same rabbit which produced the antibody) was coupled to the same volume of Protein A Sepharose. Subsequently these beads are referred to as Stau2 and PIS beads. The

coupling was performed in 1.5 ml Eppendorf tubes for 1 h rotating at 4°C, where the volume for coupling was adjusted to a minimum of 1 ml with PBS to ensure good mixing. For the production of non-crosslinked beads, the beads were washed 3 times with PBS and stored in PBS with 0.02% NaN₃ at 4°C.

For the production of crosslinked beads, the beads were washed 2 times with PBS, once with PBS including 350mM NaCl and 2 times with Hepes buffer pH 8.5. Crosslinking of the IgGs was performed with 1 ml 20 mM DMP in Hepes buffer pH 8.5 at RT for 30 min. To stop the crosslinking reaction, the beads were first rinsed and then incubated in 0.2 M ethanolamine pH 8.0 for 1 h at RT. Afterwards, two washing steps with PBS and one with water were performed prior to a short elution of not successful crosslinked IgGs with 1 ml of 0.2 M glycine pH 2.5. Re-equilibrated beads with PBS were stored at 4°C in the presence of 0.02% NaN₃.

To analyze the efficiency of binding/coupling, samples of the beads, 10 µl of the 1:1 slurry, as well as the input and non-bound IgGs were analyzed by 10% SDS-PAGE and silver staining.

2.2.7 IMMUNOPRECIPITATION OF STAU2-CONTAINING RNPs

The protocol used was adopted from Daniela Karra in the lab (D. Karra, 2008, PhD thesis).

Input material

E17 IPs: 20-24 E17 rat brains (stored at -80°C) in 2 ml 1x BEB complete (30 - 40 mg/ml)

Adult IPs: 1 adult rat forebrain (stored at -80°C) in 3 ml 1x BEB complete (30 - 40 mg/ml)

S100 IPs: for the preparation, see gel filtration experiments (section 2.2.5)

The input material was homogenized with 10 strokes at 900 rpm (for E17 brains) or 1500 rpm (for adult brains) in 1x BEB complete, which was supplemented with RiboLock (2 µl/ml), 1 mM DTT and protease inhibitors (1 tablet/10 ml). The homogenate was centrifuged at 20,000 g for 10 min at 4°C. The resulting PNS was pre-cleared with 100 µl of Protein A Sepharose for 1 hour at 4°C rotating. At the same time, 20 - 25 µl of crosslinked anti-Stau2 and PIS beads were blocked with 0.5 mg BSA (25 µl 20 mg/ml BSA stock) and 50 µg yeast tRNA (5 µl 10 mg/ml stock) in 1x BEB complete for 1 hour at 4°C rotating.

Centrifugation steps to collect the beads were carried out for 2 min at 500 g, 4°C. Beads were washed once with 1x BEB complete and then incubated with 300 µl pre-cleared PNS including 30 µg of yeast tRNAs for 1.5 hour at 4°C rotating.

Afterwards, the beads were washed 4 times with 1x BEB complete w/o RiboLock and once with PBS containing 1 mM MgCl₂ (which had RT). First, the RNase elution was carried out by addition of 150 µl of RNase mix, composed of 150 µl PBS + 1 mM MgCl₂ + 1.7 µl RNase A + T (5,000 U/ml RNase T1, 12 mg/ml RNase A) and the eluted proteins were collected after 1 h incubation at RT. The beads were then washed 2 times with 1x BEB complete w/o RiboLock and once with ice-cold water. Second, the elution of the remaining proteins bound directly to Stau2 was performed with 125 µl of glycine pH 2.5 for 15 min at RT. The eluted proteins were collected into a tube containing 25 µl of 1 M Tris-HCl pH 8.5 to immediately neutralize the low pH.

The RNase and glycine eluates were precipitated by methanol-chloroform precipitation method (Wessel and Flugge 1984). The protein pellets were redissolved in 15 µl of 100 mM Tris buffer pH 8.5 and subjected to SDS-PAGE sample preparation. As a control 3 µl of the input (PNS) and the unbound supernatant after IP were diluted up to 10 µl with PBS. IP samples were separated on 10 or 12% SDS-PAGE followed by Western blotting (see section 2.2.4.1). In general, IP from 20 µl beads and 300 µl PNS was sufficient for one Western blot, for two gels the amount of the beads and the input was doubled.

2.2.8 RNA METHODS

2.2.8.1 RNA HANDLING IN GENERAL

RNase contamination should be eliminated, therefore the following precautions were taken:

- The working space was cleaned with ethanol
- gloves were worn and frequently cleaned with ethanol
- Glassware was sterilized by baking for 6 h at 240°C
- ddH₂O was treated with 0.1% DEPC (diethylpyrocarbonate)
- Solutions were prepared from RNA grade chemicals
- Barrier tips were used for pipetting
- RNase-free non-stick tubes from Ambion were used for miRNA experiments
- Total RNA was stored at –20°C or –80°C in water

2.2.9 IMMUNOPRECIPITATION OF STAU2-CONTAINING RNPs FOR RNA EXPERIMENTS

The IP for subsequent RNA isolation was performed as described in section 2.2.7 with the following modifications: 50 µl non-crosslinked beads were incubated with 600 µl input. The blocking procedure was tested with and w/o yeast tRNAs, subsequently tRNAs were omitted. After binding of the input, beads were washed 2 times in 1x BEB complete, 0.5% NP40 and 2 times in 1x BEB complete, 0.1% NP40. After this washing step all further steps were carried out according to RNA handling rules. Beads were transferred into non-stick RNase-free tubes and washed 2 times in 5 mM Tris, 100 mM NaCl buffer. After the last washing step the supernatant was removed and RNA isolation using the *miVana*TM Kit was performed.

2.2.9.1 MIRVANATM MIRNA ISOLATION KIT

The original protocol according to the manufacturer (Ambion) was used with minor modifications.

After IP, total RNA was isolated from Stau2 RNPs bound to the beads as shown in the table. Alternatively, fractions obtained after GF were used for RNA isolation. As a positive control, RNA was isolated in parallel from the input sample (in general PNS).

Sample	Lysis/Binding buffer	miRNA Homogenate additive	Acid Phenol:Chloroform
PNS / input – 40 µl	200 µl	24 µl	240 µl
Beads – 50 µl	200 µl	20 µl	200 µl
Beads – 100 µl	250 µl	25 µl	250 µl
Fractions GF – 200 µl	500 µl	70 µl	700 µl

The organic extraction and further steps of the “Total RNA Isolation Procedure” were carried out as described in the protocol. The RNA was eluted in 100 µl pre-heated RNase-free water and subjected to RNA precipitation.

2.2.9.2 RNA PRECIPITATION AND PURITY ANALYSIS

Eluted RNA was precipitated by the addition of 50 µl 3 M sodium acetate, pH 5.5, 0.5 µl glycogen (20 mg/ml) and 1 ml 1:1 ethanol/isopropanol. The mixture was incubated o/n at -20°C. The next day, RNA was recovered by centrifugation at 20,000 g for 15 min, 4°C. The pellet was washed once with 1 ml of 75% ethanol, re-centrifuged and allowed to air-dry for a maximum of 5 min. Then the RNA was redissolved in RNase-free water (usually 8 to 15 µl) and the amount and purity was estimated by measurement at 260 and 280 nm. The remaining RNA was stored at -20°C.

2.2.10 RNA GEL ELECTROPHORESIS

For RNA gel electrophoresis, only special equipment was used, which was reserved for RNA work. A 1.5% agarose gel containing formaldehyde was prepared as follows:

agarose	1.5 g
DEPC water	73 ml
Dissolve by heating, cool down under constant stirring to 55°C	
10x MOPS	10 ml
formaldehyde, 37%	17 ml
Pour the gel under the hood	

A sample of 2 μg of RNA in 6 μl DEPC water was denatured by addition of 19 μl of formaldehyde/formamide mixture as shown in the table:

mixture	μl
formamide	12.5
10x MOPS	2.5
formaldehyde, 37%	4
Total	19

The resulting 25 μl of the mixture were incubated at 65°C for 10 min, chilled on ice and combined with 2.5 μl RNA loading dye mix.

The gel was pre-run in 1x MOPS buffer for 10 min at 5 V/cm (which makes 90 V for 19 cm measured between the two electrodes). Afterwards samples and size markers were loaded and electrophoresis was performed at 90 V for 4 h under the hood. RNA was visualized by staining with ethidium bromide in a bath of 1x MOPS.

2.2.11 3'-END RNA LABELING WITH [³²P] PCP

A 15% denaturing polyacrylamide gel containing urea (1 mm) was prepared as shown in the following table:

urea	12 g
10x TBE Buffer	2.5 ml
40% acrylamide (19:1)	9.3 ml
DEPC water	up to 25 ml
dissolve urea at RT, shaking	
APS (10%)	125 μl
TEMED	25 μl

The gel was prepared at RT and allowed to polymerize for 20-30 min.

For the RNA labeling reaction, the following mixture was prepared.

RNA	0.5 µg
DMSO	3 µl
10x T4 Ligase buffer	2 µl
0.1 mM ATP	1.2 µl
0.1 M MgCl ₂	2 µl
0.1 mg/ml BSA	2 µl
DEPC water	up to 18 µl

Then 1 µl T4 RNA Ligase and 0.5 µl of [³²P] pCp were added and the reaction mixture was incubated at 15°C for 60 min in a water bath. In the meantime, the gel was pre-run at 30 mA constant for 20 min to obtain an optimal temperature of 45-50°C. After incubation, RNA samples were desalted using the MicroSpin G-25 columns according to the manufacturer's instructions. The desalted flow-through was combined with 20 µl of gel loading buffer II, heated at 95°C for 3 min and loaded hot onto the gel. As a size control, 10 µl of the decade marker (Ambion) was used, which was prepared according to the protocol supplied. The gel was run in 1x TBE at 30 mA constant for 40 min. The running buffer was collected as radioactive liquid waste. The gel was wrapped with Saran and exposed to an Imaging Screen K from 10 min to o/n at RT.

2.2.12 END POINT RT-PCR FOR SELECTED MIRNAS

RT-PCR was performed using the *miVana*TM qRT-PCR miRNA Detection Kit from Ambion.

Set-up of the reverse transcription (RT):

RT	10 µl
5x RT-buffer	2 µl
Enzyme mix	0.4 µl
RNA (25 ng/µl)	1 µl
1x RT-primer	1 µl
RNase free water	5.6 µl

Set-up of the PCR reaction:

PCR	25 µl
RT-mix	10 µl
5x PCR-buffer	5 µl
Taq (1 U)	0.2 µl
PCR-primer set	0.5 µl
RNase free water	9.3 µl

RNA was reverse transcribed for 30 min at 37°C using a thermal cycler, afterwards the enzyme was inactivated at 95°C for 10 min. The complete 10 µl of RT-mix were used for setup of the PCR reaction, the composition is shown in the table. The PCR mixture was placed into a pre-heated thermal cycler and the following program was run.

Initial denature: 95°C for 3 min
Cycling (27 cycles): 95°C for 45 sec
 60°C for 60 sec

The PCR products (90 bp) were combined with 6x Orange LD and analyzed on 3.5% agarose gels (Top Vision LE GQ Agarose). As a size marker, 7 µl of the O'GeneRuler™ Low Range (700 – 25 bp) were used. DNA was visualized by incubation of the gel in a 1:10,000 dilution of SYBR® GOLD in TAE for 10-20 min and subsequent monitoring of the bands using a SYBR® photographic filter.

3 RESULTS

3.1 PURIFICATION OF GST-STAU2_{CT} FOR ANTIBODY PRODUCTION

3.1.1 CLONING OF STAU2_{CT} INTO PGEX-6P-2

For many experiments, the quality or specificity of the antibodies used is crucial, e.g. for immunoprecipitation (IP). To generate specific antibodies against Stau2, a new antigen consisting of GST fused to the C-terminal (CT) part of mouse Stau2 (GST-Stau2_{CT}) was produced. The C-terminal part of the Stau2 protein covers the region starting from threonin 379 until the C-terminal isoleucin 512, including the tubulin-binding domain (TBD) and the RNA binding domain (RBD) 5. The construct was initially described in Duchaine et al. 2002 where it was cloned from mouse brain into pBluescript SK(+) at the EcoRV site and later subcloned into pGEX-4T-2 at the NotI/SalI sites.

The aim was to insert Stau2_{CT} into the bacterial expression vector of the pGEX-6P series, which contain a cleavage site for the PreScission protease in order to cleave the GST-tag after purification. For maintaining the correct reading frame, pGEX-6P-2 was needed and therefore constructed from pGEX-6P-1 and pGEX-4T-2 (see section 2.2.2.1). In Figure 3.1A, the plasmid map of the empty pGEX-6P-2 vector is shown. It includes an ampicillin resistance gene for positive selection, the coding sequence for GST right before the PreScission cleavage site and a multiple cloning site (MCS). Stau2_{CT} was inserted directly after the GST sequence using NotI and SalI sites (Figure 3.1B). The vector and the insert used for ligation are shown in Figure 3.1C. Clones were tested by restriction digestion, yielding 8 clones carrying the correct construct. Clone #2 was used for subsequent expression of GST-Stau2_{CT} in BL21 cells.

3.1.2 EXPRESSION AND PURIFICATION OF THE PRESCISSION PROTEASE

The main advantage of the pGEX-6P series is the PreScission cleavage site for removing the GST-tag from expressed fusion proteins. Thus, the PreScission protease was expressed and purified. The construct (GST-3C) was obtained from Andi Geerlof (see section 2.1.4) and contains the GST-tagged protease. Therefore, on the one hand the protease can be purified using a Glutathione Sepharose™ 4 Fast Flow (GSFF) column which binds to GST.

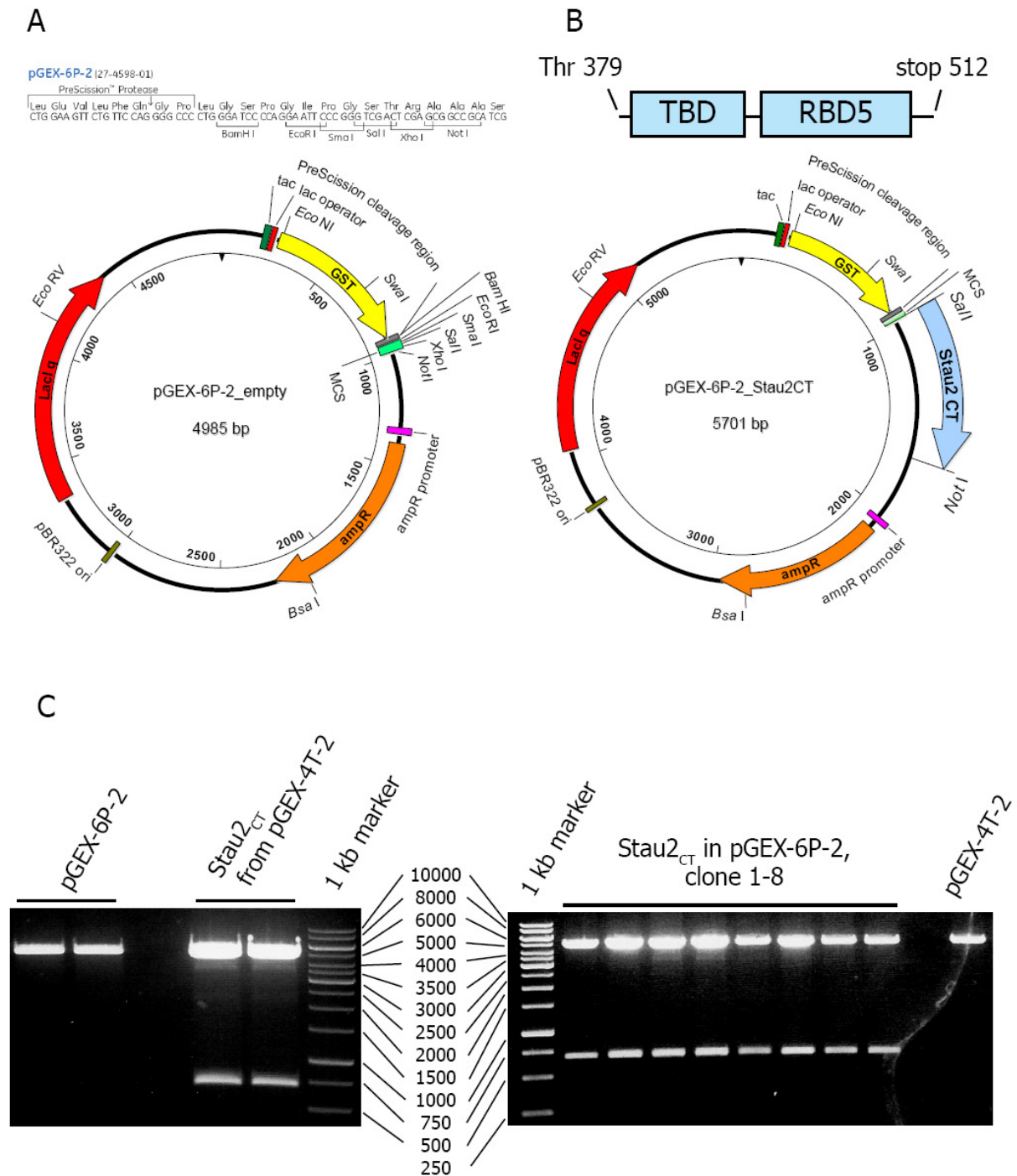


Figure 3.1 – Cloning of the Stau2_{CT} construct into pGEX-6P-2

(A) Plasmid map of the empty pGEX-6P-2, the sequence of the MCS and the PreScission cleavage site is shown in large. (B) Plasmid map of pGEX-6P-2 containing the Stau2_{CT} (blue), inserted between SalI and NotI. On top, a schematic representation of the Stau2_{CT} construct (Thr 379 - stop 512), containing the TBD and RBD5, is shown. (C) Cloning of Stau2_{CT} into pGEX-6P-2. (left) 1% agarose gel of restriction digestion (SalI/NotI) of the empty pGEX-6P-2 (4985 bp) and of the Stau2_{CT} insert (734 bp). (right) 1% agarose gel of restriction digestion (SalI/NotI) of 8 different clones after ligation, all containing the correct insert (734 bp). For comparison, the empty linearized pGEX-4T-2 was loaded.

On the other hand, this GST-tag allows to trap the protease on the beads during cleavage of the GST-tag from a fusion protein. The protease was expressed in BL21 cells as described in section 2.2.3.1. BL21 cells are deficient in both *lon* and *ompT* proteases, therefore they are commonly used for expression of recombinant proteins. As seen in Figure 3.2A, the protease was produced upon induction with IPTG and the major portion of the protein was found in the supernatant, indicating that it was soluble. The lysate supernatant was then subjected to purification on a GSFF column. As shown in Figure 3.2B, the column was saturated with GST-PreScission protease since there was still a significant amount of the protein found in the flow-through (FT) as well as in the washing step. This left the possibility to re-purify the protease from the FT or increase the volume of the column.

The eluate showed a single protein band, proving the purity and the correct size of the protease. This is also visible from the elution profile containing one symmetric peak (Figure 3.2C). The peak fractions 11 to 17, which included the main part of the protein, were pooled. The obtained concentration was 7.36 mg/ml. The specific activity of the PreScission protease usually obtained using this protocol is 1,000 U/mg. Therefore, based on the concentration and the assumed specific activity this purification yielded a protease activity of approximately 7,360 U/ml.

3.1.3 EXPRESSION AND PURIFICATION OF STAU2 PROTEINS

3.1.3.1 EXPRESSION AND PURIFICATION OF STAU2_{CT}

The purpose of the following experiments was to obtain a pure antigen suitable for antibody generation. The advantage for production of Stau2_{CT} via cleavage of the GST tag was the possibility to inject "tag-free" antigen. This prevents production of antibodies directed against the tag and therefore abolishes the need for removing them.

GST-Stau2_{CT} was expressed in BL21 cells via induction with IPTG. Comparing the amount of GST-Stau2_{CT} in the total lysate and the lysate supernatant showed that half of the protein was lost in insoluble form (inclusion bodies) in the pellet after centrifugation (see Figure 3.3A). The purification was performed by binding of GST-Stau2_{CT} to the GSFF column and subsequent cleavage of the Stau2_{CT} using the PreScission protease. A representative purification is shown in Figure 3.3A. The binding capacity of the column was exceeded by the amount of protein applied, as some protein was still found in the FT. Upon binding, GST-Stau2_{CT}, its degradation products and also some other proteins, namely DnaK, were bound. DnaK is a heat shock protein involved in correct folding of nascent proteins in *E. coli* and may co-purify with GST fusion proteins.

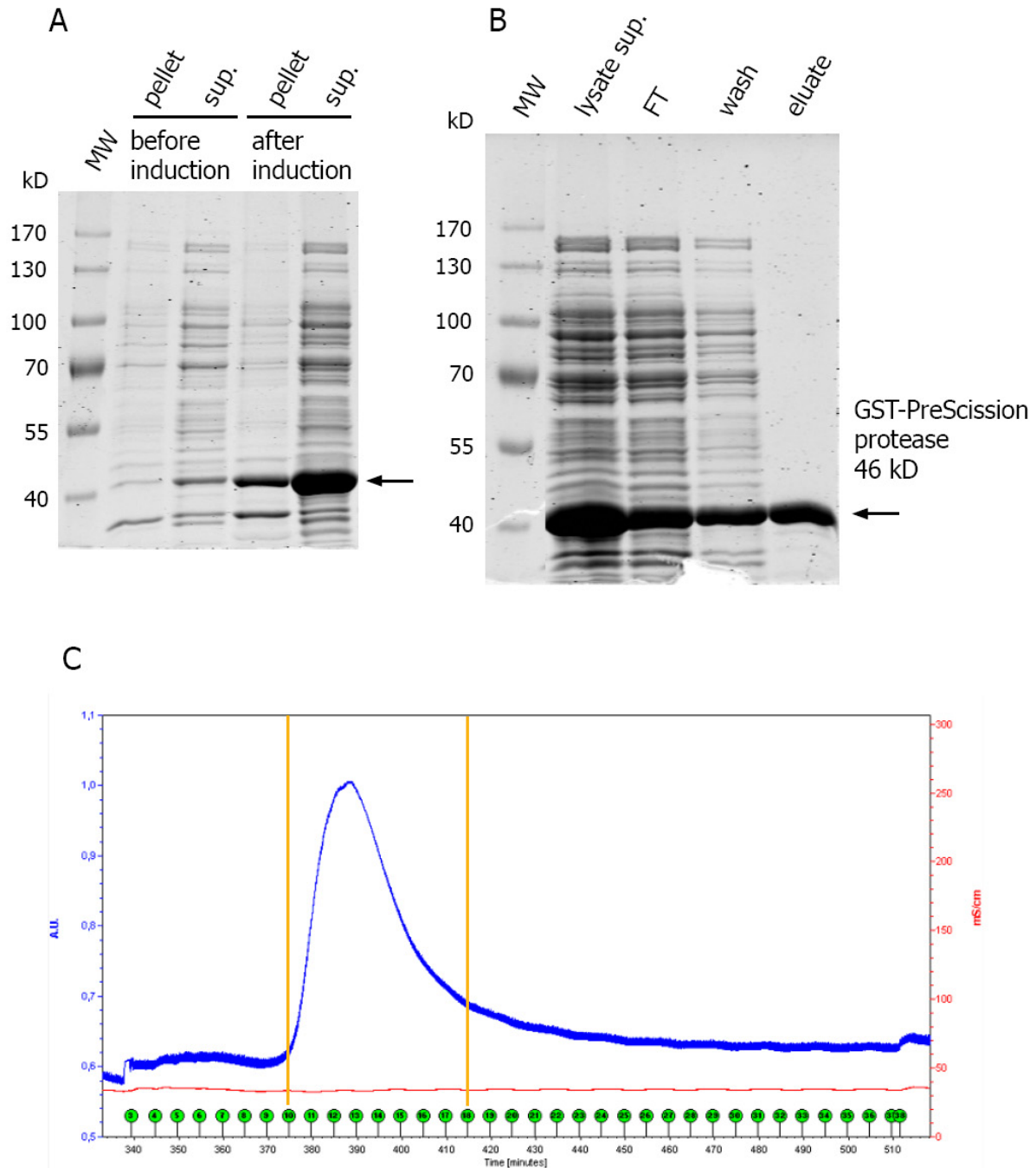


Figure 3.2 – Purification of the PreScission protease

(A) 10% SDS-PAGE and Coomassie staining: Expression of GST-PreScission protease in BL21 o/n at 20°C, induced with 0.1 mM IPTG, yielded a soluble protein of 46 kD. (B) 10% SDS-PAGE and Coomassie staining: Purification of GST-PreScission protease on a GSFF column; the eluate contains pure protein of the correct size (46 kD). (C) UV-profile of the elution of PreScission protease with glutathione; green labels the fractions, the yellow bars show the pooled fractions (11-17).

MW, molecular weight marker; sup., supernatant; FT, flow through

After cleavage, only the GST tag and the PreScission protease (which also carries a GST-tag) remained, indicating that the cleavage of GST-Stau2_{CT} was complete. However, the amount of cleaved Stau2_{CT} was much less than expected from the amount of bound GST-Stau2_{CT}. This observation was independent from the method used for quantification: Coomassie staining, Bradford, UV-measurement. After dialysis, the concentration levels were even lower. To exclude any unspecific proteolytic activity, purified GST-Stau2_{CT} and BSA were incubated over a time of 3 h with or without PreScission protease. This resulted in no decrease of the protein amounts of BSA and GST-Stau2_{CT}, therefore no unspecific degradation occurred by incubation with PreScission protease (data not shown).

Because the Bradford assay essentially measures the amount of arginine and hydrophobic amino acid residues, the amino acid composition can bias the results depending on the percentage of arginine or hydrophobic amino acids in each protein. Therefore, the ProtParam tool from the ExPasy webpage was used to calculate several protein parameters, shown in the following table. One of the parameters was the molar extinction coefficient computed from the amino acid composition of either the GST-Stau2_{CT} fusion protein or cleaved Stau2_{CT} protein. Usage of this molar extinction coefficient to calculate the concentration from the absorption at 280 nm (A_{280}) gave more reliable results compared to Bradford or conventional UV-measurement (with an averaged coefficient).

protein	Amino acids	Molecular weight (kD)	Isoelectric point	Molar extinction coefficient (/M cm)	Stability index
GST-Stau2 _{CT}	436	48.6	6.53	53205	39.68 = stable
Stau2 _{CT}	210	22.1	8.84	10095	43.74 = unstable

If the two methods (UV-measurement using the molar extinction coefficient and Bradford measurement) were compared, the following results were obtained. For GST-Stau2_{CT}, the concentration was reduced by a factor of 0.87; meaning that the Bradford method slightly overestimated the concentration. For cleaved Stau2_{CT}, an increase of the quantity by a factor of 2.45 for was found, leading to the assumption that Bradford method underestimated the concentration of cleaved Stau2_{CT}. The correction of the concentrations decreased the discrepancy between quantities of GST-Stau2_{CT} and cleaved Stau2_{CT}, but still the yield of Stau2_{CT} after cleavage and concentrating was below 20-30%. One possible reason might be the high instability of Stau2_{CT} (as seen by the stability index), making Stau2_{CT} an unsuitable antigen for injection and antibody production. Thus, the approach of purifying Stau2_{CT} via cleavage of the GST tag was abandoned.

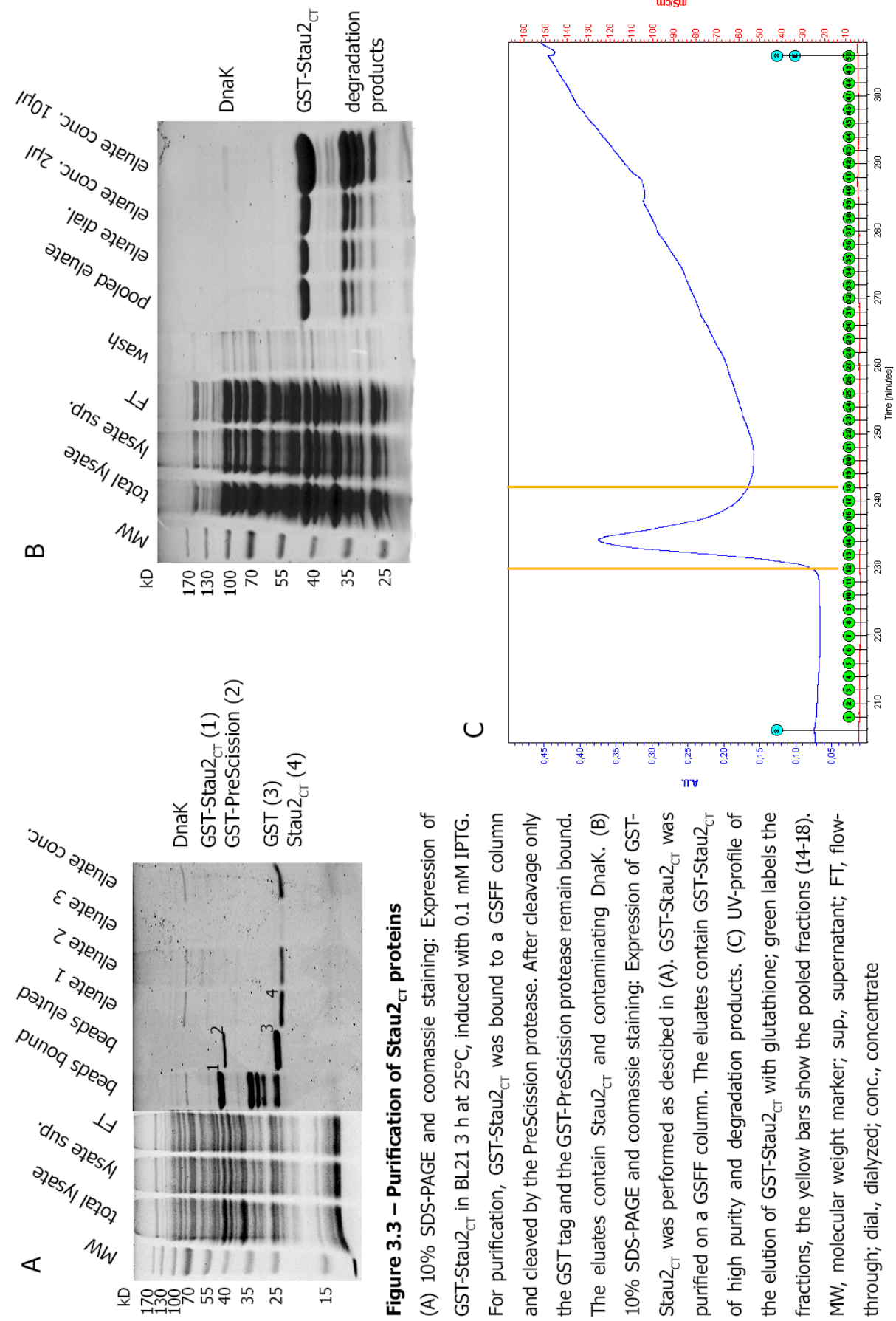


Figure 3.3 – Purification of Stau2_{CT} proteins

(A) 10% SDS-PAGE and coomassie staining: Expression of GST-Stau_{CT} in BL21 3 h at 25°C, induced with 0.1 mM IPTG. For purification, GST-Stau_{CT} was bound to a GSFF column and cleaved by the PreScission protease. After cleavage only the GST tag and the GST-PreScission protease remain bound. The eluates contain Stau_{CT} and contaminating DnaK. (B) 10% SDS-PAGE and coomassie staining: Expression of GST-Stau_{CT} was performed as described in (A). GST-Stau_{CT} was purified on a GSFF column. The eluates contain GST-Stau_{CT} of high purity and degradation products. (C) UV-profile of the elution of GST-Stau_{CT} with glutathione; green labels the fractions, the yellow bars show the pooled fractions (14-18). MW, molecular weight marker; sup., supernatant; FT, flow-through; dial., dialyzed; conc., concentrate

Instead, it was decided to produce GST-Stau2_{CT}, which was previously shown by Anke Deitinghoff in the Kiebler lab to yield specific antibodies.

3.1.3.2 EXPRESSION AND PURIFICATION OF GST-STAU2_{CT}

The following section describes the purification of GST-Stau2_{CT} to obtain a stable, highly pure antigen suitable for antibody production. Due to the importance of the quality of the antigen for antibody specificity, the purification protocol was modified to the final version described in the material and method section 2.2.3.4. An ATP/MgCl₂ incubation step was included after binding of the fusion protein to GSFF. This step should dissociate the interaction of the recombinant protein with the chaperone DnaK. Afterwards the column was connected to the BioLogicLP system (BioRad) and GST-Stau2_{CT} was eluted using a glutathione gradient. The advantage of elution using the LP system was the small volume of elution, leading to higher concentrations.

The purification process is shown in Figure 3.3B. Since there is still unbound GST-Stau2_{CT} in the FT, re-binding of the FT or increasing the volume of the Sepharose would be possible. In Figure 3.3C, the elution profile is shown. From this experiment, fractions 14 – 19 were pooled. This approach yielded a sufficient amount of stable protein which was relatively free of impurities, especially the contaminating chaperone DnaK. Just a very faint band is visible at 70 kD in the concentrated eluate, leading to the conclusion that the ATP/MgCl₂ incubation is sufficient to dissociate the interaction of the recombinant protein with DnaK. The lower bands in the eluate refer to degradation products, which were considered to be no problem for antigen purity (tested by WB, data not shown).

This purified GST-Stau2_{CT} was used as an antigen for antibody production. After testing the specificity, the generated antibody could be used for WB or IP experiments.

3.2 PROTEIN COMPOSITION OF STAU2 COMPLEXES

3.2.1 AFFINITY PURIFICATION OF ANTI-STAU2 ANTIBODIES AND PREPARATION OF ANTIBODY-COUPLED BEADS

Immunoprecipitation is a suitable method to investigate the composition of Stau2-containing particles in rat brain. Using this approach, it is possible to specifically precipitate Stau2 with all associated proteins, RNAs and other factors. For the specificity of the IP, the high quality of the antibody used is essential. Therefore, all the IP experiments were performed using affinity-purified anti-Stau2 antibodies. Two different anti-Stau2 antibodies were used: H7 derived from rabbit H7 immunized with His-tagged mouse Stau2 full-length (FL) protein (His-Stau2_{FL}) and R derived from rabbit R immunized with the C-terminal part of mouse Stau2 fused to a GST-tag (GST-Stau2_{CT}). As a control, the pre-immune sera (PIS) from the two corresponding rabbits were used in parallel IPs.

In Figure 3.4A, the affinity purification of anti-Stau2 antibodies from rabbit H7 is shown. For this purpose, the serum was applied to magnetic beads coated with the GST-Stau2_{FL} protein. As the His-tagged protein was used for immunization, a GST-tagged Stau2 protein was used for the affinity purification. It is important not to purify the antibodies on the antigen including the same tag used for immunization, as this will result in purification of additional antibodies directed against the tag itself. After binding and thorough washing, the IgGs were eluted and tested for specificity. As seen in Figure 3.4A, the serum detected primarily three isoforms of Stau2 along with a number of additional bands. After purification, the most prominent bands were the ones for the two most abundant isoforms of Stau2 (59 and 52 kD), whereas there was just a faint band for the 62 kD isoform. This reflects the levels of expression of the Stau2 isoforms in the brain. Importantly, with the affinity-purified antibody, most of the non-specific bands disappeared. As obvious from the flow-through, several rounds of purification were performed from one serum aliquot due to a high titer of anti-Stau2 antibodies.

The affinity-purified anti-Stau2 antibody as well as equivalent amounts of the PIS were then coupled to Protein A Sepharose beads, as shown in Figure 3.4B (subsequently referred to Stau2 and PIS beads). The binding was complete, as there is no antibody left in the supernatant after binding. The crosslinking of the antibodies with dimethylpimelidate (DMP) led to covalent binding to the Sepharose. Therefore, the samples of the beads after

crosslinking showed only weak bands for heavy and light immunoglobulin (Ig) G chains, which represent a minor leakage. The amount of Stau2 and PIS IgGs coupled to beads was equivalent, which is an important point for subsequent IP. The identity of the band slightly below 70 kD in the PIS beads is not known. It was also present in the affinity-purified anti-Stau2 antibody but it did not bind to the Protein A Sepharose. Both IgG-coupled beads were then ready to be used for IP experiments.

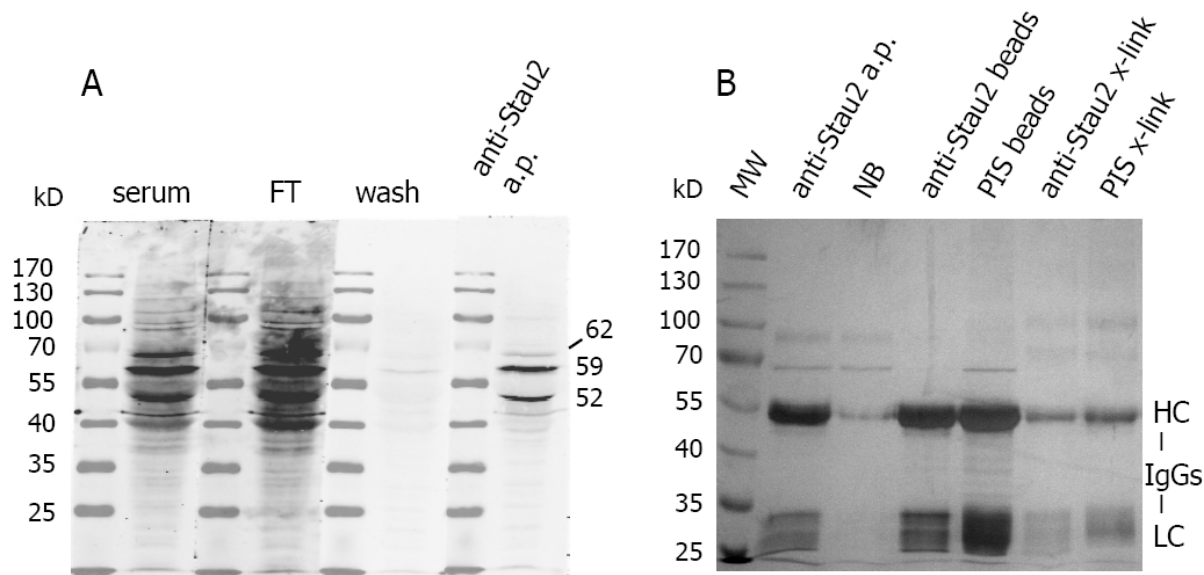


Figure 3.4 – Antibody affinity purification and coupling to Protein A Sepharose beads

(A) Affinity purification of antibodies directed against His-Stau2_{FL}. Samples of the purification steps were tested on WB from E17 brain lysates. The purified antibody recognizes three isoforms of Stau2 (62, 59, 52 kD). (B) Silver gel from coupling of anti-Stau2 antibody to Protein A Sepharose (with and w/o crosslinking). Bands represent IgGs (heavy and light chains) and show the successful coupling and crosslinking to the beads. MW, molecular weight marker; NB, nonbound; FT, flow through; a.p., affinity purified; x-link, crosslinked; HC, heavy chains; LC, light chains

3.2.2 PROTEIN CANDIDATES IN STAU2 COMPLEXES

Currently, a comprehensive proteomic analysis of Stau2 RNPs is under intensive investigation in the lab (D. Karra and M. Kiebler, in preparation). Since the main goal of this thesis was to address whether small non-coding RNAs, such as miRNAs, are present in these complexes, focus was put on few selected candidate proteins known to be involved in miRNA processing and function.

For this purpose, IP experiments were performed using anti-Stau2 antibodies. The expression of Stau2 peaks during the two first weeks after birth and then progressively

decreases until adulthood (unpublished data). Therefore, it was decided to analyze and to compare Stau2 complexes isolated from developing (E17) and adult rat brain.

As described in section 2.2.7, Stau2 complexes were immunoprecipitated from a postnuclear supernatant (PNS) of either embryonic (Figure 3.5A) or adult (Figure 3.5B) rat brain using antibody-coupled Sepharose (in this case from rabbit H7). The proteins from these Stau2 complexes were subsequently subjected to a two-step elution. First, by adding an RNase A/T1 mixture to the beads with immunoprecipitated Stau2 complexes, the RNA was digested, which resulted in release of all proteins bound indirectly to Stau2 via RNA. This is referred to as RNase elution. In a second step, a shift to a low pH led to the dissociation of antigen-antibody interactions and thereby eluting Stau2 together with all directly associated proteins. This is referred to as low pH elution. This two-step procedure allowed to distinguish between Stau2 indirect interactors via RNA and Stau2 direct protein-protein interactors. In parallel to Stau2 beads, the IP was performed with PIS beads as a negative control.

After IP, the eluates were analyzed by Western blot using indicated antibodies. To confirm the functionality of the IP, it was probed for Stau2, which was present in low pH elution of both, E17 and adult IP. Upregulated protein factor (Upf) 1, an RNA helicase involved in nonsense-mediated decay (NMD), reviewed in Chang et al. 2007, turned out to be a good positive control for the IP. It was present in the RNase elution as well as to a minor extent in the low pH elution from IPs of E17 and adult rat brain.

Ago proteins, protein activator of the interferon-induced protein kinase PKR (PACT) and FMRP are proteins known to be involved in the RISC (Peters and Meister 2007; Lee et al. 2006; Jin et al. 2004). Their presence would give a first hint for the link of Stau2 and the miRNA pathway. For the IPs from E17 rat brain, all three proteins were found in the RNase elution but not in the low pH elution. This indicates that they are RNA-dependent interactors of Stau2. In more detail, two Ago isoforms and all three FMRP isoforms showed a weak signal in the Stau2 IP but none in the control. However, it was not possible to distinguish which two of the four Ago isoforms co-precipitated because of cross-reactivity of the antibody (therefore, the result is simply referred to as co-IP with Ago). The weak co-precipitation leads to the conclusion that the interaction is specific, but the abundance of these proteins in Stau2 complexes is rather low. The intensity of the PACT signal in Stau2 IP was comparable to the signal in the input and only a very faint band could be seen in the PIS IP. Therefore, the abundance of PACT in Stau2 complexes is higher than for Ago and FMRP. eIF6 was co-precipitated with Stau2 (and to a lower extent also with the PIS) and found both in the RNase and the low pH elution. This suggests a partial direct interaction with

Stau2. Recently, eIF6 has been shown to have a repressive function on mRNA translation by regulating the recruitment and joining of the large ribosomal subunit (Chendrimada et al. 2007). eIF4E and eEF1 α are factors involved in the initiation and elongation of translation. Their complete absence in Stau2 IPs is pointing to the fact that mRNAs in Stau2 complexes are not actively translated. L7a and S6, two ribosomal proteins gave information about the association of ribosomes with Stau2 complexes. L7a is found in both RNase and low pH elution, however, S6 is present just in the low pH elution. This leads to the conclusion that Stau2 directly interacts with ribosomes, in particular with ribosomal proteins, as previously suggested (Duchaine et al. 2002).

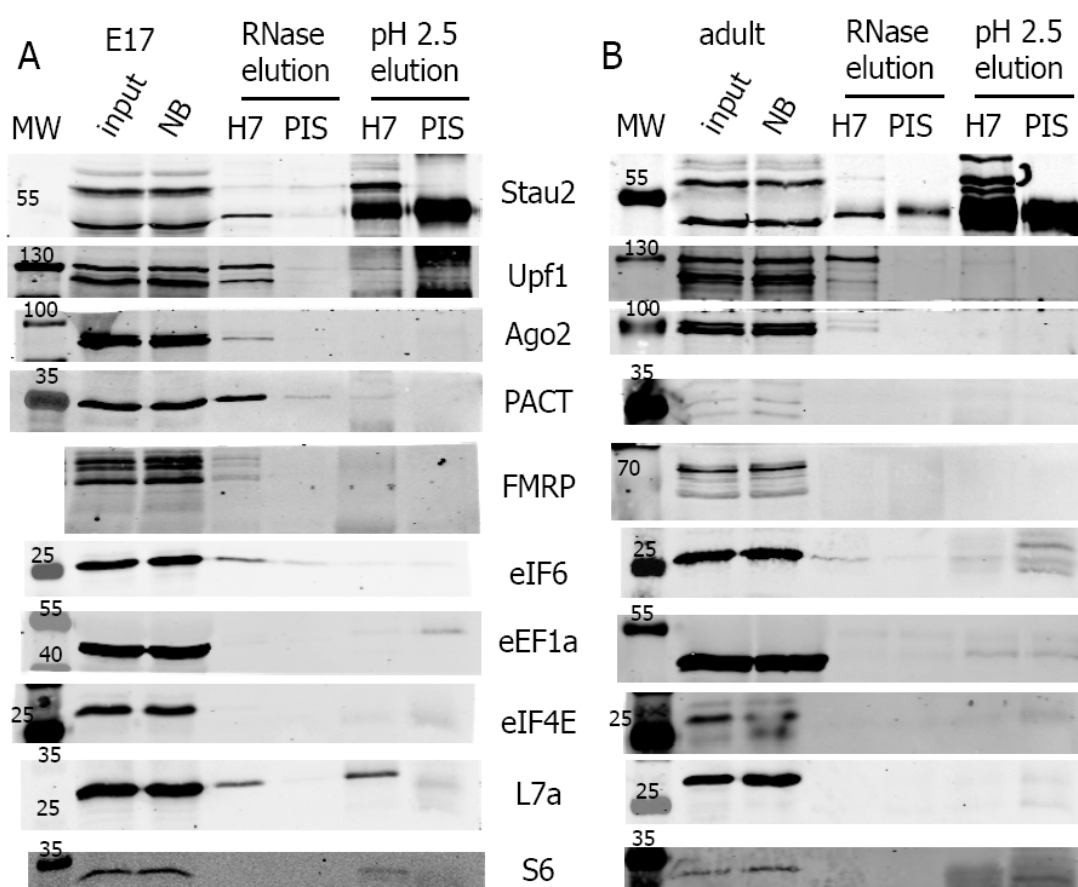


Figure 3.5 – Protein candidates in Stau2 complexes

WBs of anti-Stau2 IPs from (A) E17 and (B) adult brain lysates probed with the indicated antibodies. Input: input used for IP, NB: nonbound after IP, RNase elution: RNA was degraded and eluted proteins were collected, low pH elution: dissociates protein-protein interaction, eluate was collected. H7: anti-Stau2 antibody, PIS: negative control. The size (in kD) of the marker is depicted on top of the bands. For details see text. MW, molecular weight marker

The results for the IPs from adult rat brain were different to those from E17 rat brain. In this case, a co-precipitation was possible only with Upf1, two Ago isoforms and to a low extent also with eIF6. All these interactions were RNA-dependent. PACT and FMRP were completely absent in the adult Stau2 IP and it was also not possible to co-precipitate L7a or S6.

However, the absence of eIF4E and eEF1 α in IPs from adult rat brain proves that also in this condition, mRNAs in Stau2 complexes are not actively translated.

These differences could result from a lower IP efficiency in the adult brain. Therefore, low abundant Stau2 interactors are less likely to be found. Still, the possibility remains, that Stau2 complexes have different compositions depending on the developmental stage. The absence of the two ribosomal proteins leads to the question, whether adult Stau2 is less associated with ribosomes.

Summarizing, the IP from the adult rat brain has to be further optimized until any final conclusions concerning the differences of E17 and adult Stau2 complexes can be drawn.

3.3 RNA COMPOSITION OF STAU2 COMPLEXES

3.3.1 RNA ISOLATION FROM STAU2 RNPs

The main interest of this work was to investigate the RNA composition of Stau2 complexes, especially to search for the presence of small RNAs. For this purpose, the complexes containing Stau2 were immunoprecipitated as described in the previous section using anti-Stau2 antibodies. But instead of the two-step elution performed for detection of proteins, the beads were subjected to RNA isolation right after binding. In order to test the efficiency of the RNA isolation and the quality of the RNA obtained, a standard RNA electrophoresis of 2 μ g of RNA was performed. The quality of the RNA can be assessed by the presence of intact ribosomal RNAs, 28S rRNA (4,718 nt) and 18S rRNA (1,874 nt). Typically, the amount of 28S rRNA is twice the amount of 18S rRNA. However, the presence of rRNAs in Stau2 IP could also confirm the interaction of Stau2 with ribosomes on the RNA level. The results are shown in Figure 3.6. Three different total RNA samples were loaded: E17 PNS, adult PNS and the supernatant after 120,000 g centrifugation (S100) from E17 brains. The quality of the RNA samples was good except that the ratio between 28S/18S rRNA in the RNA from the S100 fraction was approximately 1:1. Indeed, at the bottom of the gel a cloud was visible, which could refer to degraded RNA. The reason for this can be the long storage of the RNA at -20°C before running this gel.

It is interesting to note that the amount of rRNA varies among samples. It is higher for E17 PNS compared to adult PNS, but also higher in E17 PNS compared to the S100 fraction from E17 brains. Due to the fact that the same amount of RNA was loaded, one could conclude that the ribosome content is different between E17 and adult rat brain. The variation in the rRNA amount between PNS and the S100 fraction from E17 brain results very likely from the fact that the S100 fraction is highly enriched for free cytosolic ribosomes compared to PNS, which contains membrane-associated ribosomes and polysomes too. When the IP samples are compared to the PNS samples, it is obvious that after the Stau2 IP the rRNA amount is equivalent to the PNS. This confirms the results from the protein IPs, namely the presence of L7a and S6, and therefore strongly suggests the association of Stau2 particles with ribosomes. In the control IPs with either PIS or Protein A Sepharose, only very weak or no bands for 28S and 18S rRNA were observed. This leads to the conclusion that the interaction of Stau2 with the ribosomes is specific.

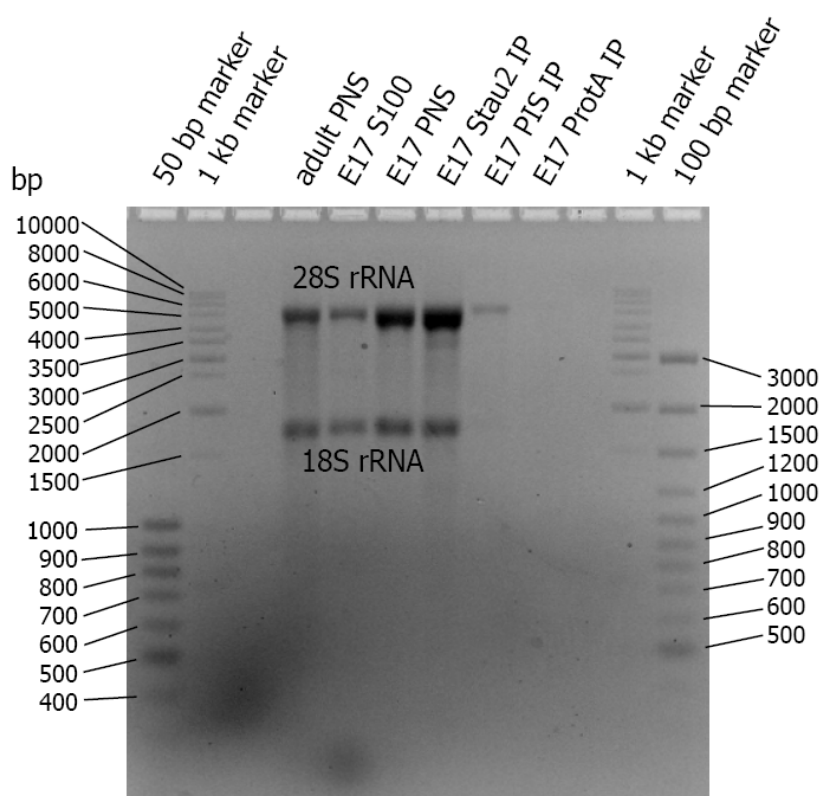


Figure 3.6 – RNA extracted from Stau2 complexes

Total RNA samples extracted from input and IPs were separated on a 1.5% denaturing agarose RNA gel containing formaldehyde. The signal for 28S (4718 nt) and 18S (1874 nt) rRNAs shows two different things: On the one hand, rRNAs were used to investigate the quality of the RNA, showing high quality of the input samples (PNS and S100). On the other hand, rRNAs are also abundant in Stau2 IP but not in the negative controls (PIS and ProtA IP).

3.3.2 RNA LABELING EXPERIMENTS – A SEARCH FOR MIRNAS

In order to clarify whether Stau2 particles contain miRNAs, a highly sensitive experimental setup to visualize small RNAs needed to be established. IP experiments with anti-Stau2 antibody were performed as described, with some modifications for subsequent optimal RNA labeling. Total RNA was isolated after IP using the *miVana*TM Kit not to lose small RNAs during the isolation procedure. Because it is not possible to visualize precise bands of small RNAs (between the size of 20 and 40 nt) on a standard agarose gel stained with ethidium bromide, it was decided to use radioactive labeling for RNA visualization. T4 RNA Ligase was used for the ATP dependent 3' labeling of RNA with cytidine 3',5'-bis [α -³²P] phosphate (pCp). The optimal composition of the labeling buffer, especially the concentration of DMSO, BSA and MgCl₂, which enhance labeling of small RNAs, was tested (data not shown). RNA was separated on a denaturing 15% polyacrylamid gel containing urea.

In Figure 3.7, the results for the labeling of RNA from IPs from E17 rat brain are shown. For comparison, two experiments are presented, in which two different Stau2 antibodies were used, directed against His-Stau2_{FL} (H7) and GST-Stau2_{CT} (R) (Figure 3.7A and B, respectively). For both antibodies, two blocking conditions, with or without yeast tRNAs to prevent unspecific RNA binding during IP, were tested. For each experiment, two different exposure times are depicted, in order to visualize also very weak signals.

The following results described in Figure 3.7 were obtained for both anti-Stau2 antibodies used. The E17 PNS represents the input used for IP. Signals from the tRNAs (80-90 nt) and presumably the 5S (120 nt) and 5.8S rRNAs (160 nt) were the most prominent labeled RNAs. In the Stau2 IP, 5S and 5.8S rRNAs were co-precipitated and exhibited the strongest signals. In control IPs with PIS or Protein A Sepharose, these RNA species were found too, but to a minor extent. It is noteworthy, that the PIS of H7 anti-Stau2 antibody gave a relatively strong background RNA signal compared to the PIS of R anti-Stau2 antibody. Thus, these results are consistent with the presence of 28S and 18S rRNAs as well as ribosomal proteins in the Stau2 IP and further support the conclusion that Stau2 complexes are associated with ribosomes.

In addition to small rRNAs, tRNAs were also co-precipitated with Stau2 beads (green asterisks). Importantly, a much higher tRNA signal was obtained in IPs where yeast tRNAs were included during blocking. There seemed to be specific RNAs of 80, 50 and 35 nt in size that co-precipitated with Stau2 but only to some extent with PIS and Protein A Sepharose

(green arrows). With a closer look at a sample of labeled yeast tRNAs alone, the pattern of the radioactive signal turned out to be similar to the one in the Stau2 IP including yeast tRNAs. The two lower bands of 50 and 30 nt in size, respectively, originate very likely from yeast tRNA degradation upon several rounds of freeze/thaw of the stock solution.

In Stau2 IP experiments without tRNAs for blocking, still RNAs at ~70 nt in size (possibly tRNAs) were co-precipitated but to a much lower extent (red asterisks). This led to the assumption that Stau2 complexes can specifically interact with structured tRNAs, however, the strength of this interaction does not resemble the situation *in vivo*. Moreover, the signal coming from degraded tRNAs could mask a signal of potential miRNAs. As a consequence of these findings, tRNAs were not used for Stau2 RNA IPs in later experiments. Alternatively, the signal at 70 nt in size could also originate from pre-miRNAs but no definite evidence can be drawn from RNA PAGE experiments.

Most interestingly, small RNAs between 50 and 20 nt in size (red arrows) were associated with Stau2 complexes. These signals were completely missing in the negative controls, therefore they can be considered as specific. For both antibodies, two bands were detected at about 22 and 40 nt in size, but weaker signals were also present at 50, 35 and for the IP with H7 antibody also at 24 nt in size. This led to the first assumption that miRNAs and another classes of small RNAs are present in Stau2 complexes in E17 rat brain.

In IPs from adult rat brain, the results were slightly different as shown in Figure 3.8. The experimental setup using two different anti-Stau2 antibodies directed against His-Stau2_{FL} (H7) and GST-Stau2_{CT} (R) (Figure 3.8A and B, respectively) was the same as for E17 brain. Also the two blocking conditions tested, with and without yeast tRNAs, as well as two different exposure times are shown.

Again, the results described hold true for both anti-Stau2 antibodies used. The use of tRNAs for blocking led to the same misleading signals (green arrows and asterisks) as in the E17 IP. Therefore, also for the adult rat brain, tRNAs were excluded from Stau2 RNA IPs.

The adult PNS shows signals from the tRNAs (80-90 nt) and presumably the 5S (120 nt) and 5.8S rRNA (160 nt). As for E17 brain, the most prominent RNAs co-precipitated in the Stau2 IP were 5S and 5.8S rRNAs as well as tRNAs (red asterisks). These results led to the conclusion that also in adult rat brain Stau2 is associated with ribosomes (in contrary to the findings on the protein level).

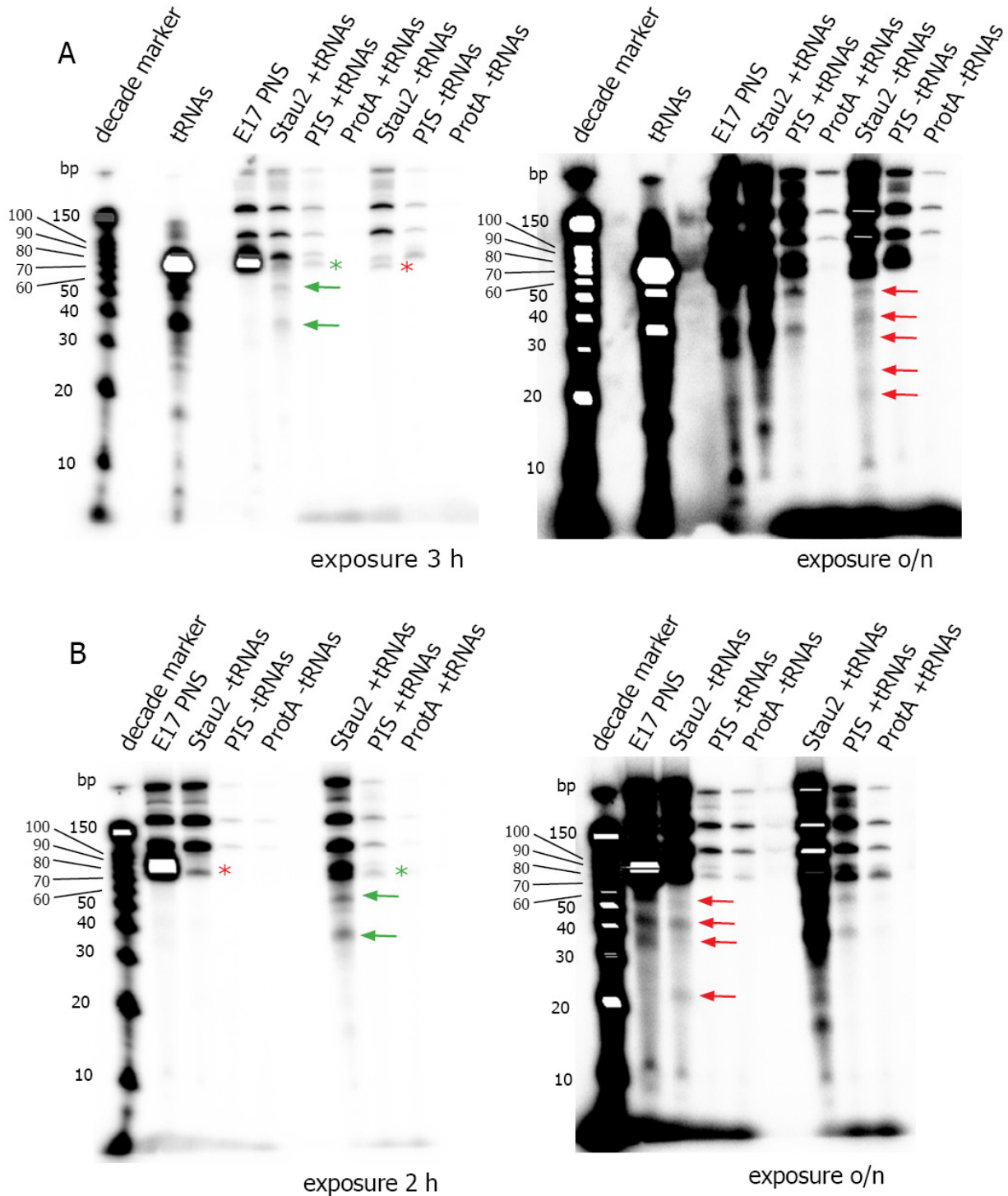


Figure 3.7 – Analysis of small RNA composition of Stau2 particles from E17 rat brain

RNA labeling with [³²P] pCp and separation on 15% denaturing (containing urea) PAGE. RNA samples were obtained from anti-Stau2 IP of E17 rat brains using the antibody from (A) rabbit H7 (anti-His-Stau2_{FL}) or (B) rabbit R (anti-GST-Stau2_{CT}). Results are shown in two different exposure times. + or -tRNAs indicates if tRNAs were used for blocking, PNS: input, Stau2: IP with anti-Stau2 antibody, PIS and ProtA: negative controls. Green arrows indicate bands resulting from tRNA blocking, red arrows indicate specific bands referring to RNAs present in Stau2 particles. The presence of miRNAs is suggested by the band at ~22 nt.

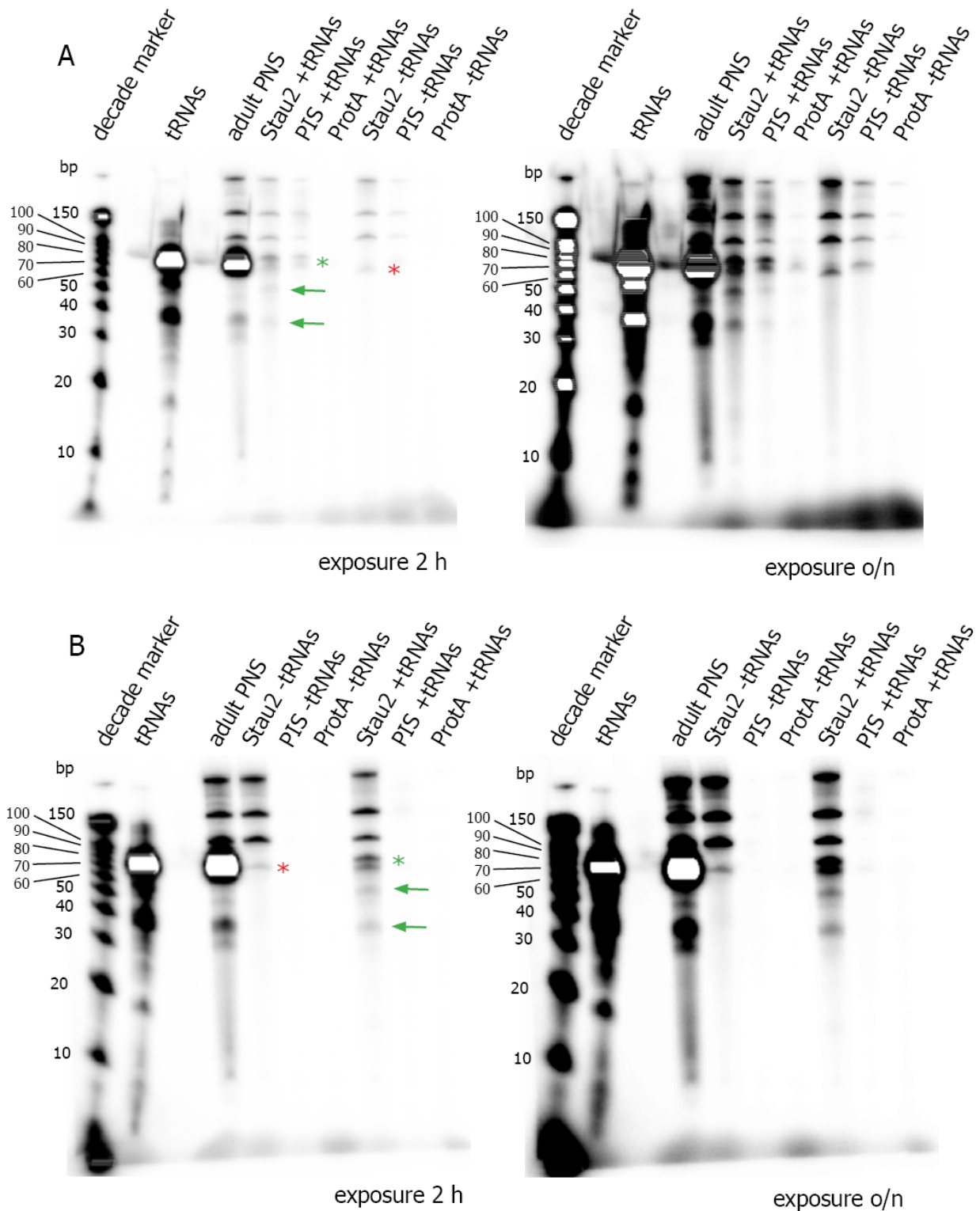


Figure 3.8 - Analysis of small RNA composition of Stau2 particles from adult rat brain

RNA labeling with [32 P] pCp and separation on 15% denaturing (containing urea) PAGE. RNA samples were obtained from anti-Stau2 IP of adult rat brains using the antibody from (A) rabbit H7 (anti-His-Stau2_{FL}) or (B) rabbit R (anti-GST-Stau2_{CT}). Results are shown in two different exposure times. + or -tRNAs indicates if tRNAs were used for blocking, PNS: input, Stau2: IP with anti-Stau2 antibody, PIS and ProtA: negative controls. Green arrows indicate bands resulting from tRNA blocking. Due to high background, no distinct bands can be seen below 50 nt in the IP samples.

Unfortunately, it was not possible to visualize small RNAs between 50 and 20 nt in size associated with Stau2 complexes. The reason for this was a high background in the Stau2 IP, which made it impossible to see distinct bands. miRNAs and other small RNAs may be present in Stau2 complexes from adult rat brain, but a reduction of the background is necessary to visualize those small RNAs. Also, the amount of RNA precipitated was lower than for the E17 brain, therefore there is still a need for optimization of the adult IP.

The results of the radioactive labeling experiments are the first indication that miRNAs but also other small RNAs might be associated with Stau2 complexes in E17 rat brain. In adult rat brain, the results are not yet clear. Altogether, the confirmation of these results with two different anti-Stau2 antibodies provides convincing evidence.

3.3.3 GEL FILTRATION EXPERIMENTS TO SEPARATE DIFFERENT STAU2 COMPLEXES

Recently, miRNAs and siRNAs were found in separate complexes in *C. elegans*, named miRNPs and siRNPs, respectively (Gu et al. 2007). They were isolated based on their different sizes by gel filtration: miRNPs appeared to fractionate at 200 kD whereas siRNPs seemed to constitute smaller, 60 kD complexes. Previous research in the Kiebler lab pioneered a similar fractionation for Stau1 and Stau2 RNPs (Mallardo et al. 2003): According to gel filtration experiments performed during this work, at least two distinct groups of Stau2-containing particles exist in adult rat brain, high molecular weight granules (above 2 MD) and smaller 700-400 kD particles. Moreover, lately even smaller complexes of Stau2, 200 kD in size, which co-fractionated with Ago and PACT proteins were observed after GF of adult rat brain extracts (A. Konecna and M. Kiebler, unpublished).

Based on these findings, the gel filtration experiments were repeated with the focus on RNA distribution, especially on detection of small RNAs in different fractions with respect to Stau2 RNPs. As input for gel filtration served the S100 supernatant from E17 rat brain which is enriched in smaller RNA-protein complexes. After gel filtration, total RNA was isolated from the fractions and subjected to the 3' labeling using pCp (Figure 3.9A). A clear enrichment of larger RNAs (>100 nt) in the fractions containing the larger complexes (fractions 4-14) and in parallel an enrichment of smaller RNAs (20-50 nt) in fractions containing smaller complexes (fractions 28-40) was observed. miRNAs were detected in fractions 30-37, which in parallel also contained Stau2 (Figure 3.9B). Interesting was the increase in signal intensity

of miRNAs and other small RNAs at 35 and 40 nt in the input (S100 fraction) compared to the PNS. If small RNAs are more abundant in this fraction, it could represent a better input for RNA IPs in order to detect miRNAs. The Western blot in Figure 3.9B showed co-fractionation of lower size Stau2 complexes with RISC marker proteins such as Ago, PACT and eIF6. These results, together with the presence of miRNAs in the same fractions, led to the hypothesis that a subset of Stau2 complexes might be associated with miRNAs and components of the RISC. However, the size of the smaller subset of Stau2 complexes was estimated to be 60 kD, what would contradict the presence of complexes, but rather suggest that they are monomers.

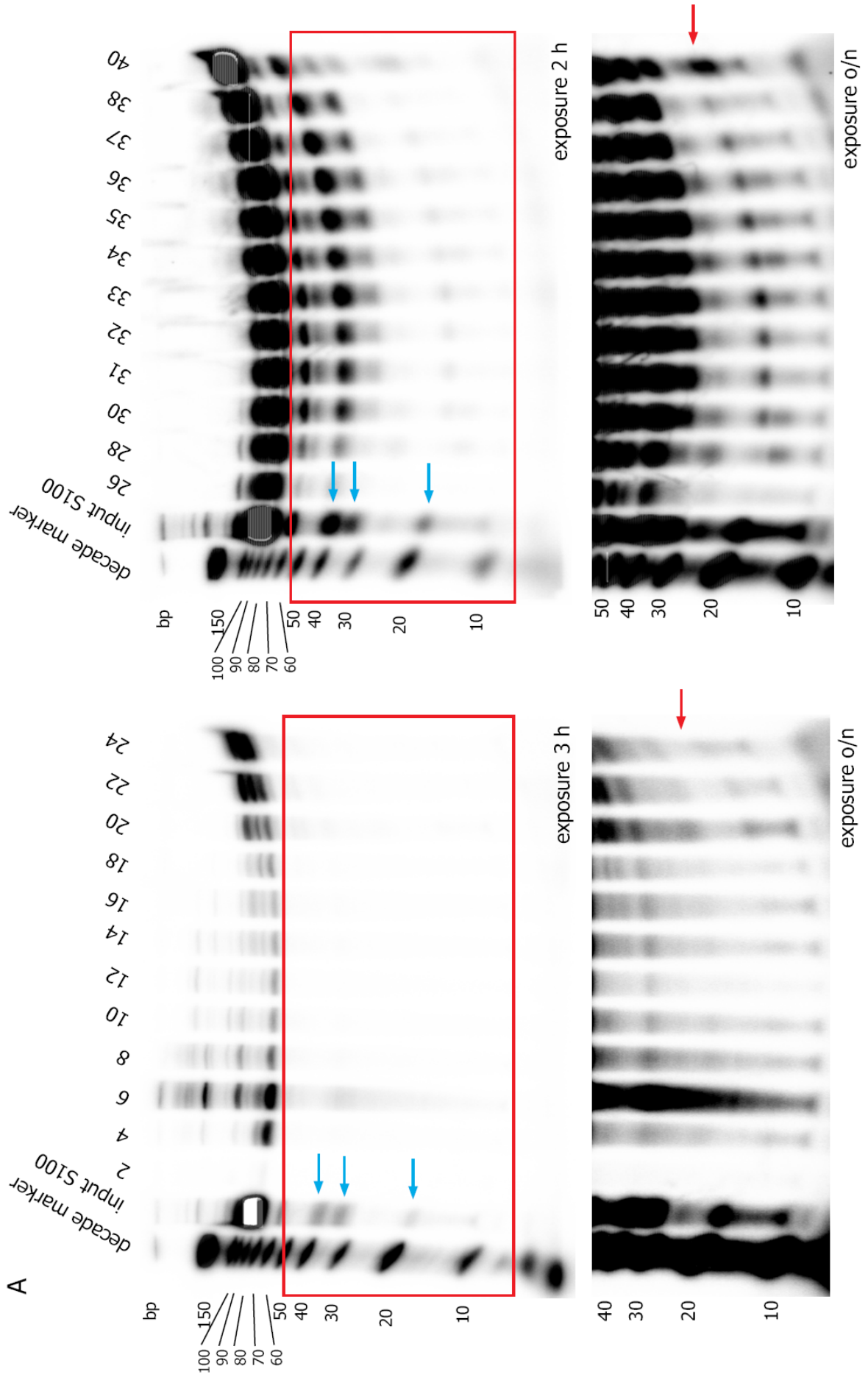
In comparison, for the adult rat brain the size of the low molecular weight complexes of Stau2 co-fractionating with Ago and PACT was estimated to be 200 kD (data not shown). This finding points to differences between Stau2 complexes in embryonic and adult brain. To further test the hypothesis of low molecular weight miRNPs, an IP was performed from the fractions obtained from E17 GF containing small Stau2 complexes (fractions 29-37), which were frozen and stored at -80°C after GF. No RNA could be detected (data not shown). Western blotting showed that Stau2 was present in the input, but no clear IP of Stau2 was seen (data not shown).

This can be explained either by that the IP did not work or it is in general not possible to perform IP from frozen gel filtration fractions due a stability problem of RNA-protein complexes. Optimization of the procedure is required in order to draw clear conclusions from this experiment.

For the distribution of small RNAs in adult rat brain, no statements can be made so far, because no signal was found for RNAs at the size of 20-25 nt (data not shown). As the level of miRNA expression is generally lower in adulthood, the experiment should be repeated with increased amounts of starting material. Furthermore, the high background has to be reduced, as discussed in section 3.3.2.

3.3.4 THE S100 FRACTION AS AN INPUT FOR LABELING EXPERIMENTS

As observed during gel filtration experiments, the S100 supernatant appears to be enriched for small RNAs (Figure 3.9A). Therefore, it may represent a better input for IP experiments to detect small RNAs. The setup of the IPs (without tRNA blocking) and the RNA labeling was performed as described in section 3.3.2.



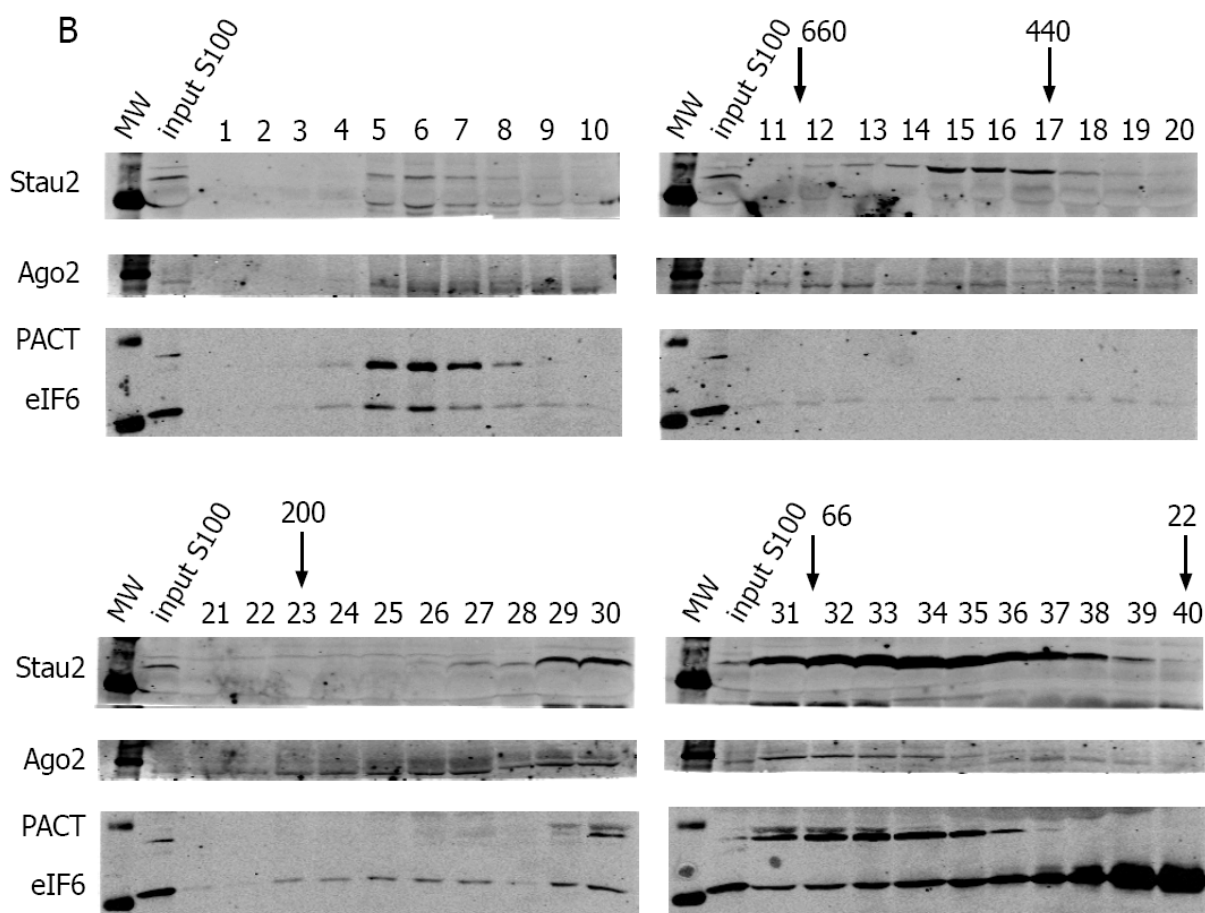


Figure 3.9 - Analysis of distribution of small RNAs by gel filtration of E17 rat brain lysate

(A) RNA labeling with [32 P] pCp and separation on 15% denaturing (containing urea) PAGE. RNA was isolated from fractions of GF (Sephacryl S-300HR) from the S100 fraction from E17 rat brains. Blue arrows indicate the small RNAs in the input. Red arrows indicate bands referring to miRNAs. An enrichment of miRNAs in fractions of lower molecular weight is visible.

(B) WB of the fractions from GF using the S100 fraction from E17 rat brain. The distribution of Stau2, Ago2, PACT and eIF6 is shown. The size of different complexes (in kD) was estimated from the elution of marker proteins and is depicted on top of the blots. A co-fractionation of Stau2 with Ago2, PACT and eIF6 was observed at 66 kD, however, the low molecular weight argues against the formation of a complex.

Figure 3.10 shows the RNA labeling after IP from the S100 fraction of E17 rat brain in two different exposure times. In parallel to the progressive enrichment for smaller RNA-protein complexes with increasing centrifugation velocity (from PNS to S40 and S100), an increase in small RNAs (blue arrows) was seen. The bands at 60, 45 and 35 nt as well as at 22 nt in size (referring to miRNAs) increased substantially in intensity in the S100 supernatant. Also in this case, two different anti-Stau2 antibodies were used for IP, purified from rabbit H7 and rabbit R, respectively. Similar to results for IPs from E17 PNS, both rRNAs and tRNAs were co-precipitated with the anti-Stau2 antibodies and to a minor extent also with the PIS and the Protein A beads.

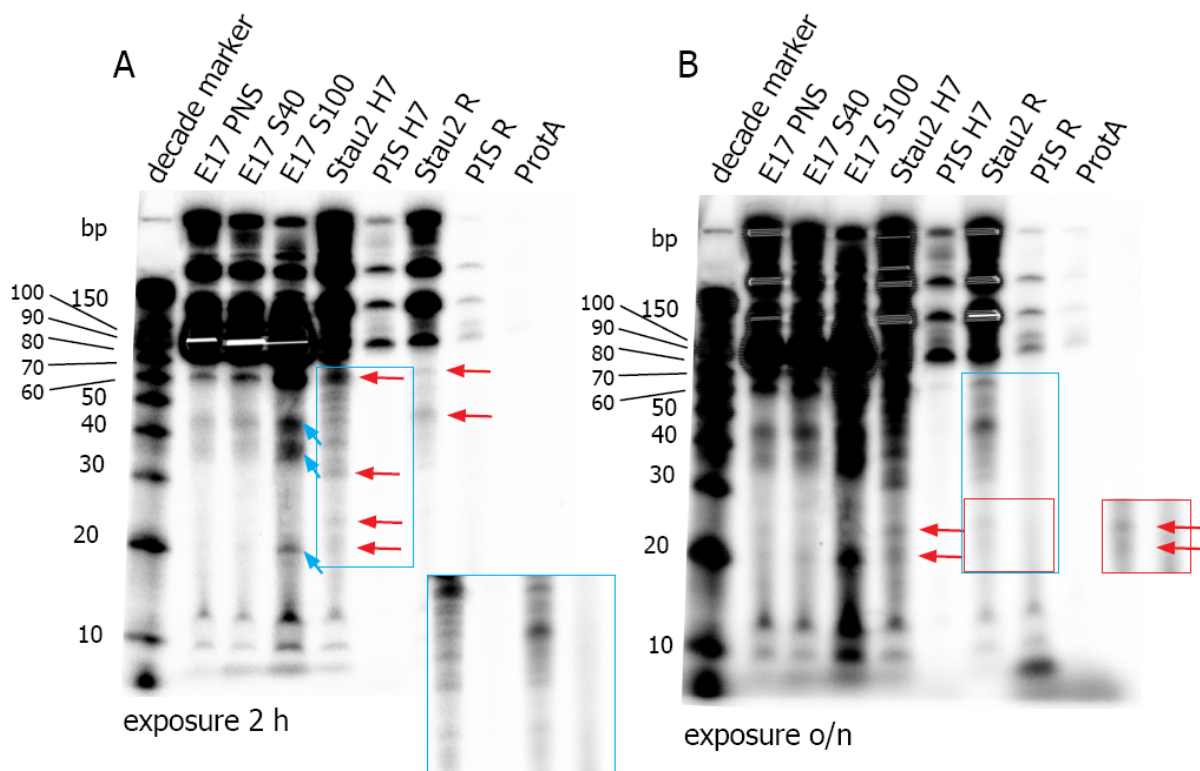


Figure 3.10 - Analysis of small RNA composition of Stau2 particles in the S100 fraction from E17 rat brain

RNA labeling with [^{32}P] pCp and separation on 15% denaturing (containing urea) PAGE. RNA samples were obtained from anti-Stau2 IP of the S100 fraction from E17 rat brains. The antibodies used, either rabbit H7 (anti-His-Stau2_{FL}) or rabbit R (anti-GST-Stau2_{CT}), are depicted on top of the lanes. Results are shown in two different exposure times: (A) 2 h, (B) o/n. S40: supernatant after spin at 40,000 g, S100: supernatant after spin at 120,000 g = input for IP, Stau2: IP with anti-Stau2 antibody, PIS and ProtA: negative controls. Blue arrows indicate the enrichment of small RNAs in the input. Red arrows indicate specific bands referring to RNAs present in Stau2 particles. In the blue box inserts of the two different Stau2 antibodies are shown for easier comparison. The presence of miRNAs is suggested by a characteristic double band at ~20/22 nt present for both antibodies.

When looking at the small RNAs between 60 and 20 nt in size (red arrows), they were again found to be associated specifically with Stau2 complexes, as the signal in the negative controls was completely missing. For rabbit H7, there were many different bands detected between 60 and 30 nt, compared to rabbit R where only two prominent bands at 60 and 45 nt were seen. In both IPs using the two antibodies, a double band between 20 and 25 nt, which is very characteristic for miRNAs, was clearly detected.

Unfortunately, it was not possible to detect small RNAs after IP from the S100 fraction from adult brain (data not shown). Again, the background was too high to see distinct bands. But also the enrichment of small RNAs, especially miRNAs, was not as prominent in the adult S100 fraction as for E17.

Taken together, these results provide evidence that miRNAs and also other small RNAs are associated with Stau2 complexes in E17 rat brain, while for adult rat brain a clear conclusion cannot be drawn yet. All results were confirmed using two different anti-Stau2 antibodies yielding similar results. Validation of these interactions by a different method was the next important step.

3.3.5 RT-PCR

The previous labeling experiments of RNA isolated from Stau2 complexes provided the first indication for the presence of miRNAs. To verify this finding, the *miVana*TM RT-PCR system from Ambion was used to validate the interaction of miRNAs with Stau2 complexes. This method allows to investigate the presence of candidate miRNAs, since it is particularly interesting to identify which miRNAs are associated with Stau2.

Five different primer sets to amplify miR-18, 26a, 128a, 134 and let7c were tested. These miRNAs were chosen based on different criteria: First, based on the PicTar software (provided by the Rajewsky lab) to predict possible miRNA – mRNA interactions. Second, based on a particular neuronal expression and known interactions with target mRNAs in neurons. miR-18 is the only predicted miRNA targeting *β-actin* mRNA, which could be an interesting issue in growth cones of embryonic neurons. On top of this, upon down-regulation of Stau2 by siRNAs, *β-actin* mRNA showed reduced expression levels (Goetze et al. 2006). miR-26a was predicted to target *CaMKIIα* and *MAP2* mRNA, which were known to be dendritically localized mRNAs in neurons (Kye et al. 2007). For investigating miRNAs in the adult brain, miR-128a was picked due to its onset of high expression in adult neurons (Kim et al. 2004). Let-7c was shown to be dendritically localized as well (Kye et al. 2007).

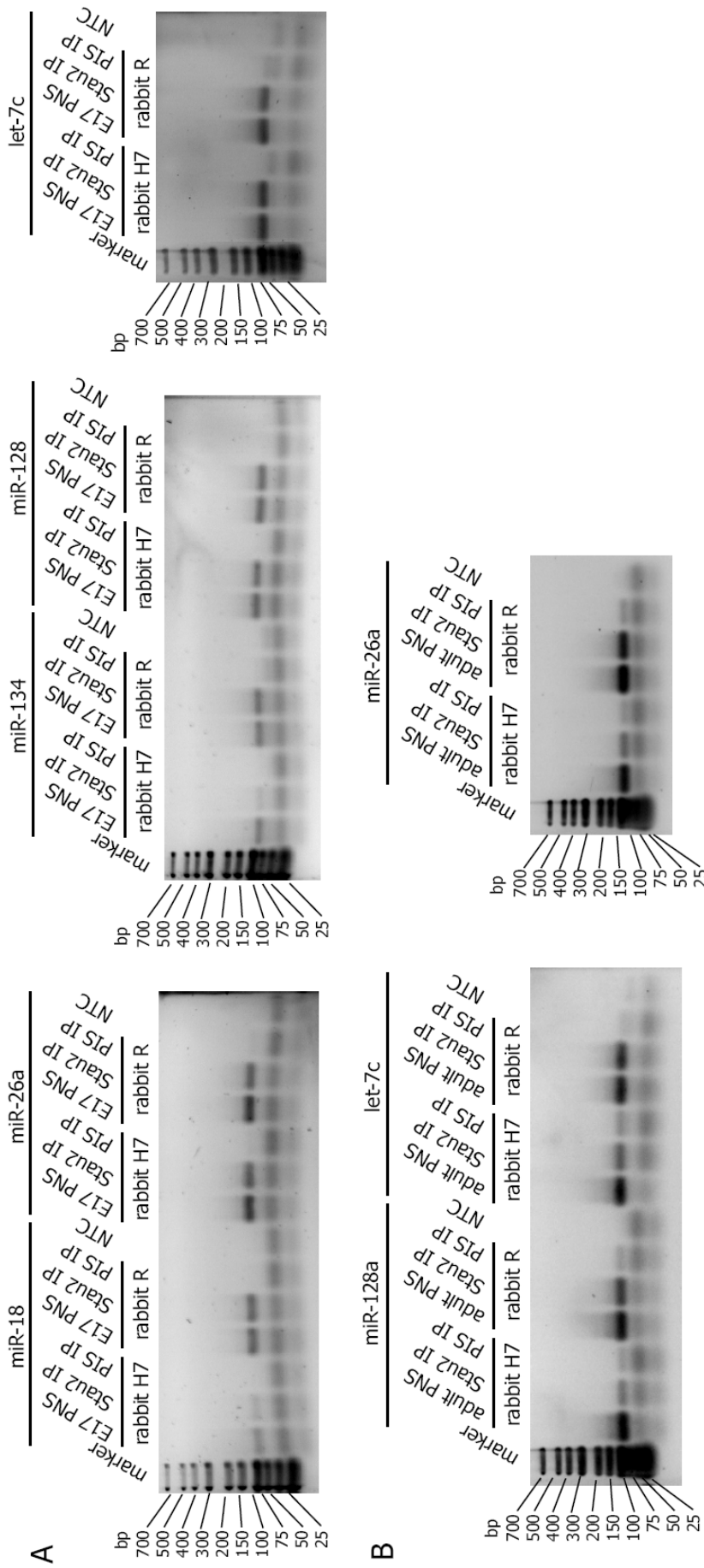


Figure 3.11 – RT-PCR – a search for candidate miRNAs in Stau2 particles

3.5% agarose gel after RT-PCR for 5 different miRNAs (miR-18, 26a, 128, 134 and let-7c), stained with SYBR gold. (A) E17 rat brain and (B) adult rat brain. RNA used as input for RT-PCR was obtained from anti-Stau2 IP using the antibody from rabbit H7 (anti-His-Stau2_{FL}) or rabbit R (anti-GST-Stau2_{CT}), as depicted in the figure. PNS: input, Stau2: IP with anti-Stau2 antibody, PIS and NTC: negative controls. Primers used are indicated on top of the gel. The bands of ~90 nt represent the PCR product of amplified miRNAs. Bands at lower size refer to PCR primers. NTC, non template control; miR, miRNA

Finally, the only validated interaction of a miRNA with a target mRNA at the synapse is the one between miR-134 and *Limk1* mRNA, therefore, miR-134 was also chosen (Schratt et al. 2006).

The *miVana*TM RT-PCR primer sets include a primer for reverse transcription and a PCR primer pair. Using this system, only mature but not pre-miRNAs are amplified. Already during reverse transcription just the indicated miRNA is transcribed with a primer consisting of a short miRNA-specific sequence and a loop structure. This yields a cDNA longer than the initial miRNA. During PCR, the cDNA is amplified with one miRNA specific primer and a second one complementary to the loop sequence, resulting in a PCR product of ~90 bp.

In Figure 3.11A, the results of RT-PCR, using the primer sets described, for IP samples from E17 rat brain are shown. Again two different antibodies were used for the Stau2 IP (rabbit H7 and R) from E17 rat brain. In general, all five tested miRNAs were expressed in the embryonic brain, as shown by the PCR product in the PNS sample. Surprisingly, all five miRNAs were amplified from the RNA of Stau2 IP samples, but not from the PIS control.

This finding was confirmed with both anti-Stau2 antibodies. This led to the conclusion that miR-18, 26a, 128a, 134 and let-7c associate with Stau2 complexes in the embryonic rat brain.

Performing RT-PCR from Stau2 IP samples from the adult rat brain showed that miR-26a, miR-128a, and let-7c were expressed (Figure 3.11B). For miR-134, however, further optimization would be necessary to reduce the formation of primer dimers. miR-18 was expressed at a very low level in adult rat brain and it could be amplified only after 35 cycles (data not shown). For the three tested miRNAs, miR-26a, miR-128a, and let-7c, the same results as for E17 were found. All three miRNAs were present in the RNA samples after Stau2 IP. For Stau2 IP using the anti-Stau2 R antibody, no or a very weak PCR product was found in the corresponding PIS control. Unfortunately, this was not the case for rabbit H7, where a weak signal was present in the PIS samples. The reason for this could be the high background in IP samples from adult brain, which was already found in the labeling experiments (see section 3.3.2). Due to the fact, that in general the PIS from rabbit R gave a lower background compared to rabbit H7, this rather reflects a problem with the specificity of the PIS from H7 than the problem of unspecific binding of anti-Stau2 antibody. Therefore, it was concluded that miR-26a, 128a, and let7c specifically associate with Stau2 complexes also in the adult rat brain.

4 DISCUSSION

4.1 PROTEIN CANDIDATES IN STAU2 COMPLEXES

Within this project, the composition of Stau2-containing complexes from rat brains was investigated using the immunoprecipitation (IP) method. A search for candidate proteins from E17 and adult rat brain yielded interesting results. The proteins tested for co-precipitation with Stau2 can be grouped as follows: mRNA decay factors, RISC-associated proteins, translational silencing and promoting factors as well as ribosomal proteins.

One important remark has to be made concerning the input material for IP experiments. Since whole rat brains were used, the input represents a mixture of different types of neurons and glia cells. Thus, the conclusions drawn hold true for rat brain but not necessarily for neurons only or even localized Stau2 complexes within cells. The big advantage of this approach, however, is that complexes from rat brain display the functions of Stau2 *in vivo*.

Cultured rat hippocampal neurons are considered to be a suitable *in vitro* system for studying neuronal processes. But since the amount of starting material needed for biochemical experiments is exceeding the possibilities of cell culture, cultured neurons are rather used for subsequent validation of the findings from rat brain.

In general, during this thesis, differences were found between results from E17 and adult rat brain, suggesting a varying protein composition of RNPs dependent on the developmental stage. This led to the hypothesis that Stau2 might have different functions through the life span of an organism. Since more protein-interactors for Stau2 were found for E17 rat brain, these differences could also result from a lower IP efficiency in the adult brain. Therefore, low abundant Stau2 interactors are less likely to be found. Optimization of the IP protocol from adult rat brain is needed before definite conclusions can be drawn.

In more detail, the results from the candidate protein search showed that Stau2 interacts with Upf1 in an RNA-dependent manner. This interaction was of high reliability, therefore it was used as a marker for successful IPs. Upf1 is an RNA helicase, involved in nonsense-mediated decay (NMD). Upf1 was further shown to interact directly with Stau1, which can recruit the helicase to the 3'-UTR of *ADP-ribosylation factor (Arf)1* and other mRNAs to elicit exon-junction complex (EJC)-independent mRNA decay (Kim et al. 2005; Kim et al. 2007).

The interaction of Upf1 with Stau2 could be of similar kind as for Stau1, being necessary for degradation of mRNAs no longer needed e.g. at the synapse.

4.1.1 STAU2 IS ASSOCIATED WITH RIBOSOMES

Previously, a connection between Stau and ribosomes has been found (Duchaine et al. 2002; Mallardo et al. 2003). Duchaine et al. reported co-sedimentation of Stau2 with ribosomal markers (L7a) and co-fractionation with 40S and 60S ribosomal subunits even after EDTA treatment, which disrupts assembled ribosomes. The group was able to co-precipitate Stau2 with a human anti-ribosomal protein antiserum. For Stau1, a co-fractionation as well as direct interaction with ribosomal protein P0 (which is an indicator for the 80S ribosome) was shown (Brendel et al. 2004). Furthermore, the interaction of Stau1 with ribosomes was mapped to the RBD3, the main dsRBD (Luo et al. 2002).

I extended those findings now by proving a direct protein-protein interaction of Stau2 with two ribosomal proteins, L7a and S6 in E17 rat brains suggesting that Stau2 may bind to the ribosome. Further support for this interaction comes from the presence of rRNAs in Stau2 complexes, namely 28S and 18S but also 5S and 5.8S rRNAs as shown in this thesis.

However, the absence of eIF4E and eEF1 α , factors involved in initiation and elongation of translation, in IPs from E17 and adult rat brain supports the idea that mRNAs in Stau2 complexes are not actively translated despite the presence of ribosomes. Consistent with these findings, it was shown that association of Stau2 with ribosomes is independent of translation (Duchaine et al. 2002).

The functional relevance for association of Stau2 with ribosomes remains to be investigated. As postulated by Krichevsky and Kosik, synaptic stimulation may cause a local release of mRNA and translational components (including ribosomes) from granules at the synapse linking RNA localization to translation (Krichevsky and Kosik 2001). Thus, a possible reason for association of Stau2 with ribosomes could simply be localizing ribosomes for immediate translation of mRNAs at their destination site.

Other means by which ribosomes can play a role in Stau2 complexes originate from the finding that the dsRBD5 of Stau2 was involved in activating the translation of *oskar* mRNA in *D. melanogaster* (Micklem et al. 2000). Since the RBD5 is not able to bind RNA, the effect on translational activation is very likely mediated via protein interaction with Stau2. One could speculate that ribosomal proteins may play a role in this regulation.

4.1.2 RISC PROTEINS IN STAU2 COMPLEXES

Furthermore, using the candidate protein search, I found evidence that Stau2 complexes contain molecules involved in silencing mRNAs. IP experiments proved the RNA-dependent interaction of Stau2 with Ago and PACT in E17 rat brain. Ago and PACT are proteins known to be associated with the RISC (Peters and Meister 2007; Lee et al. 2006). Additional support for this hypothesis came from the finding that FMRP and eIF6 also represent interactors of Stau2 complexes in E17 rat brain and for eIF6 also in adult rat brain. eIF6 and FMRP were postulated to be associated with the RISC and have repressive functions on mRNA translation (Chendrimada et al. 2007; Jin et al. 2004). Taken together, these findings are consistent with the idea of mRNAs being repressed in Stau2 complexes and not actively translated. Thus, FMRP and eIF6 could contribute to silencing of mRNAs in Stau2 complexes. Since all four proteins are part of miRNPs/RISC, the silencing could be a result of RISC recruitment to the particles.

The presence of different RISC-associated components, Ago, PACT, FMRP and eIF6 in Stau2 complexes suggests a participation of the miRNA pathway. The relevance of these findings is versatile. On the one hand, as mentioned above, the need for silencing mRNAs in Stau2 complexes could lead to recruitment of RISC from the cytoplasm to Stau2 complexes. On the other hand, one could propose exchange of mRNA or other components between Stau2-containing RNPs and P-bodies, which are known to contain RISC components (Wu and Belasco 2008). This hypothesis was derived from the finding of transient “docking” events between Stau2 and Dcp1-containing particles, observed by time-lapse videomicroscopy (Zeitelhofer et al. 2008, in press). These “docking” events could build the basis for exchange of components, leading to a hypothesis of a very complex interplay between different particles.

4.2 RNA COMPOSITION OF STAU2 COMPLEXES

4.2.1 MIRNAS ARE ASSOCIATED WITH STAU2 COMPLEXES

Additional evidence supporting the involvement of miRNAs in Stau2 complexes was provided by RNA labeling experiments. I observed a specific association of small RNAs between 50 and 20 nt with Stau2 complexes in E17 rat brain, especially a prominent band at ~22 nt, which refers to mature miRNAs. Using the high-speed centrifugation supernatant (S100) as input for the IP, I detected a double-band at 20/22 nt, which is very characteristic for

miRNAs. Specific amplification of candidate miRNAs, miR-18, 26a, 128a, 134 and let-7c, by RT-PCR proved unequivocally the presence of mature miRNAs in Stau2 complexes. For adult rat brain, no distinct bands for miRNAs could be visualized during labeling experiments due to a high background signal. However, RT-PCR successfully proved the association of miR-26a, 128a and let-7c with Stau2 complexes. miR-18 was expressed only at very low levels in adult rat brain and for miR-134 problems with primer-dimers arose. The identity of other small RNAs of higher size (30 – 50 nt) detected in Stau2 complexes by labeling experiments is still unclear. Subsequent cloning approaches will clarify their origin.

The fact that miRNAs interact with Stau2 complexes raises different hypotheses concerning the biological relevance. First, miRNAs could function in silencing of mRNA present in Stau2 complexes. It was shown that Stau1-containing RNPs move along microtubules from the cell body into dendrites, suggesting a functional role of Stau proteins in the dendritic localization of mRNAs (Köhrmann et al. 1999). Assuming that Stau2 plays a role in mRNA transport too, miRNAs provide one possibility of repressing translation during this process. Up to now there is only one published example, showing that miRNAs can play a crucial role in silencing mRNAs at the synapse. Namely, the translation of *Limk1*, a localized mRNA, which was shown to be affected by miR-134 (Schratt et al. 2006).

The fact that 5 out of 5 tested candidate miRNAs were present in Stau2 complexes was surprising at first glance. However, preliminary microarray data of the mRNA composition of Stau2 particles in E17 rat brain (A. Konecna, M. Bilban and M. Kiebler, unpublished) yielded more than 2000 different mRNAs. Provided that one particular mRNA may be regulated by different miRNAs, I expect several miRNAs to be present in Stau2 complexes. Combining these two findings, the significance of miRNAs in silencing mRNAs in RNPs might have been underestimated so far.

With a closer look at those 5 tested miRNAs, more detailed hypotheses are possible. Using PicTar (provided by the Rajewsky lab), *β -actin* mRNA was the only predicted target for miR-18. First, this mRNA was found to undergo Stau2-dependent regulation (Goetze et al. 2006; Y. Xi, P. Macchi and M. Kiebler, unpublished) and second, its presence in Stau2-containing complexes was shown (D.Karra, 2008, PhD thesis). Furthermore, actin plays a crucial role in formation and migration of neurites and the growth cone (Yao et al. 2006; Leung et al. 2006). Therefore, the presence of miR-18 in E17 Stau2 complexes leads to the assumption that translation of *β -actin* mRNA in Stau2 particles could be silenced by miR-18. miR-26a, 128a, 134 and let-7c were found in dendrites using a laser-capture based multiplex RT-PCR approach (Kye et al. 2007). In addition, miR-134 was shown to target *Limk1* and

miR-26a to target *MAP2*, respectively (Schratt et al. 2006; Kye et al. 2007). The presence of these two mRNAs in Stau2 granules (A. Konecna and M. Kiebler, unpublished; D. Karra, 2008, PhD thesis) yields two more possible pairs of mRNA-miRNA duplexes in Stau2 complexes. miR-128a, enriched in adult rat brain (Kim et al. 2004), was amplified from both developmental stages; the same was true for let-7c. Predicted targets for these miRNAs were of notable diversity. Therefore, no conclusions about possible pairs could be drawn at this stage. Still, for all miRNAs found in Stau2 complexes additional validation experiments are necessary, which are discussed in the future perspectives.

The fact that ribosomes are part of Stau2 complexes does not contradict the association with miRNAs. First, mRNAs are thought to be silenced within particles (Dahm and Kiebler 2005). Second, evidence was found that miRNAs co-purify with polysomes in a human neuronal cell line (Nelson et al. 2004) and in mammalian neurons (Kim et al. 2004). A model can be envisioned where mRNAs, miRNAs, ribosomes and Stau2 are present in one complex: The mRNA, covered by ribosomes, is silenced by a miRNA bound to its 3'-UTR. Stau2 associates either via direct binding to the ribosome or also to the 3'-UTR of the mRNA.

4.2.2 MIRNAS IN DIFFERENT STAU2 COMPLEXES

Previous gel filtration experiments in the lab allowed to distinguish distinct pools of Stau2-containing particles in adult rat brain: high molecular weight granules (above 2 MD) and smaller 700-400 kD particles (Mallardo et al. 2003); as well as smaller complexes of 200 kD, (A. Konecna and M. Kiebler, unpublished). Therefore, it was of great interest, in which Stau2-containing complexes miRNAs are present. Recently, miRNPs were shown to be rather small complexes of ~200 kD that differ from siRNA complexes (Gu et al. 2007).

I therefore performed gel filtration experiments, which aimed at separation of Stau2-containing complexes of different sizes and monitoring the association of miRNAs within these complexes. Results for E17 rat brain suggested that in low molecular weight complexes, Stau2 might be associated with miRNAs and components of the RISC. For adult rat brain, Stau2 co-fractionation with Ago and PACT in low molecular weight complexes was found too. However, at the RNA level, detection of miRNAs was not possible due to a high background. The main difference between the results of E17 and adult rat brain was the estimated size of these low molecular weight particles: 200 kD for adult, which corresponds to the results from Gu et al. 2007; but just 60 kD for E17. The small size of 60 kD would contradict the existence of particles, but rather suggests monomers. Clearly, these

differences between E17 and adult RISC and miRNA co-fractionating Stau2 complexes have to be further investigated before definite conclusions can be drawn.

4.2.3 STAU2 AND EXPORT OF PRE-MIRNAS

Stau2 was shown to be transported by the same export factor Exportin-5 which is involved in pre-miRNA export from the nucleus (Macchi et al. 2004). Since Stau2 interacts with stem-loop structures containing 12 uninterrupted base pairs *in vitro* (Ramos et al. 2000) and pre-miRNAs are folded into hairpin structures these findings are of great interest. In addition, Stau2 export was shown to depend on dsRNA mediating the interaction with Exp-5 (Macchi et al. 2004). Thus, a second function for Stau2 in the miRNA pathway emerges: Stau2 may play a role in binding pre-miRNAs and facilitating their export. However, direct evidence for pre-miRNAs in Stau2 complexes is still missing. First, the RT-PCR system from Ambion is designed to amplify mature miRNAs only. Second, the detection of RNAs at 70 nt in size by radioactive labeling can only indirectly refer to pre-miRNAs and might also be overlaid by the signal of tRNAs of the same size (70-90 nt). Thus, pre-miRNA detection by Northern blotting or RT-PCR is an immediate goal that is discussed below in the future perspectives.

4.3 FUTURE PERSPECTIVES

Since the association of Stau2 complexes with miRNAs was shown for some candidates, the immediate question to be asked is: How many and which miRNAs are present in Stau2 complexes? Therefore, I would like to obtain a detailed list of all interacting miRNAs in E17 or adult rat brain by cloning miRNAs from Stau2 IPs followed by subsequent sequencing. The obtained list of miRNAs will then allow us to compare them to microarray data for mRNAs (A. Konecna and M. Kiebler, unpublished) using a bioinformatics approach. Finally, detailed knowledge about the composition of RNAs in Stau2 complexes will result in the identification of additional mRNA-miRNA pairs in the near future.

Furthermore, I expect that the cloning approach will shed some light on the origin of other small RNAs of bigger size (30-50 nt) that were specifically found in the Stau2 complexes.

Validation of the interacting miRNAs found in those experiments will be important since the possibility of post-lysis interactions cannot be excluded (Mali and Steitz 2004). Such validation experiments can be carried out in cultured rat hippocampal neurons. First, *in situ* hybridization for miRNAs using locked nucleic acid (LNA) probes can answer the question if

these miRNAs are expressed and especially how they are distributed in neurons. Subsequent co-staining in neurons for Stau2 and miRNAs of interest can validate their association.

Furthermore, it will be important to investigate the presumable role of Stau2 in the export of pre-miRNAs. This can be achieved by Northern blotting, where, according to the size of the signal, mature, pri- and pre-miRNAs can be distinguished. As a second approach, RT-PCR with primers specific for pre-miRNA but not mature miRNAs could further clarify the association of Stau2 with pre-miRNAs.

One of the main questions left is in which RNPs Stau2 and miRNAs associate. To follow up on the preliminary results from the gel filtration experiments, these should be repeated to confirm the differences in size of small, RISC co-fractionating, Stau2 particles between E17 and adult. IP experiments need to be performed from a pool of large versus small Stau2 complexes from both developmental stages to investigate differences in protein composition. In case gel filtration experiments are not successful, attention can also be put on using density gradients for separating Stau2 particles of different sizes as done before (Mallardo et al. 2003).

Overall, the presence of miRNAs in Stau2 complexes from E17 and adult rat brain was shown within this thesis. A very interesting question left is the biological function of Stau2 in the miRNA pathway, which for sure will turn into a promising but also challenging project.

5 REFERENCES

- Aakalu, G., Smith, W. B., Nguyen, N., Jiang, C. and Schuman, E. M. (2001). "Dynamic visualization of local protein synthesis in hippocampal neurons." *Neuron* **30**(2): 489-502.
- Anderson, P. and Kedersha, N. (2006). "RNA granules." *J Cell Biol* **172**(6): 803-8.
- Ashraf, S. I., McLoon, A. L., Sclarsic, S. M. and Kunes, S. (2006). "Synaptic protein synthesis associated with memory is regulated by the RISC pathway in *Drosophila*." *Cell* **124**(1): 191-205.
- Bamburg, J. R. (1999). "Proteins of the ADF/cofilin family: essential regulators of actin dynamics." *Annu Rev Cell Dev Biol* **15**: 185-230.
- Bensadoun, A. and Weinstein, D. (1976). "Assay of proteins in the presence of interfering materials." *Anal Biochem* **70**(1): 241-50.
- Bhattacharyya, S. N., Habermacher, R., Martine, U., Closs, E. I. and Filipowicz, W. (2006). "Relief of microRNA-mediated translational repression in human cells subjected to stress." *Cell* **125**(6): 1111-24.
- Brendel, C., Rehbein, M., Kreienkamp, H. J., Buck, F., Richter, D. and Kindler, S. (2004). "Characterization of Staufen 1 ribonucleoprotein complexes." *Biochem J* **384**(Pt 2): 239-46.
- Brennan, C. M. and Steitz, J. A. (2001). "HuR and mRNA stability." *Cell Mol Life Sci* **58**(2): 266-77.
- Brennecke, J., Stark, A., Russell, R. B. and Cohen, S. M. (2005). "Principles of microRNA-target recognition." *PLoS Biol* **3**(3): e85.
- Caudy, A. A., Ketting, R. F., Hammond, S. M., Denli, A. M., Bathorn, A. M., Tops, B. B., Silva, J. M., Myers, M. M., Hannon, G. J. and Plasterk, R. H. (2003). "A micrococcal nuclease homologue in RNAi effector complexes." *Nature* **425**(6956): 411-4.
- Caudy, A. A., Myers, M., Hannon, G. J. and Hammond, S. M. (2002). "Fragile X-related protein and VIG associate with the RNA interference machinery." *Genes Dev* **16**(19): 2491-6.
- Chang, Y. F., Imam, J. S. and Wilkinson, M. F. (2007). "The nonsense-mediated decay RNA surveillance pathway." *Annu Rev Biochem* **76**: 51-74.
- Chendrimada, T. P., Finn, K. J., Ji, X., Baillat, D., Gregory, R. I., Liebhaber, S. A., Pasquinelli, A. E. and Shiekhattar, R. (2007). "MicroRNA silencing through RISC recruitment of eIF6." *Nature*.
- Chu, C. Y. and Rana, T. M. (2006). "Translation repression in human cells by microRNA-induced gene silencing requires RCK/p54." *PLoS Biol* **4**(7): e210.
- Dahm, R. and Kiebler, M. (2005). "Cell biology: silenced RNA on the move." *Nature* **438**(7067): 432-5.
- Dahm, R., Kiebler, M. and Macchi, P. (2007). "RNA localisation in the nervous system." *Semin Cell Dev Biol*.
- Davis, H. P. and Squire, L. R. (1984). "Protein synthesis and memory: a review." *Psychol Bull* **96**(3): 518-59.
- Doench, J. G. and Sharp, P. A. (2004). "Specificity of microRNA target selection in translational repression." *Genes Dev* **18**(5): 504-11.
- Dubnau, J., Chiang, A. S., Grady, L., Barditch, J., Gossweiler, S., McNeil, J., Smith, P., Buldoc, F., Scott, R., Certa, U., Broger, C. and Tully, T. (2003). "The staufen/pumilio pathway is involved in *Drosophila* long-term memory." *Curr Biol* **13**(4): 286-96.

- Duchaine, T. F., Hemraj, I., Furic, L., Deitinghoff, A., Kiebler, M. A. and DesGroseillers, L. (2002). "Staufen2 isoforms localize to the somatodendritic domain of neurons and interact with different organelles." *J Cell Sci* **115**(Pt 16): 3285-95.
- Filipowicz, W., Bhattacharyya, S. N. and Sonenberg, N. (2008). "Mechanisms of post-transcriptional regulation by microRNAs: are the answers in sight?" *Nat Rev Genet* **9**(2): 102-14.
- Filipowicz, W., Jaskiewicz, L., Kolb, F. A. and Pillai, R. S. (2005). "Post-transcriptional gene silencing by siRNAs and miRNAs." *Curr Opin Struct Biol* **15**(3): 331-41.
- Giraldez, A. J., Cinalli, R. M., Glasner, M. E., Enright, A. J., Thomson, J. M., Baskerville, S., Hammond, S. M., Bartel, D. P. and Schier, A. F. (2005). "MicroRNAs regulate brain morphogenesis in zebrafish." *Science* **308**(5723): 833-8.
- Giraldez, A. J., Mishima, Y., Rihel, J., Grocock, R. J., Van Dongen, S., Inoue, K., Enright, A. J. and Schier, A. F. (2006). "Zebrafish MiR-430 promotes deadenylation and clearance of maternal mRNAs." *Science* **312**(5770): 75-9.
- Goetze, B., Tuebing, F., Xie, Y., Dorostkar, M. M., Thomas, S., Pehl, U., Boehm, S., Macchi, P. and Kiebler, M. A. (2006). "The brain-specific double-stranded RNA-binding protein Staufen2 is required for dendritic spine morphogenesis." *J Cell Biol* **172**(2): 221-31.
- Grimson, A., Farh, K. K., Johnston, W. K., Garrett-Engele, P., Lim, L. P. and Bartel, D. P. (2007). "MicroRNA targeting specificity in mammals: determinants beyond seed pairing." *Mol Cell* **27**(1): 91-105.
- Grosshans, H. and Filipowicz, W. (2008). "Molecular biology: the expanding world of small RNAs." *Nature* **451**(7177): 414-6.
- Gu, S. G., Pak, J., Barberan-Soler, S., Ali, M., Fire, A. and Zahler, A. M. (2007). "Distinct ribonucleoprotein reservoirs for microRNA and siRNA populations in *C. elegans*." *Rna* **13**(9): 1492-504.
- Gu, W., Pan, F., Zhang, H., Bassell, G. J. and Singer, R. H. (2002). "A predominantly nuclear protein affecting cytoplasmic localization of beta-actin mRNA in fibroblasts and neurons." *J Cell Biol* **156**(1): 41-51.
- Haase, A. D., Jaskiewicz, L., Zhang, H., Laine, S., Sack, R., Gatignol, A. and Filipowicz, W. (2005). "TRBP, a regulator of cellular PKR and HIV-1 virus expression, interacts with Dicer and functions in RNA silencing." *EMBO Rep* **6**(10): 961-7.
- He, L. and Hannon, G. J. (2004). "MicroRNAs: small RNAs with a big role in gene regulation." *Nat Rev Genet* **5**(7): 522-31.
- Hengst, U., Cox, L. J., Macosko, E. Z. and Jaffrey, S. R. (2006). "Functional and selective RNA interference in developing axons and growth cones." *J Neurosci* **26**(21): 5727-32.
- Hüttelmaier, S., Zenklusen, D., Lederer, M., Dichtenberg, J., Lorenz, M., Meng, X., Bassell, G. J., Condeelis, J. and Singer, R. H. (2005). "Spatial regulation of beta-actin translation by Src-dependent phosphorylation of ZBP1." *Nature* **438**(7067): 512-5.
- Jin, P., Zarnescu, D. C., Ceman, S., Nakamoto, M., Mowrey, J., Jongens, T. A., Nelson, D. L., Moses, K. and Warren, S. T. (2004). "Biochemical and genetic interaction between the fragile X mental retardation protein and the microRNA pathway." *Nat Neurosci* **7**(2): 113-7.
- Jones-Rhoades, M. W., Bartel, D. P. and Bartel, B. (2006). "MicroRNAs and their regulatory roles in plants." *Annu Rev Plant Biol* **57**: 19-53.

- Karra, D. (2008). Isolierung und Charakterisierung von Staufen- und Barentsz- enthaltenden Ribonukleoproteinpartikeln aus Rattenhirn, Eberhard Karls Universität Tübingen, PhD thesis.
- Kedde, M., Strasser, M. J., Boldajipour, B., Vrielink, J. A., Slanchev, K., le Sage, C., Nagel, R., Voorhoeve, P. M., van Duijse, J., Orom, U. A., Lund, A. H., Perrakis, A., Raz, E. and Agami, R. (2007). "RNA-binding protein Dnd1 inhibits microRNA access to target mRNA." *Cell* **131**(7): 1273-86.
- Kiebler, M. A. and Bassell, G. J. (2006). "Neuronal RNA granules: movers and makers." *Neuron* **51**(6): 685-90.
- Kiebler, M. A., Hemraj, I., Verkade, P., Kohrmann, M., Fortes, P., Marion, R. M., Ortin, J. and Dotti, C. G. (1999). "The mammalian staufen protein localizes to the somatodendritic domain of cultured hippocampal neurons: implications for its involvement in mRNA transport." *J Neurosci* **19**(1): 288-97.
- Kim, J., Krichevsky, A., Grad, Y., Hayes, G. D., Kosik, K. S., Church, G. M. and Ruvkun, G. (2004). "Identification of many microRNAs that copurify with polyribosomes in mammalian neurons." *Proc Natl Acad Sci U S A* **101**(1): 360-5.
- Kim, Y. K., Furic, L., Desgroseillers, L. and Maquat, L. E. (2005). "Mammalian Staufen1 recruits Upf1 to specific mRNA 3'UTRs so as to elicit mRNA decay." *Cell* **120**(2): 195-208.
- Kim, Y. K., Furic, L., Parisien, M., Major, F., Desgroseillers, L. and Maquat, L. E. (2007). "Staufen1 regulates diverse classes of mammalian transcripts." *EMBO J* **26**: 2670-81.
- Kiriakidou, M., Tan, G. S., Lamprinaki, S., De Planell-Saguer, M., Nelson, P. T. and Mourelatos, Z. (2007). "An mRNA m(7)G Cap Binding-like Motif within Human Ago2 Represses Translation." *Cell*.
- Köhrmann, M., Luo, M., Kaether, C., DesGroseillers, L., Dotti, C. G. and Kiebler, M. A. (1999). "Microtubule-dependent recruitment of Staufen-green fluorescent protein into large RNA-containing granules and subsequent dendritic transport in living hippocampal neurons." *Mol Biol Cell* **10**(9): 2945-53.
- Kosik, K. S. (2006). "The neuronal microRNA system." *Nat Rev Neurosci* **7**(12): 911-20.
- Krichevsky, A. M. and Kosik, K. S. (2001). "Neuronal RNA granules: a link between RNA localization and stimulation-dependent translation." *Neuron* **32**(4): 683-96.
- Krichevsky, A. M., Sonntag, K. C., Isacson, O. and Kosik, K. S. (2006). "Specific microRNAs modulate embryonic stem cell-derived neurogenesis." *Stem Cells* **24**(4): 857-64.
- Kye, M. J., Liu, T., Levy, S. F., Xu, N. L., Groves, B. B., Bonneau, R., Lao, K. and Kosik, K. S. (2007). "Somatodendritic microRNAs identified by laser capture and multiplex RT-PCR." *Rna* **13**(8): 1224-34.
- Laemmli, U. K. (1970). "Cleavage of structural proteins during the assembly of the head of bacteriophage T4." *Nature* **227**(5259): 680-5.
- Lee, Y., Hur, I., Park, S. Y., Kim, Y. K., Suh, M. R. and Kim, V. N. (2006). "The role of PACT in the RNA silencing pathway." *Embo J* **25**(3): 522-32.
- Leung, K. M., van Horck, F. P., Lin, A. C., Allison, R., Standart, N. and Holt, C. E. (2006). "Asymmetrical beta-actin mRNA translation in growth cones mediates attractive turning to netrin-1." *Nat Neurosci* **9**(10): 1247-56.
- Liu, Q., Rand, T. A., Kalidas, S., Du, F., Kim, H. E., Smith, D. P. and Wang, X. (2003). "R2D2, a bridge between the initiation and effector steps of the Drosophila RNAi pathway." *Science* **301**(5641): 1921-5.

- Luo, M., Duchaine, T. F. and DesGroseillers, L. (2002). "Molecular mapping of the determinants involved in human Staufen-ribosome association." *Biochem J* **365**(Pt 3): 817-24.
- Macchi, P., Brownawell, A. M., Grunewald, B., DesGroseillers, L., Macara, I. G. and Kiebler, M. A. (2004). "The brain-specific double-stranded RNA-binding protein Staufen2: nucleolar accumulation and isoform-specific exportin-5-dependent export." *J Biol Chem* **279**(30): 31440-4.
- Mallardo, M., Deitinghoff, A., Muller, J., Goetze, B., Macchi, P., Peters, C. and Kiebler, M. A. (2003). "Isolation and characterization of Staufen-containing ribonucleoprotein particles from rat brain." *Proc Natl Acad Sci U S A* **100**(4): 2100-5.
- Maroney, P. A., Yu, Y., Fisher, J. and Nilsen, T. W. (2006). "Evidence that microRNAs are associated with translating messenger RNAs in human cells." *Nat Struct Mol Biol* **13**(12): 1102-7.
- Meister, G., Landthaler, M., Patkaniowska, A., Dorsett, Y., Teng, G. and Tuschl, T. (2004). "Human Argonaute2 mediates RNA cleavage targeted by miRNAs and siRNAs." *Mol Cell* **15**(2): 185-97.
- Micklem, D. R., Adams, J., Grunert, S. and St Johnston, D. (2000). "Distinct roles of two conserved Staufen domains in oskar mRNA localization and translation." *Embo J* **19**(6): 1366-77.
- Mili, S. and Steitz, J. A. (2004). "Evidence for reassociation of RNA-binding proteins after cell lysis: implications for the interpretation of immunoprecipitation analyses." *Rna* **10**(11): 1692-4.
- Monshausen, M., Putz, U., Rehbein, M., Schweizer, M., DesGroseillers, L., Kuhl, D., Richter, D. and Kindler, S. (2001). "Two rat brain staufen isoforms differentially bind RNA." *J Neurochem* **76**(1): 155-65.
- Montarolo, P. G., Goelet, P., Castellucci, V. F., Morgan, J., Kandel, E. R. and Schacher, S. (1986). "A critical period for macromolecular synthesis in long-term heterosynaptic facilitation in *Aplysia*." *Science* **234**(4781): 1249-54.
- Mourelatos, Z., Dostie, J., Paushkin, S., Sharma, A., Charroux, B., Abel, L., Rappsilber, J., Mann, M. and Dreyfuss, G. (2002). "miRNPs: a novel class of ribonucleoproteins containing numerous microRNAs." *Genes Dev* **16**(6): 720-8.
- Nelson, P. T., Hatzigeorgiou, A. G. and Mourelatos, Z. (2004). "miRNP:mRNA association in polyribosomes in a human neuronal cell line." *Rna* **10**(3): 387-94.
- Nottrott, S., Simard, M. J. and Richter, J. D. (2006). "Human let-7a miRNA blocks protein production on actively translating polyribosomes." *Nat Struct Mol Biol* **13**(12): 1108-14.
- Pearson, J. C., Lemons, D. and McGinnis, W. (2005). "Modulating Hox gene functions during animal body patterning." *Nat Rev Genet* **6**(12): 893-904.
- Peters, L. and Meister, G. (2007). "Argonaute proteins: mediators of RNA silencing." *Mol Cell* **26**(5): 611-23.
- Petersen, C. P., Bordeleau, M. E., Pelletier, J. and Sharp, P. A. (2006). "Short RNAs repress translation after initiation in mammalian cells." *Mol Cell* **21**(4): 533-42.
- Pillai, R. S., Bhattacharyya, S. N., Artus, C. G., Zoller, T., Cougot, N., Basyuk, E., Bertrand, E. and Filipowicz, W. (2005). "Inhibition of translational initiation by Let-7 MicroRNA in human cells." *Science* **309**(5740): 1573-6.
- Ramos, A., Grunert, S., Adams, J., Micklem, D. R., Proctor, M. R., Freund, S., Bycroft, M., St Johnston, D. and Varani, G. (2000). "RNA recognition by a Staufen double-stranded RNA-binding domain." *Embo J* **19**(5): 997-1009.

- Rana, T. M. (2007). "Illuminating the silence: understanding the structure and function of small RNAs." *Nat Rev Mol Cell Biol* **8**(1): 23-36.
- Russell, D. W. and Spremulli, L. L. (1978). "Identification of a wheat germ ribosome dissociation factor distinct from initiation factor eIF-3." *J Biol Chem* **253**(19): 6647-9.
- Schratt, G. M., Tuebing, F., Nigh, E. A., Kane, C. G., Sabatini, M. E., Kiebler, M. and Greenberg, M. E. (2006). "A brain-specific microRNA regulates dendritic spine development." *Nature* **439**(7074): 283-9.
- Sossin, W. S. and DesGroseillers, L. (2006). "Intracellular trafficking of RNA in neurons." *Traffic* **7**(12): 1581-9.
- St Johnston, D. (2005). "Moving messages: the intracellular localization of mRNAs." *Nat Rev Mol Cell Biol* **6**(5): 363-75.
- Tomari, Y., Du, T., Haley, B., Schwarz, D. S., Bennett, R., Cook, H. A., Koppetsch, B. S., Theurkauf, W. E. and Zamore, P. D. (2004). "RISC assembly defects in the Drosophila RNAi mutant armitage." *Cell* **116**(6): 831-41.
- Vasudevan, S. and Steitz, J. A. (2007). "AU-rich-element-mediated upregulation of translation by FXR1 and Argonaute 2." *Cell* **128**(6): 1105-18.
- Vasudevan, S., Tong, Y. and Steitz, J. A. (2007). "Switching from repression to activation: microRNAs can up-regulate translation." *Science* **318**(5858): 1931-4.
- Vo, N., Klein, M. E., Varlamova, O., Keller, D. M., Yamamoto, T., Goodman, R. H. and Impey, S. (2005). "A cAMP-response element binding protein-induced microRNA regulates neuronal morphogenesis." *Proc Natl Acad Sci U S A* **102**(45): 16426-31.
- Wessel, D. and Flugge, U. I. (1984). "A method for the quantitative recovery of protein in dilute solution in the presence of detergents and lipids." *Anal Biochem* **138**(1): 141-3.
- Wickham, L., Duchaine, T., Luo, M., Nabi, I. R. and DesGroseillers, L. (1999). "Mammalian stau1 is a double-stranded-RNA- and tubulin-binding protein which localizes to the rough endoplasmic reticulum." *Mol Cell Biol* **19**(3): 2220-30.
- Wu, L. and Belasco, J. G. (2008). "Let Me Count the Ways: Mechanisms of Gene Regulation by miRNAs and siRNAs." *Mol Cell* **29**(1): 1-7.
- Wu, L., Fan, J. and Belasco, J. G. (2006). "MicroRNAs direct rapid deadenylation of mRNA." *Proc Natl Acad Sci U S A* **103**(11): 4034-9.
- Yao, J., Sasaki, Y., Wen, Z., Bassell, G. J. and Zheng, J. Q. (2006). "An essential role for beta-actin mRNA localization and translation in Ca²⁺-dependent growth cone guidance." *Nat Neurosci* **9**(10): 1265-73.
- Zalfa, F., Achsel, T. and Bagni, C. (2006). "mRNPs, polysomes or granules: FMRP in neuronal protein synthesis." *Curr Opin Neurobiol* **16**(3): 265-9.
- Zhang, H. L., Eom, T., Oleynikov, Y., Shenoy, S. M., Liebelt, D. A., Dictenberg, J. B., Singer, R. H. and Bassell, G. J. (2001). "Neurotrophin-induced transport of a beta-actin mRNA complex increases beta-actin levels and stimulates growth cone motility." *Neuron* **31**(2): 261-75.
- Zeitelhofer, M., Karra, D., Vessey, J. P., Jaskic, E., Macchi, P., Thomas, S., Riefler, J., Kiebler, M. and Dahm, R. (2008) "High-efficiency transfection of shRNA-encoding plasmids into primary hippocampal neurons." In press.

6 APPENDIX

6.1 ABBREVIATIONS

Ago	Argonaute
amp	Ampicillin
APS	Ammonium peroxodisulfate
ATP	Adenosine triphosphate
BDNF	brain derived neurotrophic factor
bp	base pairs
BSA	Bovine serum albumin
CaMKII α	calcium/calmodulin-dependent protein kinase II α
cDNA	complementary DNA
CT	C-terminal
DEPC	Diethyl pyrocarbonate
DMP	Dimethyl pimelimidate
DMSO	Dimethyl sulfoxide
DNA	desoxyribonucleic acid
DOC	Deoxycholate
dsRBD	double stranded RNA-binding domain
DTT	Dithiothreitol
E17	embryonic day 17
EDTA	Ethylenediaminetetraacetic acid
eEF	eukaryotic elongation factor
eIF	eukaryotic initiation factor
EtBr	Ethidium bromide
FL	full length
FMRP	fragile X mental retardation protein
FT	flow-through
g	gravity (or grams for chemicals)
GF	gel filtration
GSFF	Glutathione Sepharose™ 4 Fast Flow
GST	Glutathione-S-transferase
h	hour/hours

HEPES	2-[4-(2-Hydroxyethyl)-1-piperazinyl]-ethanesulfonic acid
IP	immunoprecipitation
IPTG	Isopropylthiogalactopyranoside
kb	kilo basepairs
kD	kilo Dalton
Limk1	LIM domain kinase 1
MAP	microtubulin associated protein
MCS	multiple cloning site
mA	milli amperes
min	minutes
mRNA	messenger RNA
miRNA	micro RNA
MOPS	Morpholinopropane sulfonic acid
MW	molecular weight marker
NP-40	Nonidet™ P 40 Substitute
nt	nucleotides
NTC	non template control
OD	optical density
o/n	overnight
PACT	protein activator of the interferon-induced protein kinase PKR
PAGE	Polyacrylamide gel electrophoresis
PBS	Phosphate buffered saline
pCp	Cytidine 3',5'-bis [α - ³² P] phosphate
PCR	polymerase chain reaction
pDNA	plasmid DNA
PIS	preimmune serum
PNS	post nuclear supernatant
ProtA	Protein A Sepharose
RBD	RNA-binding domain
RBP	RNA-binding protein
RISC	RNA induced silencing complex
RNA	ribonucleic acid
RNase	ribonuclease
RNP	ribonuclearprotein particles
rpm	rounds per minute

rRNA	ribosomal RNA
RT	room temperature or reverse transcription
S	Svedberg
S100	supernatant after centrifugation at 120,000 g
SDS	Sodium dodecylsulfate
sec	seconds
siRNA	small interfering RNA
Stau	Staufen
TBD	tubulin binding domain
TBS	Tris buffered saline
TCA	Trichloric acid
TEMED	N,N,N',N'-Tetramethylethylenediamine
TRBP	human immunodeficiency virus (HIV-1) <i>trans</i> -activating response (TAR) RBP
tRNAs	transfer RNAs
u	enzymatic units
Upf1	Upregulated protein factor 1
UTR	untranslated region
V	volts
WB	Western blot

6.2 ACKNOWLEDGEMENTS

The performance of the project would not have been possible without Prof. Michael Kiebler, who gave me the opportunity to carry out my work at the Center for Brain Research. Thanks for showing a lot of interest in my data and always taking the time for discussions.

I would like to thank in particular my supervisor Dr. Anetta Konecna for her great support during my whole thesis and her patience to answer any question concerning the theoretical and practical outline of the project.

Special thanks go to Florian Mair for his encouragement, support and bringing balance in my life as well as for useful comments and discussions concerning my thesis.

I further owe thanks to my family, especially for their interest in my education as well as their confidence in me and my work.

Last but not least I would like to thank all my laboratory colleagues at the Center for Brain Research for providing nice working conditions, especially Martin, Georgia, Anetta and Ingrid for being good friends, Sebastian for his patience during orderings, Sabine for organizing and chocolate, Martina for funny times and help in the lab as well as Jacki for showing interest in my project (and my bench).

6.3 CURRICULUM VITAE

Personal Data

Name	Sabine Spath
Address	Malfattigasse 45/9, 1120 Vienna
Citizenship	Austrian
Date and place of birth	04. 09. 1982 in Vienna
Email	sabine.spath@gmx.at
Telephone	0043/6504982100

Education

March 2007 - present	Diploma thesis in the lab of Prof. Michael Kiebler, Center for Brain Research, Division of Neuronal Cell Biology
September/October 2006	Practical work in Cell Biology at the Novartis Institute of Biomedical Research, lab of Dr. Tamas Schwaighoffer
March/April 2006	Practical work in Immunology at the University of Vienna, lab of Prof. Pavel Kovarik
October 2005	Completion of the first level of „Molecular Biology“, passed with distinction, for the second level of studies specialization in Neuroscience, Immunology and Cell Biology
October 2002 - present	Studies of „Molecular Biology“ and „Psychology“ at the University of Vienna
June 2002	Graduation from HTL, passed with distinction
1997 – 2002	Higher Technical School (HTL) for Chemical Industry, Vienna
1993 – 1997	Grammar School, Gänserndorf

Scholarships and awards

2003-2006	A performance scholarship in "Molecular Biology" (1st, 3rd and 4th year of the studies) was received
February 2001 – July 2001	Leonardo studentship for a trainee period in The Netherlands

Work experience

September 2003 – October 2006	Technical assistance at Boehringer Ingelheim, Vienna, in the Process Science department, working on process development in plasmid- and protein-analyses
February 2001 – July 2001	Studies in The Netherlands, founded by Leonardo, at TNO – Nutrition and Food research in the field of biosensors, working on the projects „Mycotoxins in food“ and „Hormone detection in milk“
July 2000	Practical work at the Novartis Research Institute Vienna
August 1999	Practical work at B.Braun (chem. pharm. company), Maria Enzersdorf

Languages and additional skills

Mother tongue	German
Foreign languages	fluent in spoken and written English
Computer skills	profound knowledge in the most common office programs as well as Adobe Photophop and InDesign
Drivers license	for group B (cars < 3500 kg), since 2000

Publications

B. van der Gaag, S. Spath, H. Dietrich, E. Stigter, G. Boonzaaijer, T. van Osenbruggen and K. Koppal. „Biosensors and multiple mycotoxin analysis“. Food Control, 14, 2003 (251-254).